CONTRACT NO. A132-102
FINAL REPORT
JULY 1993

Development of a Modular System for Acidic Deposition Monitoring

CALIFORNIA ENVIRONMENTAL PROTECTION AGENCY

AIR RESOURCES BOARD
Research Division

DEVELOPMENT OF A MODULAR SYSTEM FOR ACIDIC DEPOSITION MONITORING

Final Report
Contract No. A132-102

Prepared for:

Research Division
California Air Resources Board
2020 L Street
Sacramento, California 95814

Submitted by:

University of California, Davis
Department of Crocker Nuclear Laboratory
Davis, California 95616-8569

Prepared by:

Thomas A. Cahill
Kenneth Bowers
Teresa A. James
Paul H. Wakabayashi

JULY 1993

ABSTRACT

In order to effectively monitor dry acidic deposition in the forests of California, a simple and inexpensive monitoring system is needed for large-scale deployment. While the current California Acid Deposition Monitoring Program (CADMP) monitor performs satisfactorily, it is cumbersome and expensive for statewide application, especially in remote sites. To simplify and reduce the cost of particulate and gaseous sampling procedures for the CADMP, the University of California, Davis (UCD), developed for the ARB the Modular System for Acid Deposition Monitoring (MSAM). This sampler provides continuous monitoring on a 14-day cycle and could reduce the cost and complexity of field operations. A large part of the UCD project involves establishing comparability between the MSAM and the existing CADMP sampler before considering large-scale statewide deployment of the MSAM sampler.

The study was conducted in two phases. In Phase I, the MSAM was tested in Sacramento for three one-week periods from April 8 to 29, 1992. The data analyses showed good agreement between collocated MSAM units and the ratio for the two collocated MSAM samplers was nearly 1.00 (0.808 to 1.36, except for ammonium and nitric acid). The statistical comparisons between the MSAM and CADMP sampler were satisfactory (within 20 percent) for sulfate, sulfur dioxide, total nitrates, ammonia, and nitric oxide. However, the Phase I tests did find some discrepancies between MSAM and the CADMP samplers for particulate nitrate, ammonium, and mass. After review of the design of the MSAM sampler, the problems were identified and modifications were made.

Phase II compared the MSAM and CADMP samplers under field conditions. From August 5 to November 6, 1992, the MSAM was deployed at an intensive study site at Barton Flats in the San Bernardino National Forest. The data analyses showed the improvement of the MSAM sampler in Phase II. In the first three periods, the results showed good agreement between the two units for mass concentrations. In the case of NH_3, the species showed a marked improvement from Phase I to Phase II (CADMP/MSAM = 0.33 for Phase I and 0.84 for Phase II). After examining the data from the Phase II trials, it was concluded that the MSAM sampler performed well except for the collection of total nitrate.

Nitrate collection differences were due to the use of a Teflon filter to capture and retain nitrate particles. Data from Phase I, when the MSAM employed a single Nylasorb filter, showed that MSAM total nitrate measurements agreed very well with CADMP total nitrate measurements (CADMP/MSAM = 0.90). During Phase II, the single Nylasorb filter was replaced with a Teflon-Nylasorb filter combination to reduce the chances of filter clogging. The filters were placed in a double cassette. It was later determined that because of the filter cassette's construction, the nitric acid that passed through the Teflon filter could be absorbed by the plastic support grid and the plastic filter cassette walls before reaching the Nylasorb filter. This would reduce the amount of nitric acid collected by the Nylasorb. In addition, the MSAM Teflon filters were not analyzed for at least eight weeks. This gave the nitrate particles time to volatilize off the Teflon filter. UCD

DISCLAIMERS

The statements and conclusions in this report are those of the contractor and not necessarily those of the California Air Resources Board. The mention of commercial products, their source or their use in connection with material reported herein is not to be construed as either an actual or implied endorsement of such products.

ACKNOWLEDGMENTS

The work here described in this report was funded by the California Air Resources Board (ARB). The project officer was Nehzat Motallebi of the Research Division of the ARB; her suggestions and comments were very useful and are greatly appreciated. Without her valued input, this report would not have been possible. We are also grateful to Lowell Ashbaugh for his suggestions and comments to this report. We are also in debted to Nehzat's colleague, Brent Takemoto, who has helped with the organization of this report and provided useful suggestions and comments throughout this project. We would also like to thank Nehzat's supervisor, Manjit Ahuja, who also provided useful suggestions and comments throughout the project. And for Paul Miller and David Jones of the San Bernardino National Forest Service, whose assistance in the coordination and maintenance of the MSAM sampler at Barton Flats, California was also greatly appreciated.

RECOMMENDATIONS

By use of a compact sampling system, the MSAM can reduce the costs for equipment and by providing 14 day average and four hour time resolved data, can reduce the amount of analysis. We expect an initial equipment cost of approximately $11,000.00 for each site and a maximum analysis cost of approximately $5,000.00 per site per month. Over 380 analyses will be provided per month at an average cost of approximately $13 per analysis. (These prices are subject to change.) Each particulate analysis will provide data on the elemental composition (hydrogen and sodium through lead) of the aerosol samples. Through several assumptions that have been demonstrated to work well in the IMPROVE network, values from sulfate, soil, and organic mass can be calculated. In addition a reconstructed mass can be calculated from the elemental data and compared to the gravimetric mass.

From the tests completed in this project the MSAM sampler gas performed well, with the exception of the ability of the MSAM sampler to collect total nitrate. UCD has, from experience, that problem of nitrate collection is related to the volatilization of nitrates off the Teflon filter. UCD has experienced loss of nitrate during and after sampling. UCD recommends that this can be corrected by removing the Teflon filter from the total nitrate filter pack.

Once the Teflon is removed, the total nitrate will be collected on the Nylasorb, an excellent substrate for the collection of nitrates. At which point, UCD believes that the MSAM sampler will achieve its original goal set by the proposal. The goal being the creation of an acid deposition sampler that was both low costing and easy to operate to sample aerosols in California's forested areas.

recommends that, in the future, the Teflon filter be removed, leaving only the Nylasorb filter to collect the total particulate nitrate.

At the end of Phase II, UCD continued testing the sampler, investigating mass concentration problems from Phase I and checking the new impregnated filter protocols. The testing included collocation of the Interagency Monitoring of Protected Visual Environments (IMPROVE) particulate sampler for standard purposes. The modifications done between Phases I and II showed that mass concentration agreement between each of the filters in the MSAM sampler and IMPROVE sampler were within five percent.

Based on the tests completed in this project, we concluded that the MSAM sampler performed satisfactorily, except for collections of total nitrate. UCD believes that, in a short period of time, with further modifications and testing the MSAM sampler can be used to monitor dry particles and gas levels in forested areas throughout the state.

CONTENTS **Page**

TABLE OF CONTENTS

CONTENTS **Page**

LIST OF TABLES

CONTENTS Page

LIST OF FIGURES

1.0 INTRODUCTION

This report, submitted to the California Air Resources Board, provides information on the Modular System for Acid Deposition Monitoring (MSAM) sampler, developed at the University of California, Davis (UCD). In the report, a discussion of the sampler design, analytical techniques and experimental processes are included as part of the development of the MSAM sampler.

The MSAM sampler design was derived from existing samplers used in collecting particles and gases important to the research of acid deposition and from limiting factors created when sampling in forested areas. The analytical techniques used were based upon existing laboratory procedures from various groups who have experience in analyzing particulate and gaseous aerosols. After construction, the MSAM sampler was tested against three samplers that have been or are being used by several governmental agencies for the collection of aerosols in their various programs. The samplers used in the tests were the Stacked Filter Unit (SFU), California Acid Deposition Monitoring Program sampler (CADMP) and the Interagency Monitoring of Protected Visual Environments (IMPROVE) particulate sampler.

This report will first introduce the MSAM sampler by providing a brief discussion of the basic components of the MSAM sampler and also includes the selection and capture of aerosols. Following this discussion, a description of the analytical techniques used to extract information from the various sampling techniques is presented. After this presentation, the experimental design, data summary, and test evaluation for each of the three phases of the development of the MSAM are discussed. Finally, a project summary is provided with findings and recommendations for the MSAM.

1.1 Background

The University of California, Davis (UCD) has been collecting aerosol data for over twenty years. Through the use of the cyclotron, located on the campus of UCD, Department of Crocker Nuclear Laboratory, researchers have produced data analysis of aerosols with sensitivities less than a microgram per cubic meter. During the earlier days, UCD bought commercially available samplers to collect aerosols. However, these samplers were incompatible with some of the technologies available at UCD. With facilities on hand at UCD, including Crocker Nuclear Laboratory and the Institute of Toxicology and Environmental Health (ITEH), UCD started to construct its own samplers.

UCD has produced several samplers to collect aerosols, including the Stacked Filter Unit (SFU), Davis Rotating-drum Unit for Monitoring (DRUM) and the Interagency Monitoring of Protected Visual Environments (IMPROVE) particulate samplers. The latter is being used in a network of over fifty sites throughout the United States, mostly located in the National Parks. These samplers are also maintained in other countries

2.0 MATERIALS AND METHODS

The section entitled "Sampler Specification" will introduce the layout of the MSAM sampler's basic components, filter packs and laboratory work. This section is followed by a complete discussion of analysis techniques, quality assurance, precision and accuracy of the MSAM program. The final section will deal with an overview of the three test phases involving the MSAM sampler.

2.1 Sampler Specifications

The MSAM (Modular System for Acid deposition Monitoring) is a particulate and gas absorptive filter sampler integrated with a two stage rotating surface impactor (Figure 1). The two stage impactor is a newly designed modification of the highly successful eight stage DRUM (Davis Rotating-drum Unit for Monitoring) sampler (Cahill et al., 1987) in combination with principles also used in the SMART (Solar Monitor for Aerosols in Remote Terrain) sampler (Bowers et al., 1991) and the 3 stage IMPROVEd DRUM currently under development. The MSAM sampler also borrows technologies from the IMPROVE particulate sampler (Figure 2).

The MSAM sampler collects integrated 14-day gas and particulate samples along with four hour size-time resolved particulate aerosols in two size fractions. The pollutant gases and vapors are collected by absorptive filters. Integrated particulate matter is collected by a Teflon filter. The 14-day averaged filters will collect gases and particulate matter giving a true average and greater sensitivity than 12 or 24 hour sampling once every sixth day. By continuous sampling, pollutant episodes are assured of being monitored. In contrast, one day in six sampling has only a 17% chance of monitoring those episodes. Episodes are averaged over 14-day blocks.

Shorter term variations will be documented in the results from the Drum stage. Proton Induced X-ray Emissions (PIXE) analysis of the Mylar strip from the rotating DRUMs in 2 mm increments will give elemental concentration data in four hour time resolution. In this manner, frontal passages and diurnal patterns such as upslope-downslope wind patterns are discernible (Figure 3a and 3b). In addition, these time resolved data will provide elemental signature and time indicators to characterize pollution episodes. These concentration patterns can be important in understanding deposition in mountainous terrain (Cahill, 1989).

The anthropogenic aerosols important for acid deposition predominate in the lower lobe of the bimodal ambient aerosol distribution ($\sim 0.01\mu m \leq Dp \leq 2.5\mu m$). Particles in this size range strongly interact with sunlight ($0.3\mu m \leq Dp \leq 1.0\mu m$). Particles less than $0.3\mu m$ constitute a significant fraction of the aerosol mass, but do not contribute to visibility degradation. The particles in the $1.0\mu m$ to $2.5\mu m$ size range are not a significant factor in visibility because of the comparably low relative amount to that of particles less than 1.0 µ including Quetta, Pakistan and Santiago, Chile. With this large network, the Air Quality Group's laboratory was organized to handle the over five hundred samples per week processed therein. The IMPROVE program has been highly successful with a sample collection rate of over 95%.

The IMPROVE network's system was the basis for developing the MSAM sampler which could be integrated into a small or large network of the samplers. Some of the key components of the MSAM sampler come directly off the IMPROVE particulate sampler. These include the cyclone for aerosol size selection and the critical orifice for flow regulation.

1.2 Objectives

The principle objective of this project was to develop and demonstrate a monitoring system that could be economically deployed throughout the state and to provide data of comparable quality to the standard CADMP system. The MSAM provides significant cost savings versus the current CADMP system and allows for expansion of the network to remote sites. The technologies and procedures used in the MSAM also provide comparability to the national IMPROVE and the international IMPROVE-type networks. The MSAM sampler borrows and expands on previous sampler technology that the UCDs' Air Quality Group has worked with in the past.

The MSAM sampler was developed with remote sampling in mind. The sampler is easy to maintain in the field, with only a 10 pound filter pack to replace every two weeks. Once the filter pack has been exposed for two weeks, the filter pack is returned to UCD for archiving and subsequent analysis. Although the diurnal patterns and some of the short term weather patterns are not seen because of the long average, the filters represent seasonal trends important to local and regional areas due to inversions and agricultural activities. Because of the number of filters involved, this has the added benefit of reducing the cost of analysis.

After the initial prototype was designed and built, it was tested in two phases. But because of unforeseen problems, a third test was included to evaluate the sampler compared to an IMPROVE particulate sampler. The first phase involved the comparison of two MSAM samplers, one SFU sampler and one CADMP sampler. This was to test the precision and accuracy of the MSAM sampler. The second phase tested the MSAM sampler in actual field conditions using a third party to maintain the sampler (US Forest Service). The second phase also worked out the logistics and laboratory procedures for maintaining a sampler in the field and any of the problems that had developed in Phase I. The third phase tested the final version of the sampler with an IMPROVE sampler at UCD.

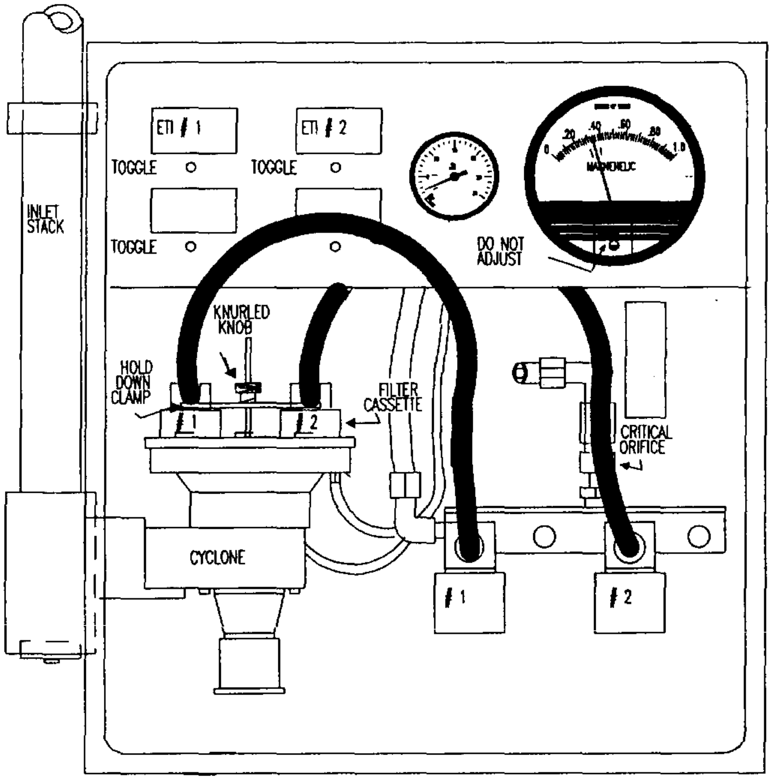

Figure 2. Diagram of the IMPROVE sampler.

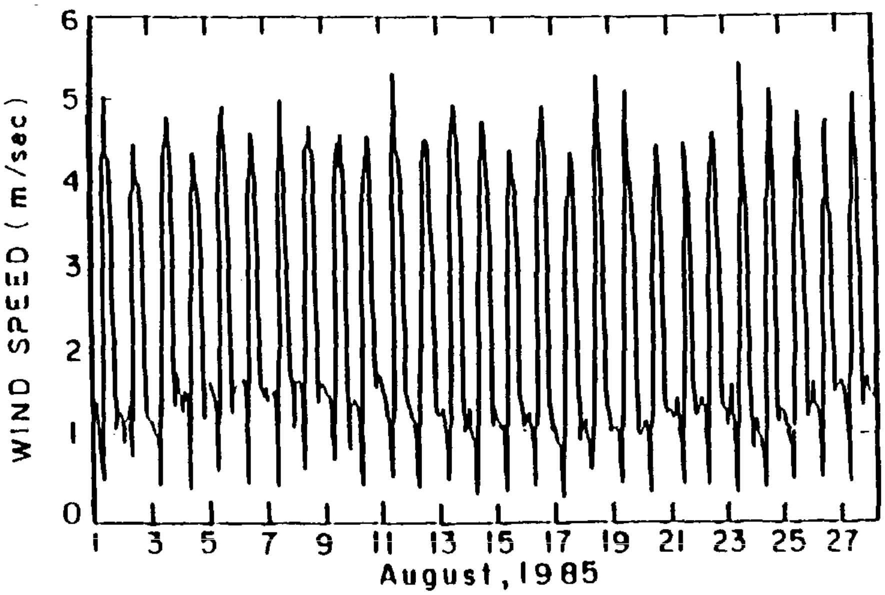

Figure 3a. Hourly wind speeds at Elk Creek, Sequoia National Park, August 1985 (From Cahill, 1989)

m. Since this size range is in the minimum of the bimodal distribution, these particles will not contribute strongly to the aerosol mass. For these reasons we have separated the DRUM stages at 0.3μm, resulting in a visibility stage (0.3μm ≤ Dp ≤ 2.5μm) and a very fine optically inactive stage (0.07μm ≤ Dp ≤ 0.3μm). Many of the anthropogenic tracer elements (Arsenic for smelter, Selenium for coal fired power plant emissions) occur in the optically inactive stage. The 0.07μm cut-point of the optically inactive DRUM stage is a factor of impactor dynamics. Extremely small impactor cut-points are very difficult to design and operate. Extremely small particles ($PM_{0.07}$) will be collected on a 14 day Teflon filter.

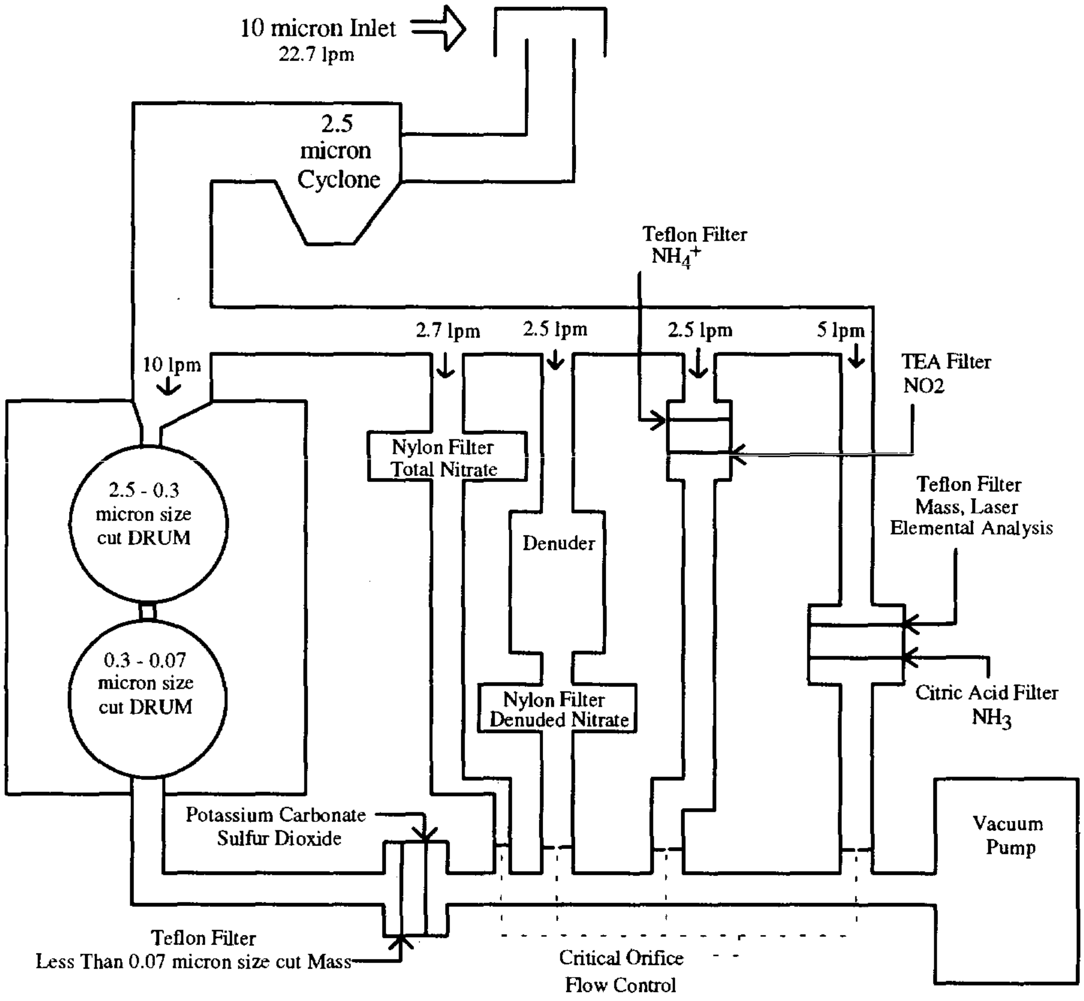

Figure 1. Schematic of MSAM sampler.

The mailable filter pack consists of several filter cassettes and an impactor. The various filter cassettes and DRUM impactor are divided into 5 channels. They are the DRUM-SO_2 channel, Total Nitrate channel, Particulate Nitrate channel, Teflon-triethanolamine (TEA) channel, and Teflon-Citric Acid channel.

The DRUM-SO_2 channel consists of a two stage DRUM impactor followed by a filter cassette with a Teflon particulate filter and a potassium carbonate filter. The two stage DRUM impactor is a hybrid of the 8 stage Davis Rotating-drum Unit for Monitoring (DRUM) sampler (Rabbe et al, 1986). The two stage DRUM impactor allows 4 hour time resolved sampling of atmospheric particles. The first stage DRUM collects particles from 0.3 to 2.5 μm in diameter. This range includes the visibility affecting particles ($0.3\ \mu m \leq Dp \leq 1.0\ \mu m$) and those slightly larger. Particles between 1.0 μm and 2.5 μm are in the minimum of the bimodal distribution of atmospheric particles and a minor contributor to the 0.3 to 2.5 μm particle loading. The second stage DRUM collects particles between 0.3 and 0.07 μm. The second stage particles are below visibility affecting size, but still make up a large portion of the aerosol mass, especially of sulfate aerosols. The samples will be collected on drums mounted with an Apiezon coated Mylar substrate. The DRUM stages will be analyzed by PIXE techniques.

Following the two stage DRUM impactors will be a filter cassette to collect the remaining particles and SO_2 gas. The cassette will have a Teflon particulate matter afterfilter to remove the $Dp < 0.07\ \mu m$ particles remaining after the two stage DRUM impactors and a potassium carbonate impregnated cellulose filter for SO_2 gas collection. The impregnated filters will be supplied and analyzed by Desert Research Institute (DRI) of Reno, Nevada. The Teflon afterfilter will be analyzed at UCD for mass, optical absorption, and elemental content by PIXE, Proton Elastic Scattering Analysis (PESA) and X-ray Re-Fluorescence (XRF). The afterfilter and gas absorptive filter give a 14 day integrated sample.

The total and particulate nitrate channels consist of two single filter cassettes with a nylon filter. The total nitrate is measured on $PM_{2.5}$ with no denuder. The particulate nitrate channel will use a denuder to remove nitric acid vapor. The denuder is made of concentric aluminum tubing coated with sodium carbonate based on the design used in the IMPROVE network. Nitric acid vapor concentrations will be calculated as the difference between the denuded and total nitrate channels. Since a separate determination of nitrate volatilization is not necessary, total and particulate nitrate will be measured on a nylon filter only. The flow through the nylon filters will be controlled by critical orifices. The nylon filters will be supplied and analyzed by DRI.

To assure that nitric acid vapor is not absorbed until desired, on the total nitrate filter and in the denuder prior to particulate nitrate collection, all up stream surfaces will be Teflon coated. A seasoned Teflon surface efficiently transmits the nitric acid vapor. The denuder to be used in this project will efficiently pass fine particles while collecting the reactive nitric acid vapor. The aluminum surface has a large capacity to absorb nitric acid vapor (John et al., 1988). In recent tests, the aluminum denuder does not appear to have infinite

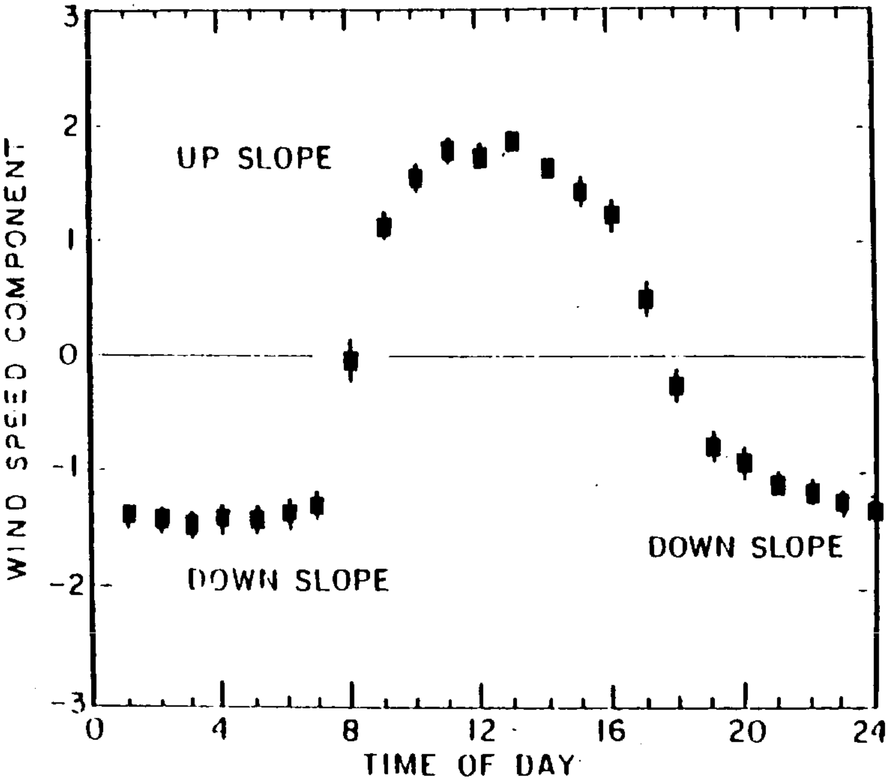

Figure 3b. Mean diurnal wind speed at mid-elevation, Sequoia National Park (From Cahill, 1989)

2.1.1 MSAM Layout

The MSAM will provide very simple field operations. The filter packs are self contained and will be prepared and loaded in the laboratory as a packaged unit. All sample and substrate handling and flow adjustment will be taken care of at the laboratory. Flow adjustments will be corrected for altitude by simulating the elevation pressure at the laboratory.

The overall design of the monitoring system consists of a mailable filter pack and an on site field stand. The on site aluminum stand supports a fiberglass enclosure consisting of a sampling inlet followed by a 2.5 µm cut point cyclone. Since the entering aerosol will be sized by the cyclone, the cut size of the inlet is not important, although for the inlet to be used the cut size is approximately 10 µm. The MSAM sampler will use the standard IMPROVE cyclone which is a 3.66 cm design of Walter John and George Reischl of the Air and Industrial Hygiene Laboratory. A Gast pump, model RAAV 131EB, is also permanently housed at the site. The Gast pump will require the most power by drawing 2.6 amps from a 110 volt line. The rest of the sampler will take up an additional 0.4 amps, giving a total of 3.0 amps needed to operate the sampler.

Once leak checking has been completed, the filter pack will be hooked up to a device to simulate air pressures found at the elevation to which the filter pack is to be installed. The flow rate is then adjusted and calibrated across each of the filters by using a mass flow meter.

The loaded and calibrated MSAM unit will be mailed to the field site where the field operator will attach the vacuum and electrical connections and insert the inlet. The operator will record the beginning vacuum reading and time. At the end of the sampling period the operator will again record the vacuum reading and the time. The vacuum and electrical connections and inlet will be removed and the unit capped and mailed back to the laboratory.

At the laboratory, after the sampling period, the pressure drop across the second drum stage jet will be remeasured along with the flow rates before removing the filters or drums. The drums will then be removed and the Mylar strips mounted for PIXE analysis. The Teflon filters from the fine particle and afterfilter stages will be recovered and post-weighed, post-lasered, and mounted for PIXE and PESA analysis. The potassium carbonate, citric acid, TEA impregnated filters and the nylon filters will be recovered and placed in petri dishes. The petri dishes are then stored in a freezer until they are shipped. When a set of filters (25-50) is completed , the filters are packed in blue ice and shipped to Desert Research Institute (DRI) for analysis. Care must be taken with all filters to avoid contamination or degradation of the sample or substrate. The filter pack is then cleaned and prepared for the insertion of fresh filters and drums.

2.1.3 Gas and Particulate Sampling Systems

2.1.3.1 Cyclone

The collection efficiency of the IMPROVE cyclone was characterized at the Health Sciences Instrumentation Facility at the University of California at Davis. The efficiency was measured as a function of particle size and flow rate using two separate methods: PSL and SPART. The PSL method uses microspheres of fluorescent polystyrene latex particles (PSL) produced by a Lovelace nebulizer and a vibrating stream generator and analyzed by electron micrographs. The SPART method uses a mixture of PSL particles produced by a Lovelace nebulizer and analyzed by a Single Particle Aerodynamic Relaxation Time (SPART) analyzer. The aerodynamic diameter for 50% collection, d_{50}, was determined for each flow rate. The relationship between diameter and flow rate is shown in Figure 4.

capacity. To increase the efficiency of the denuder, the denuder is coated with sodium carbonate.

The Teflon-TEA channel will consist of a double filter cassette containing a Teflon filter followed with a TEA (triethanolamine) impregnated cellulose filter for NO_2 collection. The Teflon filter will be analyzed for NH_4^+ ion. The filters will be analyzed by DRI through wet chemistry techniques.

The Teflon-Citric Acid channel consists of a Teflon filter followed by a citric acid impregnated cellulose filter. The Teflon filter will be a stretched Teflon total filter for collection of particles less than 2.5µm. The Teflon filter will be analyzed at UCD for mass, optical absorption of soot carbon by Laser Integrated Plate Method (LIPM), and elemental content by PIXE/XRF and hydrogen by PESA. The citric acid filter will collect ammonia (NH_3) gases. The citric acid filters will be analyzed by DRI.

The total flow through the MSAM sampler will be 22.7 liters per minute. Ten liters per minute will be utilized in the DRUM-SO_2 channel. The remaining 12.7 liters per minute will be divided among the remaining filter cassettes.

Although the impregnated filters have not been run for 14 day periods before, drying and clogging of the filters is not expected to be a problem. Our experience with the IMPROVE network carbonate impregnated filters and nylon filters indicates that even in cases when the filters ran for an extended period, drying and clogging was not a problem. This is being further tested in our current developmental work.

2.1.2 Laboratory and Field Operations

Since all filter handling will be done in the laboratory, the laboratory procedures are somewhat more extensive than in some programs. However, field procedures will be minimized.

After all filter cassettes and drums are installed into the mailable filter pack, the unit will be leak checked and the pre-exposure vacuum reading across the second drum stage jet will be recorded. The unit is designed such that if the low pressure side of the jet is less than 0.53 atmospheres, the critical orifices of the filter channels will function properly. The vacuum at the filter channels will be somewhat lower than the reading at the second stage drum due to the drum channel after-filter cassette pressure drop; assuring that the orifices at the filter stages will remain critical. The gaseous absorptive filter's pressure drops will also be measured to determine the amount of glycerol on the filter. The amount of glycerol is an important contributor to flow rate. If the filter is too heavily loaded with glycerol, the pressure drop across the filter will be to great to allow a suitable flow rate for collecting the gases. If the pressure drop is too little, this will indicate that the filter's moisture content will be too low to effectively collect gases.

particles between 0.3 μm and 0.07 μm. The Teflon after filter will collect the remaining very small particles as an integrated 14 day sample. The second impactor stage jet will be approximately 0.0129 cm by 0.8 cm. This second stage jet will have a high pressure drop and act as a critical orifice to control the air flow (Hinds, 1982; Roberson and Crowe, 1975). Following exposure, the Mylar strip from the drums will be mounted and archived for PIXE elemental analysis. The elemental analysis will provide the concentrations of elements from sodium through lead.

2.1.3.3 Flow Rate Control and Measurement

The flow rate through each filter of the MSAM sampler is maintained by a critical orifice, located between the filter and pump. The device in the sampler is a removable brass plug with a small orifice. We have a range of available orifice diameters; in addition, the orifice can be slightly enlarged or decreased in the field. As long as the pressure after the orifice is less than 52% of the pressure in front of the orifice, the air flow will be critical, that is, limited by the speed of sound and will not be affected by small changes in pump performance or filter loading.

The flow rate of a critical orifice varies predictably with temperature and pressure. Except under very unusual conditions, the flow rate variation is minor. For example in Table 1, a critical orifice designed for 10 liters per minute (lpm) at 20°C at 1500m elevation controls the flow rate at much better than ±10% except under very cold conditions at sea level (not a likely occurrence in California). An additional advantage to a critical orifice is that the flow rate can be readily calculated from theory and checked in use as needed.

To assure that the critical orifice is functioning properly, pressure readings will be made when the MSAM units are prepared for field use and also upon return. Field readings of the drum channel pressure will be taken at the beginning and ending of sampling. In addition, field flow audits will confirm the total flow rate.

If critical conditions are maintained in the drum chambers, then the nitrate and 2.5μm filter channels will also be critical. The vacuum side of the orifice controlling the nitrate and SFU channels will be greater than at the fine stage drum due to the pressure drop of the afterfilter/carbonate cartridge. Thus, unless the filters clog, there should be no problem maintaining critical conditions. In addition the flows will be checked with a low pressure drop meter placed in line with each channel.

Table 1. Flow rate (liters per minute) controlled by critical orifice designed for operation at 1500 meters elevation and 20°C

Elevation/Temp.	-20°C	0°C	20°C	40°C
Meters (Sea Level)	11.10	10.69	10.32	9.98
1500 Meters	10.73	10.33	10.00	9.64
3000 Meters	10.35	9.97	9.62	9.31

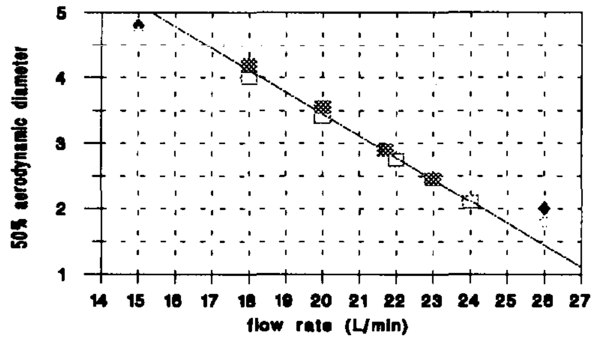

Figure 4. Relationship between 50% aerodynamic diameter and flow rate for the IMPROVE cyclone. The solid symbols are from PSL and the open symbols from SPART.

The best-fitting straight line in Figure 4 is based on measurements for both methods for flow rates between 18 and 24 L/min. The equation is:

$$d_{50} = 2.5 - 0.334 * (Q - 22.75)$$

with a correlation coefficient of r^2=0.991. In order to maintain a constant cut point of 2.5 µm, it is necessary to maintain a constant volume flow rate of 22.8 L/minute.

2.1.3.2 DRUM Impaction Technique

The MSAM's two stage DRUM impactor is a hybrid of the 8 stage Davis Rotating-drum Unit for Monitoring (DRUM) sampler (Rabbe et al, 1986). The DRUM sampler (Cahill et al, 1987) itself is the product of combining two well-tested techniques (the single orifice multi-stage impactor of the Battelle design and the rotating drum collection concept of the Lundgren design) into a single, well-engineered package. The two stage DRUM channel of the sampler will be a two stage rotating surface impaction device. Particles are collected on an Apiezon greased Mylar strip wrapped around a 6.2 cm drum. The drums will rotate at a rate of once in 14 days, giving a four hour time resolution. The unit consists of two sequential orifices impacting on two slowly rotating drums, plus an after filter. The unit impacts aerosols onto Mylar strips (lightly coated with Apiezon-L grease to eliminate bounce-off) mounted on rotating drums. After sampling, this results in two Mylar strips with linear streaks of size-resolved aerosol deposits that are analyzed by PIXE. After the winter of 1994, a second substrate, Teflon, should be made available. In addition to PIXE analysis, PESA will also be option. PESA will provide hydrogen off the Teflon strip which can be reconstructed as organic matter and total mass.

The first stage of the two stage DRUM channel will collect particles between 2.5 µm and 0.3 µm. The jet will be a slot approximately 0.0215 cm by 0.75 cm. This jet will have a low pressure drop. The second stage of the two stage DRUM channel will collect specific site data are provided. An additional area is allocated to support DRUM research activities. A refrigerator freezer is provided to retain perishable samples and supplies.

2.2.1 Mass Measurements

Integrated particulate mass concentrations are measured on the Teflon filters. The filters are weighed, pre-exposure and post-exposure, on a Cahn microbalance with a precision of ±2.5μg. The flow rate on which the concentration are based will be controlled by a critical orifice.

Gravimetric mass analysis is performed at the microgram level utilizing a Cahn 25, 27 or 31 Electrobalance modified with a zero area bail and vertical counterweight. Polonium anti static strips are used to reduce electrostatic effects in the weighing cavity and on individual filters. Earth grounded conductive mats are used on the weighing table surface and technician foot surface to negate electrostatic effects. A segregated laboratory area is used to control human traffic and to stabilize the temperature of the weighing environment. The area is cleaned with a high efficiency HEPA vacuum daily and tacky floor covering is installed to minimize dust artifact.

Gravimetric analysis of the MSAM samples requires the collected or differential mass be determined through two weighings. Teflon filters are assigned a unique media identification, pre-weighed, post-weighed, analyzed and archived. The two weighing operations are identical and referred to as PRE and POST. Laboratory and field controls are utilized to determine mass artifact in the same manner.

To assure quality control, the electrobalances are calibrated twice a day. After the balances are calibrated a series of control Teflon filters are weighed, once in the morning and once in the afternoon. In addition to calibrations, a standard weight is measured on the electrobalance after every sixth filter to check for any drift in the calibration.

2.2.2 Absorption Measurements

Optical absorption will be measured on the Teflon filters by LIPM. LIPM is a technique for measuring the optical absorption of red laser light by particles on aerosol filters. This optical absorption is proportional to the amount of soot carbon on the filter. A very good correlation has been found between the absorption based on LIPM and that based on more expensive carbon combustion methods. The correlation coefficient over several years worth of data for many sites is approximately 0.87.

The LIPM system is used to measure the optical absorption of the particles on the fine Teflon filters. The absorption by the particles on the filter is smaller than the absorption by particles in the atmosphere because of the layering of particles on the filter. A correction to the measured value, based on the areal density of particles on the filter, is

2.1.3.4 Filter Media

The filter media used are based upon those used in the Air Resources Board's (ARB) California Acid Deposition Monitoring Program (CADMP) sampler. All of the filter media used in the MSAM sampler are the same, except Teflon for elemental analysis, as in the CADMP sampler. The filter media include an impregnated potassium carbonate cellulose filter for SO_2 analysis, an impregnated triethanolamine (TEA) cellulose filter for NO_2 analysis, an impregnated citric acid cellulose filter for NH_3 analysis, Nylasorb nylon filter for both total and particulate nitrate and sulfate analysis, and Teflon filters for NH_4^+ ion, mass, absorption and elemental analysis. Teflon filters are used instead of the CADMP's Zeflour filters because UCD's elemental and light absorbing carbon analysis requires a thinner substrate than Zeflour for increased sensitivities.

The two stage DRUM impactor substrate consists of the Mylar wrapped drum that is coated with a thin layer of Apiezon grease. The grease reduces particles bouncing off the Mylar from impaction. UCD is also in the process of developing a Teflon substrate, which would be analyzed by PIXE and PESA techniques. From the hydrogen provided by PESA, organic matter as well as mass can be reconstructed. The Teflon substrate should be available in early 1994.

2.2 Analytical Techniques

When the samples return to UCD from the field, the filters and drums from the MSAM are archived and fresh filters are loaded into the sampler. The sample handling is in a building constructed in 1992 by the University to support the Air Quality Group research efforts. It is located adjacent to Crocker Nuclear Laboratory. It consists of two separate areas: the administrative area and the sample handling laboratory.

The sample handling laboratory consists of 690 square feet for general handling and a separate 140 square feet for specialized gravimetric and absorption activities. The areas are climate controlled and entry is situated such that there is no pass through foot traffic. Entrance to both areas requires that passage be made over a sticky floor mat material to capture dust and foreign particles. The laboratory area floor and work surfaces are vacuumed daily with a high efficiency HEPA cleaner.

The specialized gravimetric area is equipped with electrostatic control mat surfaces. A double ended voltage regulator system provides stabilized voltage to the LIPM laser power supply and programmed controllers turn equipment off and on to provide for stabilized operations.

The general handling area is subdivided into work station locations to support receiving and shipping operations, sample tracking, download, upload, leak check and data entry activities. Provisions for communication with sample operators and reference to their the MDL's for S, K, Fe, Pb, and Se are about 4 ng/m^3, 1.5 ng/m^3, 0.4 ng/m^3, 0.5 ng/m^3, and 0.06 ng/m^3, respectively, for a typical analysis. For increased costs these detection limits can be further reduced by longer exposure in the proton beam. In addition, PIXE is non-destructive. Therefore, a sample can be archived and re analyzed if necessary. This will provide a quality control factor and an opportunity to pursue future concerns. PIXE has gone through a formal interlaboratory intercomparisons with other similar elemental analysis techniques. Table 2 gives the result on one of the intercomparison.

Table 2. Results of formal interlaboratory intercomparisons-ratios to standards

Method	Number of groups reporting data[a]	Solution standards[b]	Rock standards[c]	Aerosol standards[d]	Aerosol samples[e]
PIXE	7	1.03±0.16	0.99±0.29	0.99±0.19	0.98±0.08;1.01±0.16
XRF	8	0.97±0.12	1.07±0.20	1.03±0.14	0.97±0.08; 1.08±0.15
λ-XRF	3	1.19±0.34	1.12±0.47	1.37±0.50	--
AA,ES[h]	3	0.88±0.17	0.40±0.31	0.47±0.29	1.04[f],0.84[g]
ACT	--	--	--	--	0.76±0.15[g]
NAA	1	0.97±0.08	--	--	--

[a] Camp et al 1974; each result represents the mean and standard deviation from all laboratories using the method for all elements

[b] Two samples, each including Al, S, K, Mn, Fe, Zn, Cd, and Au

[c] Two samples, each including Al, Si, K, Ca, Ti, Mn, and Fe.

[d] Two samples, each including Al, Si, S, K, Ca, Ti, Mn, Fe, Cu, Zn, Se, Br, and Pb

[e] Camp 1979; three samples or more, including up to 20 elements, of which S, Ca, Ti, Fe, Cu, Zn, Se, Br, and Pb are intercompared. Each result represents a single laboratory with the result being the mean and standard deviation for each element as compared to the referees.

[f] Laboratory reported S and Pb only.

[g] Laboratory reported S only

[h] Atomic absorption; emission spectroscopy.

PESA uses the proton scattering during PIXE analysis to quantify hydrogen in the deposit on the Teflon filters (DRUM stage after-filter and fine filter) (Cahill et al., 1987). Due to the hydrogen content of Mylar substrates, PESA is not applicable to these substrates. Hydrogen by PESA is a convenient and inexpensive means of determining the organic mass collected on a Teflon filter. After the hydrogen associated with components such as ammonium sulfate is removed, the remaining hydrogen is an excellent means of calculating the organic mass. For sites in the western United States the correlation of organic mass by hydrogen and organic mass by carbon is excellent. A correlation coefficient of 0.89 and a slope of 0.98 is typical. Figure 6 is an example of organic mass by hydrogen (OMH) versus organic mass by carbon (OMC) at Yosemite National Park. An advantage to using OMH is that its precision is much better than that for OMC during periods of low organic mass, particularly in the winter.

Using several basic assumptions (such as assuming an oxide state for soil elements, and elemental sulfur as ammonium sulfate) the summation of the analyzed components will reconstructs the gravimetric mass.

made at the time of data processing. A schematic of the system is given in Figure 5. Light of 633 nm wavelength from a He-Ne laser is diffused and collimated to provide a uniform beam of light of approximately 0.7 cm^2 at the sample. The light transmitted through the sample is collected with an Oriel 7022 photodiode detection system. The decrease in light intensity is provided by both absorption and large-angle scattering. (Light undergoing small angle scattering will be collected by the detector.) The blank Teflon filter does not absorb light, but it does scatter light: therefore, it is necessary to measure the transmission of the blank filter. For the particles on the filter, the absorption is the primary cause of decrease in light intensity, with only a small amount of scattering.

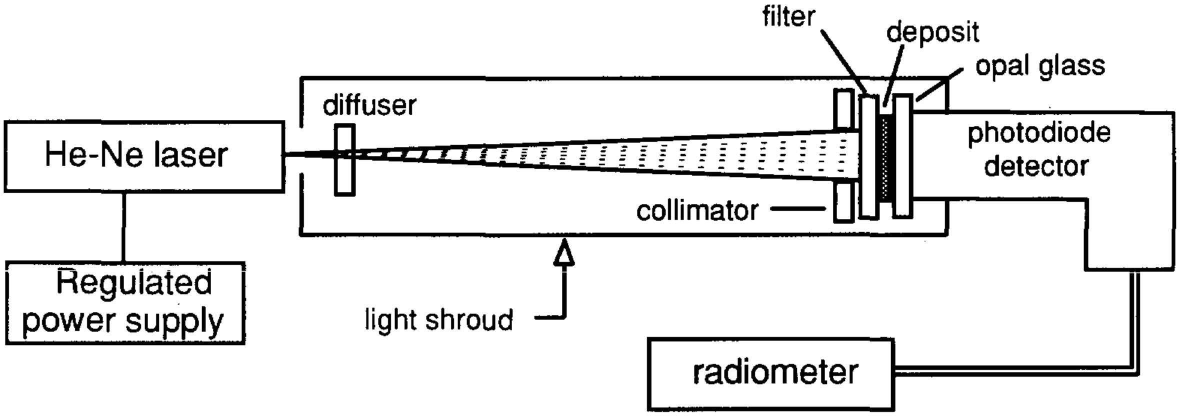

Figure 5. Setup of UCD Laser Integrating Plate Method apparatus.

For quality assurance, the laser is allowed to warm-up for a duration of at least one hour to allow it to stabilize. After warm-up, 10 standard filters are checked once a day to determine if there is any drift of the laser or detector.

2.2.3 Elemental Analysis

At Crocker Nuclear Laboratory at UC Davis the Teflon filters and the Mylar drum strips will be analyzed by PIXE. In addition, the Teflon filters will be analyzed by PESA and XRF. In PIXE analysis a beam of 4.5 MeV protons is directed onto the filter. The excitation of the atoms of the deposit produces x-rays characteristic of the elements in the deposit. The x-rays are quantified to describe the quantity of each element (from sodium to lead) that was collected (Cahill, 1986).

2.2.3.1 PIXE (Proton Induced X-ray Emissions)/PESA (Proton Elastic Scattering Analysis)

PIXE has several advantages for particulate analysis. All elements from sodium to lead can be quantified in a single analysis. The analysis is rapid and inexpensive. Using PIXE, in conjunction with XRF, the detection limits for our analysis are very low; for example

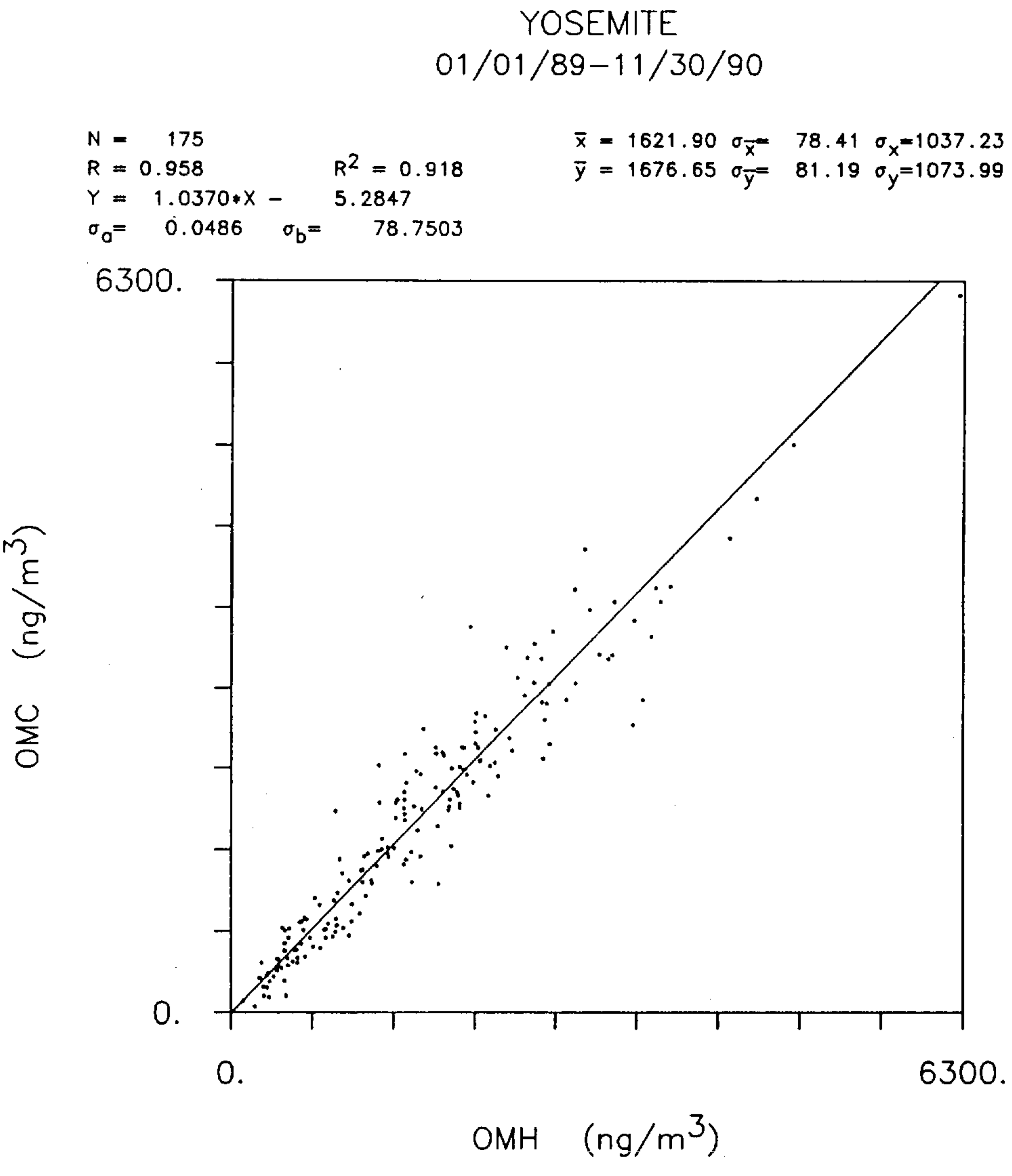

Figure 6. Organic mass calculated from carbon by combustion (OMC) and organic mass calculated from hydrogen by PESA (OMH) at Yosemite National Park, Turtleback Dome, IMPROVE site. Hydrogen from IMPROVE Channel A, carbon from IMPROVE Channel C.

The requirement that the Teflon filters be analyzed for all elements from sodium to lead non-destructively limits the methods to one of several energy-dispersive x-ray techniques, of which the major types are Particle Induced X-ray Emission (PIXE) and X-ray Fluorescence (XRF). The two methods are similar, differing primarily in cross-section, background and analytical area. The accuracy of the two methods both depend on the accuracy of the elemental standards, available through commercial vendors and the National Institute of Standards and Technology (NIST).

PIXE is able to measure all elements from sodium to uranium in a single spectrum, while XRF requires multiple measurements using incident x-rays of different energies. The advantage for PIXE is that this avoids erroneous calibrations for portions of the element list. In general, XRF systems have more difficulty analyzing elements below sulfur than do PIXE systems.

The uniformity of the cross section for PIXE is also a disadvantage, because it does not permit maximizing the sensitivity for selected trace elements without long and expensive analyses. We were able to improve the sensitivity for elements heavier than Fe by adding a second PIXE detector, but the gain was not enough to measure Se routinely. XRF has a lower minimum detectable limit (mdl) for a range of elements with absorption energies slightly below that of the incident x-rays. Thus, to maximize the system for elements in the region of Se, the incident x-rays should be produced by an Mo anode.

The protocol that we have now developed for the normal UCD analysis is to combine the strengths of the two methods, using PIXE for the lighter elements (below Fe) and for overall normalization, and XRF for the elements Fe to Pb. The samples are first analyzed by XRF for Fe-Pb. They are then analyzed with the PIXE/PESA system for H and Na-Pb. The comparison for overlapping elements is then part of the Quality Assurance protocols, providing increased quality control.

There are several advantages of this hybrid method over a PIXE-only or XRF-only system. An advantage over a PIXE-only system is the ability to lower mdl's for a range of elements at a reasonable cost. An advantage over an XRF-only system is the ability to perform other measurements concurrently using the accelerator beam. We have been measuring hydrogen using Proton Elastic Scattering Analysis (PESA) since 1984.

PIXE whenever the XRF configuration was changed. The system calibration was verified using 20 elemental standards at the beginning of the session and a tray of filters from a previous session was re analyzed. Again the analysis was performed only after the precision requirements were met. The calibration is periodically checked throughout the session. At the end of the session, the standard and re analysis trays are reanalyzed. After the PIXE run is completed, the XRF and PIXE values are compared. Figure 8 shows a drawing of the XRF system.

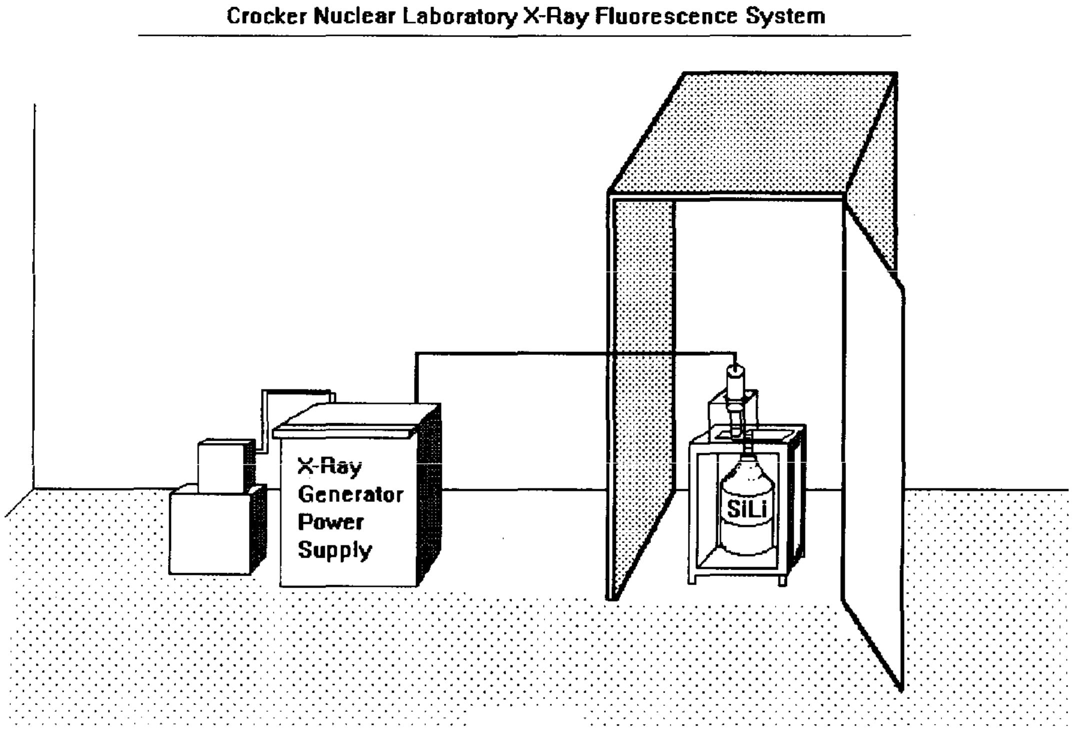

Figure 8. X-ray Fluorescence System

2.2.4 Soluble Species Measurements

The impregnated filters and nylon filters will be obtained from Desert Research Institute of Reno, Nevada (DRI). DRI will provide the filters, analysis, and analytical quality control. They will analyze extracts from the citric acid impregnated cellulose filters for NH_3 and extracts from the TEA impregnated cellulose filters for NO_2 by automated colorimetry. Extracts from the potassium carbonate impregnated cellulose filters will be analyzed for SO_2 and extracts from the nylon filters will be analyzed for NO_3^- by ion chromatography. Extracts from the nylon filters will also be analyzed for NH_4^+ by automated colorimetry.

An additional advantage over an XRF-only system is in throughput. We can rapidly increase the number of samples without overloading either the single-anode XRF or PIXE system. XRF requires 5 to 15 times the analysis time. We can quickly triple the throughput when necessary.

The concurrent analyses by Particle Induced X-ray Emission (PIXE) and Proton Elastic Scattering Analysis (PESA) provided 70% of the concentrations in the database. The system was calibrated using a set of 30-40 commercial and National Institute of Standards Technology (NIST) elemental standards whenever the system configuration was changed. The system calibration was verified using 20 elemental standards at the beginning of the session and a tray of filters from a previous session was reanalyzed. Scatter plots of the major elements were prepared and checked for consistency. If the calibration and re analysis were within the accepted 4%, the regular analysis was allowed to proceed. At the end of the session, the standard and reanalysis trays were re analyzed. Figure 7 shows a cross-section of the analysis chamber used in typical PESA/PIXE set-up.

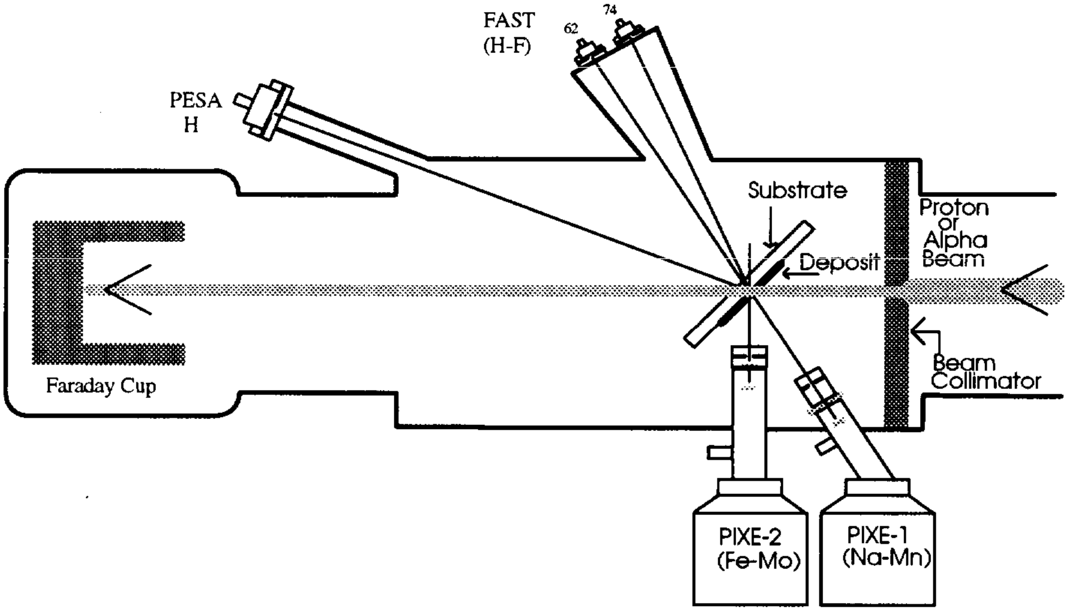

Figure 7. Diagram of PIXE/PESA system

2.2.3.2 XRF (X-ray Re-Fluorescence)

X-ray Re-Fluorescence (XRF) was added to the routine network analysis beginning with samples collected in June 1992. We use a single Mo anode, which is optimal for elements in the region of selenium. This permits us to reduce the sensitivity of a selected range of elements while retaining the reliability of PIXE for the overall range of elements. Using XRF for the heavier elements also allows us to reduce the time of the PIXE analysis. The XRF system was calibrated using the same set of 30-40 elemental standards as used by device is returned to Davis with the completed data sheet. If there is a discrepancy, the measurement is repeated.

Site visits will be made by UCD personnel in order to (1) clean and refurbish the sampler, (2) perform a complete flow rate calibration, (3) make any predetermined modifications of the sampler, and (4) discuss protocols with the operator. The field person will follow the standard operating procedures for field maintenance. All results from the site visit will be retained in the file folder for that site. This includes a summary of the visit, a check list of the maintenance, a description of all changes made, and the results of the flow rate calibration. A key part of the maintenance is to detect any potential problems with the pumps before they produce any loss in data. (With the critical orifice system the pumps can lose efficiency and still maintain the proper flow.) Records of pump replacements and maintenance are also retained in a folder for each site. In preparation for a site visit, the UCD field person will review the history of the flow rate and the history of the operations using the site operations data base. The field person will prepare time plots of both flow rate measurements made with every sample, and time plots of sulfur measured by PIXE and Ion Chromatography. The field person will review the site with the quality assurance manager and with the sample handling manager. The field person will discuss any problems with the site operator via telephone. The first step in the field maintenance will be to perform a four-point calibration of the modules prior to any modification. This will be compared to the previous calibration constants. After the maintenance is completed, another four-point calibration of the sampler will be performed. If the field person is not returning immediately to Davis, the calibration constants will be sent via FAX to Davis for inclusion in the data base. After returning the Davis, the field person will update all hard copy and data bases and discuss the results with the quality assurance manager. The field manager will maintain documentation on all flow calibrations for all audit devices. The field manager will also document all external audits and maintain a site document with position, elevation, and photographs.

2.3.2 Sample Handling

Any major changes in the sample handling procedures will be presented to the Air Quality Group steering committee before implementation. The sample handling manager will be responsible for maintaining the computer and hard copy documentation on sample handling procedures. Any revisions will be made in the Sample Handling SOP document and summarized in the SOP revisions file organized by date. These files will be available to all personnel, including the quality assurance manager and project manager.

All new personnel will be trained by the sample handling manager. The new personnel are expected to become familiar with the written standard operating procedures. The sample handling manager will train all personnel when procedures are revised. After training, the sample handling manager will supervise the processing of sample modules to and from the field.

2.3 Quality Assurance

2.3.1 Sampler Maintenance and Sample Collection

Flow audit devices are used during installation, site visits, and mail audits. They consist of a plug with a calibrated orifice that fits into the sampler inlet and a magnehelic. The device is calibrated at Davis using the UCD standard spirometer and dry gas meter apparatus. The spirometer is the primary reference standard, while the dry gas meter provides verification. A four-point calibration is made of the audit device and calibration constants adjusted to 20°C. (The magnehelic readings are regressed against the spirometer flow rates for four flow rates covering the range to be used.) The calibration constants are written on the audit magnehelic, retained in hard copy in file folders, and stored in a data base of audit devices and parameters. In addition to the calibration magnehelic, the flow rates are also checked with a Sierra Top Track Mass Flow Meter. The Mass Flow Meter is also measured against the UCD standard spirometer and dry gas meter apparatus. The calibrations are repeated before and after site visits and mail audits.

The flow rate of the sampler will be set and calibrated at Davis using the UCD site-simulation facility that consists of the UCD standard spirometer and dry gas meter apparatus, and an extra pump with manometer. The ambient pressure is simulated using the pump and manometer. The critical orifice for each module will be adjusted for the filter type and site elevation. The input data, calibration constants and nominal flows will be saved in the sampler folder for that site and entered into the flow rate database. Entries in the calibration data base are never deleted, providing a history of sampler calibrations. If the sampler is installed by UCD personnel, a one-point calibration of the flow rate will be performed. If the results do not agree with the Davis results, a four-point calibration will be done and compared to the Davis results. If necessary, the critical orifice will be adjusted and the new nominal flow rate determined. A hard copy of the results will be stored in the sampler folder for that site. Any revised calibration constants and nominal flows will be saved in the flow rate data base file with the current date. If the sampler is installed by other than UCD personnel, a one-point calibration of the flow rate will be performed by the installing personnel. If the results do not agree with the Davis results, and a reason for the discrepancy cannot be determined, a site visit will be made by UCD personnel. A site description for the site will be prepared using the standard site form. A standard set of photographs of the sampler and environment will be obtained and stored in the folder for the site. The site operations data base includes all significant events for the site including installation date. The data base can be organized by site, by date, by outstanding problems. An entry is made whenever a problem occurs and when it is resolved.

A mail audit or a field audit (by UCD personnel) will be performed every six months. In a mail audit, an audit device and a detailed description of the protocol is mailed to the operator. The results are phoned back to Davis. If the results indicate no discrepancy, the mean and standard deviation of the controls will be calculated and recorded. A table of historical monthly means and standard deviations for reweight and controls will be maintained.

2.3.4 Laser Integrating Plate Method Analysis (Absorption)

The sample handling manager will be responsible for training all new personnel in the operation of the laser system and in the standard operating procedures. The sample handling manager will also be responsible for training all personnel when the procedures are revised.

The laser system will be cleaned and calibrated once each working day, at 0800. The system will be calibrated to give an intensity reading of 750 when there is no sample. A tray of standard filters will be measured and recorded in the laser log. If there is a discrepancy for any standard, the calibration is repeated. After every fifth filter, the intensity with no filter is checked. If the reading is not 750, the laser output is adjusted.

Documentation will be maintained for calibration of the laser system and for the results from the set of standard filters.

2.3.5 PIXE/PESA Elemental Analysis

The PIXE manager will be responsible for training all new personnel in the standard operating procedures. The PIXE manager will also be responsible for training all personnel when the procedures are revised.

A set of analysis instruction files is prepared from the computer files derived from the field log sheets. These files include flow rates, durations, volumes, volumes per unit area, and level I validation flag. The instruction file includes a skip if the sample has been invalidated. At the same time that the instruction files are prepared, a hard copy analysis sheet is prepared and printed. This is to be used for notes and documentation during analysis. The physical sample trays are compared to the analysis sheets to verify that no valid samples are omitted. The analysis sheets are reviewed by the PIXE manager to verify that the volumes per unit area are all within limits.

The PIXE system is given a complete calibration whenever the system is changed, such as a new detector or a change in detector geometry. This requires analysis of a complete set of elemental standards from a commercial source (Micromatter, Inc.) and from the National Institute of Standards and Technology. The Micromatter standards have a nominal precision of ± 5%, but by using a wide range of standards and smoothing the results, the calibration values are better than that for any single standard. All PIXE analyses are calibrated by this smoothed fit to multiple standards. All the Teflon filter samples from a single season in the MSAM network would be analyzed in one single

Upon receiving the sample module from the field, the field log data is entered into the data base. If a 10% discrepancy with nominal or difference between initial and final readings is obtained, a message is displayed. The data entry person verifies the entry; if the problem remains, the problem is recorded in the site operations data base. The sample handling manager has the option of invalidating the sample. In this case, the filter is archived but not analyzed. If it is allowed to pass, the quality assurance manager will review the results after the analysis of the filter is completed.

Documentation will be maintained describing (1) status of all filters in the sample handling process, including shipment and receipt of the sampler modules to and from the site; (2) shipment of filters to cooperating laboratories; (3) efficiency of sample collection at each site; (4) identification of all invalidated samples and reasons for invalidation; and (5) telephone communications with site operators and cooperating laboratories. The laboratory staff will also interact with the site operations data base. When problems are noted, an entry will be made. If the problem cannot be solved immediately, the unresolved flag will be set. Documentation of all computer programs used in sample handling and data entry will be maintained. Any revisions will be indicated and dated.

The sample handling manager will be responsible for archiving all Teflon filters before and after elemental analysis. For the first year, these will be stored in standard slide trays. After one year, samples will be stored in a more compact form in special containers. Samples are always available for possible reanalysis.

2.3.3 Gravimetric Analysis (Mass)

The sample handling manager will be responsible for training all new personnel in the operation of the microbalance and in the standard operating procedures. The sample handling manager will also be responsible for training all personnel when the procedures are revised.

The microbalance(s) will be cleaned and calibrated twice each working day, at 0800 and 1300. The balance will be calibrated using a class 1.1 (formerly class M) standard. A standard weight with a mass similar to a Teflon filter will be measured and recorded and plotted with previous values. If there is any discrepancy, the calibration is repeated. Two blank filters will be measured, one measured one month earlier and stored in a cassette, and the other a new blank filter. The same two filters are measured in both calibrations for every analysis day.

Documentation will be maintained for the class 1.1 and standard weight for each calibration. This log will also record the relative humidity. The differences between the 0800 and 1300 measurements of the blank filters will be recorded. This is denoted 'reweight'. Each month the mean and standard deviation of the reweights will be calculated and recorded. The difference for a given filter for the first measurement and the measurement one month later will be recorded. This is denoted 'control'. Each month the

2.3.6 XRF High Sensitivity Elemental Analysis

The PIXE manager will be responsible for training all new personnel in the standard operating procedures for the UCD XRF system. The PIXE manager will also be responsible for training all personnel when the procedures are revised.

The XRF system uses the same instruction files as the PIXE system. A separate set of analysis sheets is prepared.

The XRF system is given a complete calibration whenever the system is changed, such a new detector or a change in detector geometry. This consists of a set of elemental standards from a commercial source (Micromatter, Inc.) for elements to be observed in the XRF analysis. The XRF system calibration is checked at the beginning of each working day using a subset of the 25 PIXE standards this is followed by a reanalysis of tray that was analyzed during the previous run. The ratio of measured to nominal values for the standards are calculated and recorded. The calibration is considered acceptable if the standard deviation is less than 5%. The cross sections in the table are renormalized to force the mean ratio to be 1.0. If the conditions are not met, the system is checked for problems. The concentrations from the reanalysis procedure are compared to the concentrations determined during the previous analysis. When the calibration is acceptable, a set of blank Teflon filters is analyzed to determine the signal-to-noise ratio for the XRF spectra. Following the PIXE analysis of these samples, scatter plots of S, Fe, and Zn for XRF vs. PIXE are prepared and examined. If necessary, the XRF values are renormalized so that the slopes are near 1.0. If there are further discrepancies, the XRF calibration is reviewed and some of the samples are reanalyzed by XRF.

Technicians will periodically monitor the data acquisition and analysis. The acquisition check involves verifying that the identification of the sample, as read by a remote video monitor, agrees with the computer identification.

Documentation will be maintained for the calibration, including standards, reanalysis plots, calibration tables, and renormalization values. The analysis sheets will be archived. Documentation containing the computer codes and any revisions will be maintained.

2.3.7 Data Processing: Determination of Artifacts and Precision

Calculations for artifacts are determined from the field blanks' means and standard deviations. They will be produced during a given season and compared to historic values by plotting the field blanks as a function of time. Any variations from historic values will be investigated for each site. If there are any significant differences with the means of the field blanks, the problem is researched. If no differences are found, the mean of the field blank is incorporated with all data as an artifact. The minima and 1% values of the raw ambient masses per filter will be determined and compared to the field blanks. In the assumption that the ambient concentrations go to zero 1% of the time, the 1% values analytical session and all the impactor samples in another. This permits better quality control of the data. The PIXE/PESA system calibration is checked at the beginning of the analytical session. The calibration consists of (1) analyzing a set of 25 PIXE standards (Mg, Al, Si, GaP, CuS, K, Ca, V, Cr, Mn, Fe, Ni, Zn, Se, CsBr, Sr, CdSe, Au, and Pb); (2) analyzing a set of clean Mylar PESA standards; (3) analyzing a tray of samples from the previous MSAM analytical session. In step (1), the ratio of measured to nominal values are calculated and recorded. The calibration is considered acceptable if the mean ratio is between 0.90 and 1.10 and the standard deviation is less than 5%. The calibration curves are renormalized to force the mean ratio to be 1.0. If the conditions are not met, the cyclotron beam tune and electronics are checked for problems. When the system is corrected, the standards are reanalyzed. The mean from step (2) is used to define the hydrogen calibration. The concentrations from step (3) are compared to the concentrations determined during the previous analysis. Regression plots for H, S, Fe, and Zn are prepared and examined. If the slopes differ significantly from 1.0, or the measured differences are significantly different than the calculated precisions, the calibration and analytical systems are reviewed. The analysis of regular samples can proceed only after the quality assurance manager validates the calibration. When the calibration is acceptable, a set of blank Teflon filters is analyzed to determine the signal-to-noise ratio for the PIXE and PESA spectra. The PIXE/PESA system calibration, including reanalysis procedure, is repeated at the end of the analytical session and at any time when a system shift is suspected. Any discrepancies must be reconciled by the quality assurance manager before the samples are allowed to pass level I validation.

Technicians monitor the data acquisition and analysis through the session. The acquisition check involves verifying that the identification of the sample, as read by a remote video monitor, agrees with the computer identification. The cyclotron operator is provided with real time detector counting rates, and the upper and lower limits allowed. The technician will also monitor the detector counting rates, and inform the cyclotron operator if the upper or lower limits as specified on the data sheet are exceeded. If the data acquisition time routinely exceeds the preset time, the technician will determine the reason, and have the cyclotron operator increase the beam intensity. The technician will also monitor the detector saturation levels, and have the cyclotron operator reduce the beam intensity if either saturation is over 45%. The technician will monitor the ratio of Fe concentrations of the two detector systems. (The UCD PIXE system has two detectors, one optimized for elements below Fe and one for elements above Fe.) This ratio is displayed on the data analysis screen for each sample. The technician will periodically record this value on the analysis sheet. The technician will contact the senior staff scientist on call if this ratio exceeds 1.10 for peaks with adequate statistics.

Documentation will be maintained for the calibration, including standards, reanalysis plots, calibration tables, and renormalization values. The routine hard copy output of the data acquisition and analysis programs will be archived. This includes live times and other parameters. The analysis sheets will be archived. Documentation containing the computer codes and any revisions will be maintained.

2.4 Accuracy and Precision

2.4.1 Artifact

Artifact is defined as any increase or decrease of material on the filter that positively or negatively biases the measurement of ambient concentration. The five major types of artifact are

- contamination of the filter medium;
- contamination acquired by contact with the cassettes or in handling;
- adsorption of gases during collection that are measured as particles;
- volatilization during collection and in handling;
- fall-off during handling after collection.

The first three are positive artifacts and the last two negative. The first contamination artifact is determined by analysis of laboratory blanks. The sum of the two contamination artifacts is determined by analysis of dynamic field blanks (DFB's). These are handled as normal filters, except that no air is drawn through.

We do not correct for the two negative artifact types, volatilization and fall-off. The measured low temperature organics may be much less than in the atmosphere because of volatilization of particles during the remainder of the sampling. We assume that any volatilization of nitrate and chlorine from nylon is not significant. The fine mass on the Teflon filter will underestimate the ambient mass concentrations in high nitrate areas because some nitrates collected on Teflon will volatilize.

2.4.2 Verification by Distributions

The blanks may not always provide reasonable values for the artifact. In order to verify an estimate from field blanks, we examine the distribution of values for ambient samples in two ways. We first examine the minimum of the ambient values for a large set of samples. If we can reasonably assume that the ambient mass of a given variable is occasionally much less than the artifact, then the minimum measured values of the ambient samples should equal the artifact. To avoid statistical problems, we often examine the 1% level, rather than the actual minimum.

We also examine the intercepts of regression plots of the variable with concentrations of related variables that have no problems with artifact subtraction.

should approximately equal the artifact value. On the basis of the above data, the best artifact and standard deviation are determined for each measured parameter.

The relative precisions are plotted for each replicate pair against the mean. (The relative precision is the absolute difference times 0.7 divided by the mean.) The relative precision for large means will be compared with the current estimate of relative analytical mean. (For small means the replicate precision will be affected by any constant uncertainty. The constant portion is reflected in the standard deviation of the field blanks and should not be included twice.) Unless there is a significant change, the current value is retained.

All calculations for artifact and precision determinations will be included in files arranged by season and parameter type, including all plots. The artifact and precision values are stored in data bases for access by the data processing programs and scientific personnel. A document containing computer codes with any revisions will be maintained.

2.3.8 Level II Validation

In Level II validations, the following linear correlation plots are created for each season:

3S vs. SO_4 for each site
3S vs. SO_4 for all MSAM sites

- 3S from DRUM vs. 3S from Teflon Filter for each site
- 3S from DRUM vs. 3S from Teflon Filter for all MSAM sites
- 3S from DRUM vs. SO_4 from ion chromatography for each site
- 3S from DRUM vs. SO_4 from ion chromatography for all MSAM sites
- fine mass vs. reconstructed mass for each site
- fine mass vs. reconstructed mass for all MSAM sites
- fine mass vs. hydrogen for each site
- fine mass vs. hydrogen for all MSAM sites
- denuded nitrate vs. total nitrate for each site
- denuded nitrate vs. total nitrate for all MSAM sites

Investigations of any discrepancies between the sulfur-sulfate are determined by plotting the two species and verifying that the slopes are 1.0 and identifying any outlying pairs. The outliers are researched to determine if there is reason for the discrepancies and the sample is either corrected or invalidated. The same is done in the other species for both intra laboratory checks and inter laboratory comparisons. When an anomalous point is encountered, time plots are also produced for both variables on the same plot to help determine which point disagrees with nearby values.

The quality assurance manager will prepare a summary of the level I and level II validation results and present them to the Air Quality Group steering committee. If acceptable, the data will be considered validated. The data and the hard copy summaries will be sent to the contract representative. After 6 months the data will be made available to the public via network connections. Any corrections noted by the UCD scientific staff and the contract representative's staff should be made during this 6-month period.

The precision in the average flow rate has two components: the precision in the measured values and the uncertainty in assuming that the average flow rate during collection equals the average of the flow rates measured before and after collection. The precision in a measured value is less than 3%, as estimated from internal and third-party audits. Most audits indicate that the total precision/accuracy of the difference between an audit and an MSAM measurement is approximately 3%. Since the precisions of most audit devices are 2-3%, the MSAM flow rate precision must be less than 3%.

The second component of the precision is present because all flow control devices introduce uncertainty. A critical orifice device is extremely reliable, avoiding large errors at extreme temperatures, but does allow small variations in flow rate with temperature. A difference in average temperature during the sampling period from the average temperatures before and after collection will produce an incorrect value of flow rate. If the 24-hour mean temperature were 10°C higher than the average of the two measured temperatures, than the error in average flow rate would be 2%. We allow such unusual conditions by using a conservative value for the precision in the volume of 3%. This value has been used in all calculations for the MSAM and IMPROVE samplers. Calculating site-specific or seasonal precisions would complicate the calculations without significantly changing the overall precision estimate of the concentrations.

2.4.6 Analytical Precision

1. Counting Statistics

There will be uncertainty associated with counting statistics whenever the measurement is based on the number of counts from a detector. Gravimetric and LIPM analyses do not involve counting statistics. We are not provided the information on counting statistics for ion chromatography and automated colorimetry. Counting statistics are generally negligible for ion chromatography and automated colorimetry. However, the statistical precision must be included for PIXE, XRF, and PESA because of a relatively large background in the spectra and the absence of direct artifact subtraction. This will be discussed in more detailed in the section on PIXE.

2. Nonstatistical Analytical Precision

For simplicity we will assume that the nonstatistical component of the analytical precision may consist of a constant mass/filter (σ_a) and a constant fraction (f_a). Theory indicates that some methods, such as gravimetric analysis, have only a σ_a component. The constant fraction form (f_a) is appropriate for uncertainty associated with normalization and calibration. In x-ray systems, f_a represents the uncertainty in normalizing each analysis to an incident beam intensity. In ion chromatography f_a includes the precision in preparing an aliquot. X-ray methods have only a f_a component. For ion chromatography and carbon combustion we will assume both components are present.

2.4.3 Definitions of Variables

Variables calculated prior to sample measurement:
B = artifact mass (ng/filter) = mean of the DFB's or secondary filters
σ_{dfb} = standard deviation of the DFB's used to determine B
σ_a = component of analytical precision that is a constant mass per filter.
f_a = component of analytical precision that is a constant fraction.
f_v = fractional volume precision = fractional flow rate precision

Variables measured or calculated with each sample:
A = mass measured on real sample (ng/filter)
V = volume (m^3)
area = area of deposit on the filter (cm^2) , determined from the mask size
f_s = analytical precision associated with counting statistics, expressed as fraction
c = concentration (ng/m^3)
$\sigma(c)$ = precision of c (ng/m^3)

2.4.4 Concentration

The mass of material on the filter is equal to the difference between the mass measured on the sample and the artifact determined from field blanks filters. The concentration equals this number divided by the volume:

$$c = \frac{A - B}{V} \tag{1}$$

2.4.5 Volume

The volume is the product of the average flow rate and the sample duration. The sample duration is determined using an elapsed time indicator based on line frequency. The actual time of start and stop is determined by the field operators replacement of the MSAM filter pack. The fractional precision of the volume is the quadratic sum of the fractional precisions of flow rate and duration. Since the fractional precision of the duration is always much smaller than that of the flow rate, it can be safely neglected.

The flow rate is measured before and after the collection each using two independent methods. The first method measures the pressure drop across the cyclone using a magnehelic and employs the standard measuring orifice equation. The second method uses an inline mass flow meter at the laboratory. The average flow rate is normally an average of mass flow rates before and after collection. If the mass flow readings are determined to be in error, then the magnehelic measurements are used.

Thus, the precision in the difference (A-B) is equal to the standard deviation in the DFB's

$$\sigma(A\text{-}B) = \sigma_{dfb}\,. \tag{6}$$

The precision in the concentration may be written as

$$[\sigma(c)]^2 = \left(\frac{\sigma_{dfb}}{V}\right)^2 + (f_v{*}c)^2. \tag{7}$$

We define the minimum detectable limit as the concentration that is equal to 2σ. The exact expression is given by

$$\mathrm{mdl} = \left(2\frac{\sigma_{dfb}}{V}\right)\left(\frac{1}{\sqrt{1-4f_v^2}}\right). \tag{8}$$

The right- term equals 1.002 for f_v=0.03. The difference from 1.00 is negligible compared to the uncertainties in σ_{dfb} and V. We will use the simpler expression

$$\mathrm{mdl} = 2\frac{\sigma_{dfb}}{V}\,. \tag{9}$$

2.4.8 PIXE, XRF, and PESA Analysis

In PIXE, XRF, and PESA, the spectral background for a sample is estimated using a spectrum of a blank Teflon filter. This procedure removes any contaminants, if present. These spectra of blank filters indicate that any elemental artifact is extremely small. Therefore the concentration is calculated using B=0. We use a variation of Equation 1, because PIXE, XRF, and PESA determine mass per unit area rather than mass per filter. This areal density in ng/cm^2 is proportional to the number of counts in the peak, with the proportionality factor depending on the element, the number of protons, and the detector live time. The spectral analysis program is provided the ratio of deposit area divided by sample volume. The concentration is calculated using

$$c = k * N * \frac{\mathrm{area}}{V}\,, \tag{10}$$

where area is the area of deposit on the filter, N is the number of counts in the peak, and k is a constant depending on the element, the number of protons, and the detector live time.

None of the three methods have a constant component to the precision, so that σ_a=0. All have constant fractional components, (f_a), associated with normalizing to the incident beam. The value of f_a is measured every analytical session using replicate analyses for elements with negligible statistical precision. It has never varied significantly from 4%. We have maintained a constant value of f_a=0.04 in the data processing since 1988.

Measurements by all three methods have a statistical component to the precision, (f_s), based on the number of counts in the peak and in the background under the peak. Assuming a Poisson distribution, N counts in the peak, and N_b background counts under the peak, the fractional statistical precision is given by

$$f_s^2 = \frac{1}{N}\left(1+2\frac{N_b}{N}\right). \tag{11}$$

The precision of the concentration is given by

$$[\sigma(c)]^2 = c^2 * (f_s^2 + f_a^2 + f_v^2)\,. \tag{12}$$

The precision is calculated separately for each variable at the time of spectral analysis using f_a=0.04 and f_v=0.03. The quadratic sum of these two is 0.05. At small concentrations the statistical term is dominant, while at large concentrations the precision approaches 5%. For sulfur, the average precision for all sites and seasons is slightly larger than 5%.

The minimum detectable limit for each PIXE variable is calculated from the background in the spectrum at the location of the peak and the relationship between counts and concentration for that peak. The mdl is defined as the concentration at which the number of valid counts equals 3.3 times the square root of the background counts under the peak. The mdl defines the lower limit that a variable can be reliably observed in the spectrum, although it is possible to find peaks with concentrations slightly below the mdl. At the mdl, the analytical precision is approximately 50% of the mdl. The mdl is calculated separately for each variable at the time of spectral analysis.

2.4.9 Ion, SO_2, and NH_3 Analysis

The equations for these three methods are the same, except for SO_2, where the concentrations are multiplied by 2/3 to convert from SO_4 to SO_2. The methods are characterized by significant artifact and unknown statistical precision.

The standard deviation of the DFB's includes the precision in the artifact and the analytical precision. (As in the case of gravimetric analysis, we do not equate the precision in the artifact with the standard deviation of the DFB's.) The standard deviation is a quadratic sum of the precision of the artifact B, the constant analytical precision, and the fractional analytical precision:

$$\sigma_{dfb}^2 = [\sigma(B)]^2 + \sigma_a^2 + [f_a * B]^2. \tag{13}$$

The precision of the mass/filter of the sample is

$$[\sigma(A)]^2 = \sigma_a^2 + [f_a * A]^2. \tag{14}$$

The precision of the difference (A-B) is obtained by quadratically adding the precisions of A and B,

$$[\sigma(A-B)]^2 = [\sigma(A)]^2 + [\sigma(B)]^2. \tag{15}$$

The precision of the concentration is therefore given by

$$[\sigma(c)]^2 = \left[\frac{\sigma(A-B)}{V}\right]^2 + [f_v * c]^2 = \left[\frac{\sigma(B)}{V}\right]^2 + \left[f_a * \frac{A}{V}\right]^2 + [f_v * c]^2 . \tag{16}$$

This can be written in terms of the constants as

$$[\sigma(c)]^2 = \left[\frac{\sigma_{dfb}}{V}\right]^2 + \left(\frac{2B}{V}\right) * f_a^2 * c + \left(f_a^2 + f_v^2\right) * c^2 . \tag{17}$$

Note that the constant analytical precision, σ_a, does not appear in Equation 17. This portion of the precision is included indirectly in σ_{dfb}.

For small c, the first term in Equation (17) is dominant, while for large c, the third term is dominant. The second term is never dominant; the maximum contribution for most parameters is less than 10%.

The minimum detectable limit is defined as the concentration that is twice the precision. Solving Equation 17 for the concentration gives

$$\text{mdl} = \left(2\frac{\sigma_{dfb}}{V}\right)\left(\frac{\sqrt{1-h-g}+g}{1-h}\right) , \tag{18}$$

where

$$g = \left(\frac{2B}{\sigma_{dfb}}\right) f_a^2 \qquad h = 4(f_a^2 + f_v^2) .$$

Retaining the second order terms would increase the estimate of the mdl less than 2% for ion chromatography and automated colorimetry. The simplified form that drops second order terms is used in the data processing:

$$\text{mdl} = 2\,\frac{\sigma_{dfb}}{V} . \tag{19}$$

2.4.10 Optical Absorption

The calculation of the coefficient of absorption does not follow Equation 1. The Laser Integrating Plate Method (LIPM) system measures the absorption of particles on the filter by comparing the intensity of light at the beginning of the particle layer and the intensity at the end. The exposed side of the filter is always placed toward the detector, so that the light first passes through the filter medium. Because of the large and variable opacity from filter to filter (caused by scattering), it is necessary to measure the optical transmission before (I1) and after (I2) collection. The intensity I1 indicates the amount of light at the beginning of the particles and I2 the light after passing through the particles. In the data processing system, the absorption measured on the filter is labeled LRNC for 'laser not corrected'. (The ambient coefficient is considered a composite variable and is labeled BABS.) For area in cm^2 and volume in m^3, the equation for the uncorrected coefficient of absorption in 10^{-8} m^{-1} is

$$\mathrm{LRNC} = \left(\frac{\mathrm{area}}{\mathrm{V}}\right) 10^4 \ln\left(\frac{\mathrm{I1}}{\mathrm{I2}}\right) . \qquad (20)$$

Because of layering effects inherent in collecting particles on a filter, the absorption measured on the filter (LRNC) is less than the ambient absorption (BABS). The parameter BABS is discussed in Appendix 7.2

The precision of the LRNC is based on replicate analyses of control filters measured twice each day for several years. Define σ_i as the average standard deviation of the controls. We have used a value of $\sigma_i = 2$ units since 1988. (The intensity with no filter is set to 750 units. A typical blank filter has an intensity of 366 units.) The equation for the precision of the uncorrected coefficient of absorption is

$$[\sigma(\mathrm{LRNC})]^2 = \left(\frac{\mathrm{area}}{\mathrm{V}} * 10^4 * \sigma_i\right)^2 \left(\frac{1}{\mathrm{I1}^2} + \frac{1}{\mathrm{I2}^2}\right) + (f_v * \mathrm{LRNC})^2 \qquad (21)$$

The minimum detectable limit is defined as twice the precision in the measurement for a sample with low absorption. Although this will vary from filter to filter because of differences in initial intensity, we will use a single expression for a typical filter, setting I1=I2=366 units. The approximate expression for the mdl in 10^{-8} m^{-1} is then

$$\mathrm{mdl} = \frac{\mathrm{area}}{\mathrm{V}} * 155 \qquad (22)$$

2.4.11 Ambient Coefficient of Absorption (BABS)

BABS has an unusual position in the data base. The uncorrected coefficient of absorption, LRNC, is stored in the internal data base, but is not provided for external users. The external users are only provided with the corrected (or ambient) coefficient.

The first and smallest correction is associated with the integrating plate method. In the integrating plate method any scattering with angles large enough to miss the plate causes an increase in apparent absorption. In order to quantify the effect of the large angle scattering, a series of comparisons were made between the integrating plate system and an integrating sphere system. The integrating sphere system, is somewhat more difficult to use routinely, but eliminates the scattering component. Comparison of the results indicates that approximately 3% of the apparent absorption by LIPM is associated with scattering. The measured coefficient is therefore multiplied by 0.97.

A larger correction is associated with a shielding effect inherent with any measurement of particles on a filter. The absorption of particles on a filter is less than the ambient absorption of particles because other particles on the filter can shield a given absorbing particle. This is true for both integrating plate and sphere. To quantify the effect we made a series of measurements of the same aerosol with differing areal concentrations on the filter. The hypothesis is that the shielding factor would depend on the mass per unit area (areal density) of both scattering and absorbing particles. There are fewer absorbing particles, but the effect for them is larger per unit mass than for scattering particles. A form was chosen that included two exponents of the areal density of particles measured by gravimetric analysis in $\mu g/cm^2$. The equation used is

$$R = 0.36\ \exp\left(-\frac{\rho t}{22}\right) + 0.64\ \exp\left(-\frac{\rho t}{415}\right) \tag{23}$$

where the constants were determined by fitting data from independent studies at Davis and Los Angeles.

The equation for the ambient coefficient of absorption in $10^{-8}\ m^{-1}$ is derived from the uncorrected coefficient using:

$$BABS = LRNC * \frac{0.97}{R}\ . \tag{24}$$

The uncertainty in R is estimated to be 10% of (1-R), based on the precision of the fit for the test data. The equation for the precision of the corrected coefficient of absorption is:

$$\sigma(BABS) = \left(\sigma(LRNC) * \frac{0.97}{R}\right)^2 + \left(0.10 * \frac{1-R}{R} * b\right)^2 \tag{25}$$

The minimum detectable limit is defined as twice the precision in the measurement for a sample with low absorption. Although this will vary with the intensity for a clean filter, it is more convenient to use a single intensity of 390 units for a typical clean filter. The expression for the mdl is then approximately

$$mdl(BABS) = mdl(LRNC) * \frac{0.97}{R} \tag{26}$$

The concentration of absorbing particles can also be estimated from the coefficient of absorption using the absorption efficient ε in m^2/g. For high temperature elemental carbon, such as diesel emissions, the value of ε is typically 10 m^2/g. However, the comparison of BABS and the concentration of light absorbing carbon, LAC, indicates that the BABS method yields a concentration that is approximately twice that of LAC. The two variables are moderately correlated (r=0.74 for western IMPROVE sites). There are three possible explanations: (1) the UCD integrating plate and integrating sphere methods both give values of b_{abs} that are high by a factor of 2; (2) the absorption efficient of 10 m^2/g is not appropriate for the low temperature elemental carbon produced by fires; or (3) there are more absorbing particles than those measured as LAC in the quartz-combustion method.

2.4.12 Slope and Intercept for Perpendicular Fit

The validation procedures include examination of correlation plots between two variables. Because both variables have associated uncertainty, it is necessary to construct the regression line that minimizes the perpendicular deviations of the points from the straight line. To do this it is first necessary to calculate the various means:

$$< x >= \frac{1}{n}\sum_{i=1}^{n} x_i \qquad < y >= \frac{1}{n}\sum_{i=1}^{n} y_i$$

$$< x^2 >= \frac{1}{n}\sum_{i=1}^{n} (x_i)^2 \qquad < y^2 >= \frac{1}{n}\sum_{i=1}^{n} (y_i)^2 \qquad < xy >= \frac{1}{n}\sum_{i=1}^{n} x_i y_i \tag{27}$$

The variances are calculated from the means:

$$S_x =< x^2 > -(< x >)^2 \qquad S_y =< y^2 > -(< y >)^2 \qquad S_{xy} =< xy > - < x >< y > \tag{28}$$

The correlation coefficient is

$$r^2 = \frac{(S_{xy})^2}{S_x S_y} \tag{29}$$

The expression for the slope involves the difference between the x and y variances:

$$S_d = \frac{S_y - S_x}{2} \tag{30}$$

We will the equation for the line to be y = a+bx. The slope b is given by:

$$\text{slope} = b = \frac{S_d - \sqrt{(S_d)^2 + (S_{xy})^2}}{S_{xy}} \tag{31}$$

The intercept a is given by:

$$\text{intercept} = a = < y > - b < x > \tag{32}$$

To calculate the precisions in a and b, we first calculate the parameters f and g:

$$f = \frac{S_y + b^2 S_x}{S_{xy}} \qquad g = f - 2b \tag{33}$$

The precision of the slope is:

$$\sigma_b^2 = \frac{fg}{n-2} \tag{34}$$

The precision of the intercept is:

$$\sigma_a^2 = [< x > \sigma_b]^2 + \frac{2g\, S_{xy}}{n-2} \tag{35}$$

2.4.13 Pairwise Precision

The pairwise relative precision is included on the plots for replicate analyses or for the same parameter by different analytical methods. For replicate analyses with negligible statistical or constant precision, this parameter gives the relative analytical precision.

For multiple measurements of a single quantity, z, the absolute precision is the standard deviation and the relative precision is the standard deviation divided by the mean. The standard deviation is defined as

$$(\text{stdev})^2 = \frac{n}{n-1}\left[< z^2 > - (< z >)^2\right] \tag{36}$$

Suppose there are only two measurements of each quantity, x and y. The standard deviation for this pair is given by Equation 36 with n=2:

$$(\text{stdev})^2 = 2\left[\frac{x^2 + y^2}{2} - \left(\frac{x+y}{2}\right)^2\right] = \frac{1}{2}(x-y)^2 \tag{37}$$

If D is the absolute difference $|x - y|$ and M is the mean, the standard deviation and relative precision are:

$$\text{stdev} = \frac{1}{\sqrt{2}} D \qquad P = \frac{1}{\sqrt{2}} \frac{D}{M} \tag{38}$$

Suppose there are n such pairs. The overall precision is the root-mean-square of the individual precisions. The absolute precision, P_{abs} is the sum of the individual standard deviations, while the relative precision, P, is the sum of the individual relative precisions:

$$P_{abs}^2 = \frac{1}{2n} \sum_{i=1}^{n} D_i^2 \qquad P^2 = \frac{1}{2n} \sum_{i=1}^{n} \left(\frac{D_i}{M_i} \right)^2 \tag{39}$$

These can also be written in terms of the x's and y's as:

$$P_{abs}^2 = \frac{1}{2n} \sum_{i=1}^{n} (x_i - y_i)^2 \qquad P^2 = \frac{2}{n} \sum_{i=1}^{n} \left(\frac{x_i - y_i}{x_i + y_i} \right)^2 \tag{40}$$

2.4.14 Pairwise Chi-Square

The pairwise goodness-of-fit parameter, χ^2, is also included on the plots for replicate analyses or for the same parameter by different analytical methods. This parameter, compares the differences with the precision of the differences as determined for the precision of x and y included in the data base. It is thus the best method of determining whether the differences are within the predicted precision.

If σ_x and σ_y are the calculated precisions for x and y, the precision of the difference is:

$$\sigma_d^2 = \sigma_x^2 + \sigma_y^2 \tag{41}$$

The goodness-of-fit parameter, χ^2, is:

$$\chi^2 = \frac{1}{n} \sum \left(\frac{D}{\sigma_d} \right)^2 = \frac{1}{n} \sum \frac{(x_i - y_i)^2}{\sigma_x^2 + \sigma_y^2} \tag{42}$$

Large values of χ^2 indicate that there are probably sources of difference not included in the estimate of precision.

2.5 Design of Collocated Tests

The data were collected in three major comparison tests. The first test (Phase I) involved the direct comparisons of the MSAM sampler to that of the CADMP sampler. This was done at the California Air Resources Board Monitoring Laboratory Division (MLD) located at 13th and T streets in Sacramento. The Stacked Filter Unit (SFU) sampler provides additional comparisons to the MSAM and CADMP samplers. The data from this test showed a few, easily correctable, flaws in the MSAM sampler design. Following the redesign of the MSAM sampler, the second test (Phase II) was conducted at Barton Flats, located in the San Bernardino Forest. Phase II served two purposes. The first determined if the modifications completed after Phase I were successful. The second purpose developed standard protocols for the field deployment of the MSAM sampler. Following the completion of Phase II, a third test (Phase III) was conducted to continue tests of mass concentration. In Phase III the MSAM sampler's mass concentration was compared with the IMPROVE sampler's.

2.5.1 Phase I Comparisons at ARB/MLD

The MSAM was tested at the Air Resource Board CADMP site in Sacramento. The site was located on top of the ARB MLD building on the corner of 13th and T Streets. The MSAM sampler operated for 3 one-week periods from April 8 to 29, 1992. For the first 2 weeks, the MSAM operated with a co-located conventional CADMP sampler (operated with daily 24 hour samples) and a UCD SFU Sampler (also operated with daily 24 hour samples). For the third week the CADMP was returned to its standard schedule of two 12-hour samples every six days while the SFU continued to operate daily. In addition, a second MSAM sampler operated for quality assurance purposes.

Because of time constraints of personnel at the MLD building, it was decided to train a UCD employee to operated the CADMP. A training session was held, however, both the ARB and outside reviewers have found that experience in operating the CADMP is essential for quality data return.

With the comparisons of the ARB's CADMP sampler, the first version of the MSAM sampler were evaluated. Once the problems of the MSAM sampler from the first tests were isolated and the problem resolved, Phase II could begin. The filters from the CADMP sampler were analyzed as specified in the standard operating procedures of the CADMP sampler.

2.5.2 Phase II Comparisons at Barton Flats, CA

During the period from August 5, 1992 to November 6, 1992, the Modular System for Acid deposition Monitoring (MSAM) sampler continued with Phase II testing. Phase II testing sampled with a co-located CADMP sampler at Barton Flats. The dates of the comparison are as follows:

1. August 05, 1992 to August 18, 1992
2. September 22, 1992 to October 06, 1992
3. October 09, 1992 to October 23, 1992
4. October 23, 1992 to November 06, 1992 (Invalid due to system leak)

During the final period of October 23, 1992 to November 06, 1992, the MSAM sampler developed a leak due to a faulty hose fitting. The hose fitting was redesigned so this will not occur again. This invalidates the final sample, but the data are included to show the determination of an invalid sample.

Kenneth Bowers setup of the sampler in cooperation with Paul Miller and Dave Jones. Dave Jones, who works with the Pacific Southwest Forest Experiment Station, US Forest Service, conducted the changes of the MSAM sampler at the field site at Barton Flats. At the end of the Phase II, Teresa James took final readings and ending calibrations of the unit before the subsequent return of the entire MSAM unit to UC Davis.

This was the first field test of a full 14 day sample period. During the time the MSAM sampler monitored, the CADMP collected aerosol on its one day in six protocol with two 12 hour samples (6 AM - 6 PM and 6 PM - 6 AM). Unfortunately, the data does not compare directly. Because the MSAM sampler provides a true 14 day average sample, a comparison with the CADMP sampler would present a high degree of uncertainty. During a 14 day sample period, the CADMP sampler collects on only 2 or 3 of the days. This means that the CADMP sampler operates only 14% to 21% of the time compared to the MSAM sampler. The CADMP sampler average value over 14 days should be taken as an estimated 14 day average with a large uncertainty.

2.5.3 Phase III Comparisons at the University of California, Davis

During the month of December 1992, a series of side by side measurements with the well-tested IMPROVE particulate sampler was conducted. The IMPROVE sampler was designed and built by the University of California, Davis to collect $PM_{2.5}$ using the same cyclone incorporated by the MSAM sampler. These samplers are used by the National Park Service as a part of their visibility monitoring program. These tests were specifically aimed to determine if the modifications to the MSAM had resolved the mass differences.

3.0 RESULTS AND DISCUSSION

The results of the three phases are presented in a chronological order. The results will show a progressive improvement of the MSAM sampler as faults were identified and corrected. Each phase is presented in its own section with a short discussion of the data, summary of the findings and suggested corrections to the problems.

3.1 Comparison at Air Resources (ARB)/Monitoring Laboratory Division (MLD)

The sample collection at the ARB/MLD was the first opportunity to test the MSAM samplers. Table 3 shows the filters and analysis of the MSAM sampler used in Phase I. The schematic of the MSAM sampler is seen in Figure 19. Following the conclusion of sample collection at the ARB/MLD, the aerosol filters were archived and delivered to their respective laboratories. The filters analyzed by ion chromatography and automated colorimetry were sent to DRI. Filters requiring mass, laser and elemental analysis measurements were completed by the Air Quality Group, UC Davis. From the analysis results, the following conclusions were drawn:

1. There is excellent agreement between co-located MSAM units. (within 10 percent, except for species HNO_3 and NH_4^+)

2. There is good agreement between the MSAM units and the SFU. (within 20 percent for mass and $SO_4^=$)

3. There is fair agreement between the MSAM units and the CADMP. (within 30 percent for elements total NO_3^-, NH_4^+, $SO_4^=$, and NO_2)

4. With certain modifications, agreement between the MSAM and CADMP can improve.

Table 3. Filters and Analysis Used for MSAM Sampler (Phase I)

CHANNEL	AIR FLOW RATE	MEASUREMENT
IMPACTOR-SO_2-CITRIC ACID	10.0 lpm	Stage B: $PM_{2.5-0.3}$, Elemental analysis (Na-Pb) Stage C: $PM_{0.3-0.068}$, Elemental analysis (Na-Pb) Afterfilter: $PM_{\leq 0.068}$, Elemental Analysis (H, Na-Pb) Citric acid impregnated filter: Automated Colorimetry (NH_3) K_2CO_3 impregnated filter: Ion Chromatography (SO_2)
TEFLON	5.0 lpm	$PM_{2.5}$ Mass, B_{abs}, Elemental analysis (H, Na-Pb)
TEFLON-TEA	2.5 lpm	Teflon filter (backup): $PM_{2.5}$ Mass, B_{abs}, Elemental analysis (H, Na-Pb) TEA Impregnated filter: Automated Colorimetry (NO_2)
TOTAL NITRATE	2.5	Nylasorb filters: Ion Chromatography (Total NO_3^-, NH_4^+)
PARTICULATE NITRATE	2.7	Nylasorb filter: Ion Chromatography (Particulate NO_3^-)

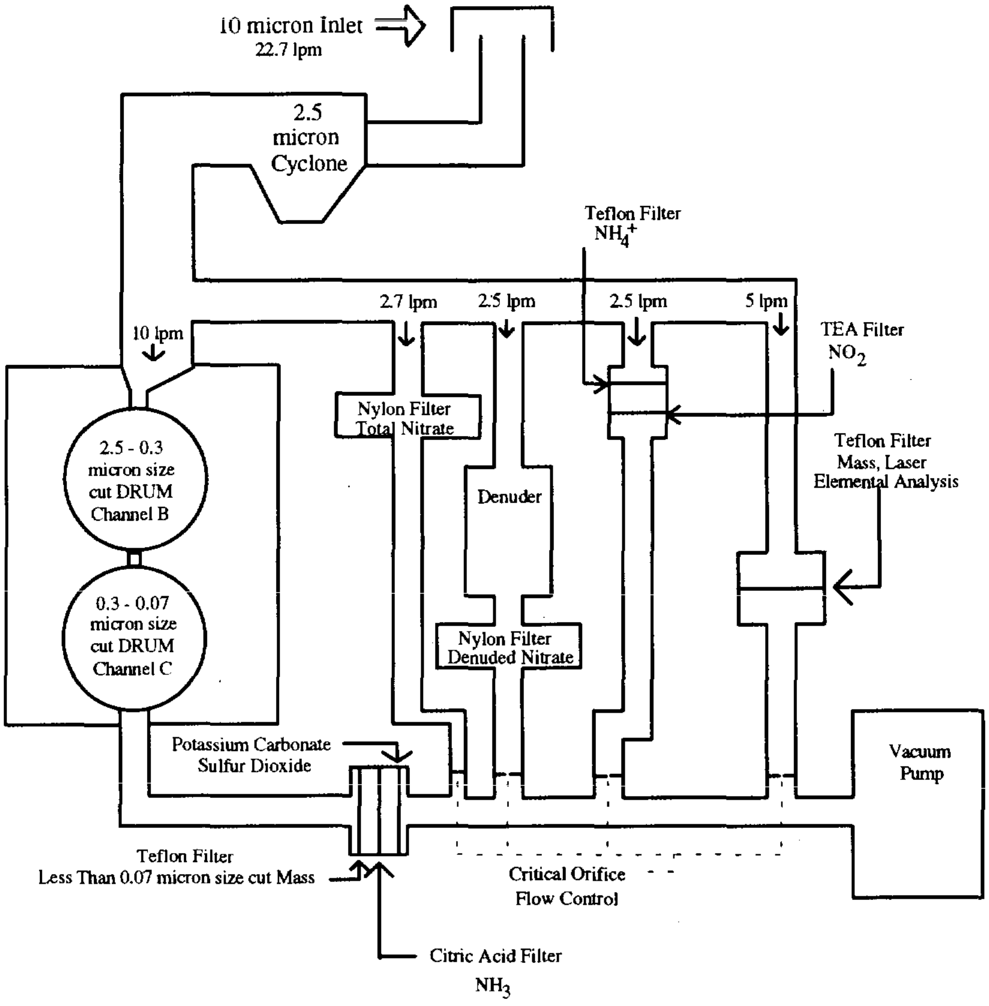

Figure 9. Schematic of MSAM sampler during Phase I testing.

3.1.1 Summary of Data

Table 4 shows the various ratios between the two MSAM, SFU and CADMP samplers filter data. In Table 4, the ratio for the two collocated MSAM samplers are nearly 1.00 (0.808 to 1.36, excluding NH_4^+ and HNO_3) among wet chemistry filters. The two stage impactor's data also are in good agreement. Figures 10 and 11 represent the correlation of the two stage impactors from the two co-located MSAM samplers. Figure 10 shows the correlation of the sulfur and iron found on the B channel of the MSAM (2.5 μm $\leq$ Dp $\leq$ 0.3 μm). Figure 11 shows the correlation of sulfur and iron found on the C channel (0.3 μ m $\leq$ Dp $\leq$ 0.07 μm). As these graphs show, they produced similar results (r^2=0.82-0.95).

Table 4. Ratios of various samplers during Phase I testing

SPECIES	DATE	MSAM1:CADMP	MSAM1:MSAM2	CADMP:SFU	MSAM:SFU
TOTAL NO_3^-					
	8-14 April	0.909	1.041		
	15-21 April	0.956	1.187		
	22-29 April		1.361		
PARTICULATE NO_3^-					
	8-14 April	1.433	0.946		
	15-21 April	1.646	1.035		
	22-29 April		0.990		
HNO_3					
	8-14 April	0.314	2.151		
	15-21 April	0.305	4.656		
	22-29 April		30.000		
MASS					
	8-14 April	2.122	1.115	0.293	0.623
	15-21 April	1.485	0.808	0.744	1.105
	22-29 April		1.087		1.241
NH_4^+					
	8-14 April	1.187	1.758		
	15-21 April	1.109	1.253		
	22-29 April		2.088		
NH_3					
	8-14 April	1.421	1.019		
	15-21 April	1.937	1.070		
	22-29 April		0.976		
$SO_4^=$					
	8-14 April	1.188	0.981	0.949	1.127
	15-21 April	1.086	0.968	0.992	1.077
	22-29 April				1.164
SO_2					
	8-14 April	1.379	1.038		
	15-21 April	1.794	1.058		
	22-29 April		0.984		
NO_2					
	8-14 April	1.067	1.018		
	15-21 April	0.704	1.000		
	22-29 April		0.989		

The data found in Table 4 and Tables 10, 17 and 18 of Appendix A show that the MSAM and SFU samplers are in good agreement. For example, in Table 10 from Appendix A, during the week of April 8-14, 1992 the values for sulfate for the two MSAM samplers are 1.195 and 1.218 compared to a value of 1.060 for the SFU sampler. For comparison, for the same time, the CADMP sampler reported a value of 1.006. During the second week (April 15-21) the values show a greater similarity with values of 1.052, 1.087, 0.977 and 0.969, the two MSAMs, SFU and CADMP, respectively. The SFU and two MSAM samplers also provided comparable data for mass concentration as shown in Table 17 of

Appendix A. Although these results are encouraging, the main purpose of the Phase I trial was to determine the comparability of the MSAM and CADMP sampler.

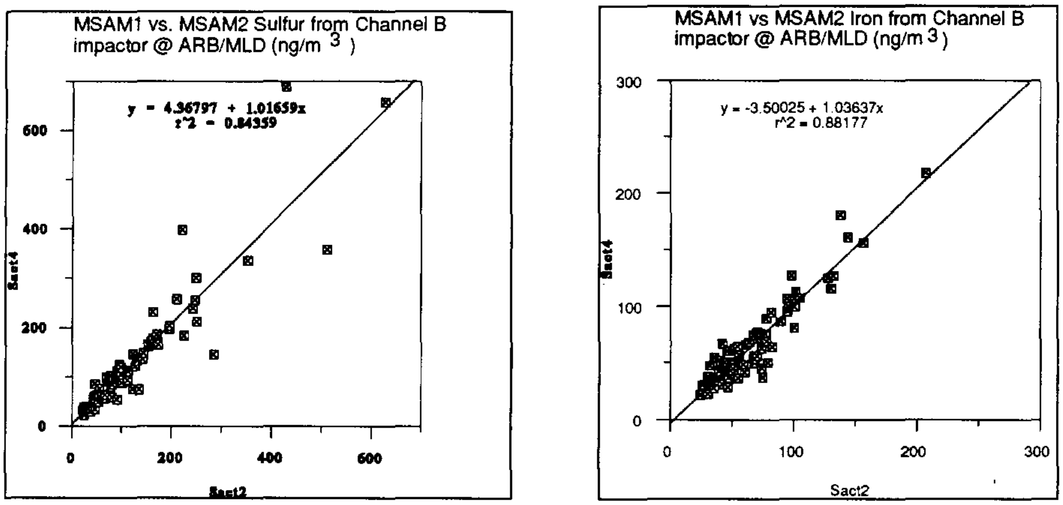

Figure 10. Correlation plots of Sulfur and Iron, $PM_{2.5-0.3}$, between two co-located MSAM samplers at Air Resources Board MLD CADMP site.

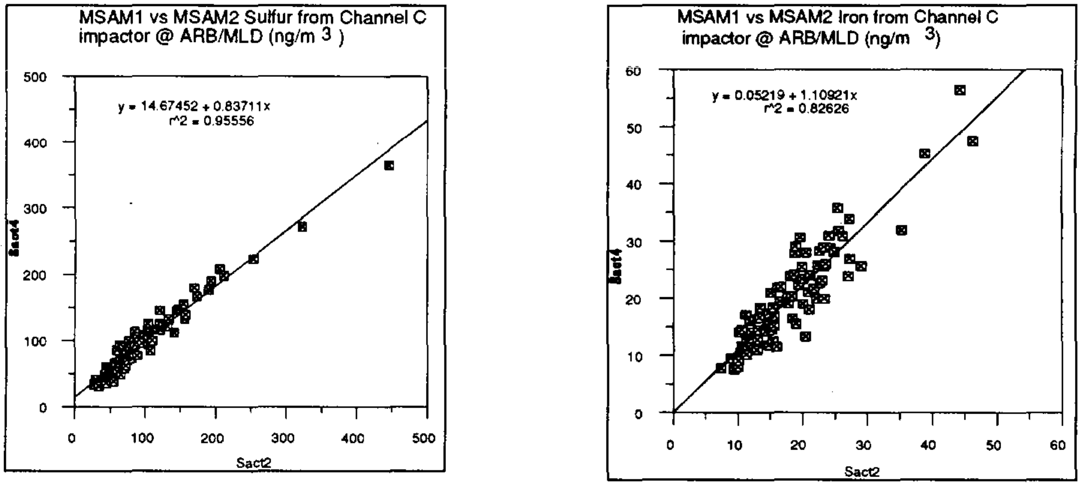

Figure 11. Correlation plots of sulfur and iron, $PM_{0.3-0.07}$, between two co-located MSAM samplers at the ARB MLD CADMP site.

In the results between the MSAM and CADMP comparisons, there is good agreement among most of the species tested for during Phase I as evidenced in Figure 12. Figure 12 shows the comparison between the MSAM and CADMP for all the species. As shown earlier, the CADMP and MSAM had equitable values of sulfates. Similar results were found with NH_4^+, total nitrate and NO_2, as evidenced in Tables 11, 12 and 16, of Appendix A, respectively. However, the MSAM and CADMP sampler's agreement in the other species did not fare as well. In Table 12 of Appendix A, the denuded nitrates from the MSAM and CADMP are compared along side total nitrates. In the Table the MSAM reports more denuded nitrates than the CADMP. This carries over Table 13 of Appendix A displaying the nitric acid that is derived from subtracting the denuded nitrates from the total nitrates. This problem was later resolved in further tests by coating the denuder with sodium bicarbonate. This, in effect, produced a more efficient denuder, thus stripping more of the nitric acid gases from the air stream.

Tables 14 and 15 of Appendix A indicate higher than anticipated amounts for SO_2 and NH_3 for the MSAM sampler as compared to the CADMP sampler. The discrepancies between the amounts were later determined to be filter related. The filters used to collect SO_2 and NH_3 are impregnated cellulose filters. These filters contain glycerol to keep the filters moist for sampling. When fresh filters are sent to the laboratory, the filters may contain different amounts of the glycerol. The amount of glycerol will vary from batch to batch. Some of the filter may have an excess amount of glycerol as was the case during Phase I. The filters created an excessive pressure drop and drove off some of the glycerol. The glycerol residue could found in the cassette following the filter. The reduced pressure drop would increase the flow rate and from past experience this occurs over a matter of minutes. Because the flow rate is an averaged flow rate between the initial and final flow rate, the true averaged flow rate would be lower than expected. Since the volume is calculated from the flow rate, volume was considerably less than expected, artificially the raising concentration values for SO_2 and NH_3. The problem was solved in two ways. The first solution developed a better quality check of the impregnated filters. Not only will the filter packs be checked for flow rates but also for pressure drops. If the pressures drop is over a nominal level , the filter will be replaced and checked again. The second solution moved the citric acid filter from the impactor stage cassette to the Teflon only cassette. The new configuration allows for reduced pressure drops across both the citric acid and potassium carbonate impregnated filters.

The final problem displayed in Table 17 of Appendix A shows higher than expected values for mass concentrations for the MSAM sampler than those of the CADMP sampler. Since these filters precede the heavily loaded glycerol impregnated filter, the volumes for the Teflon filters are also affected and there by increasing the concentration artificially. With the above solutions for the glycerol filters, the mass concentrations are corrected.

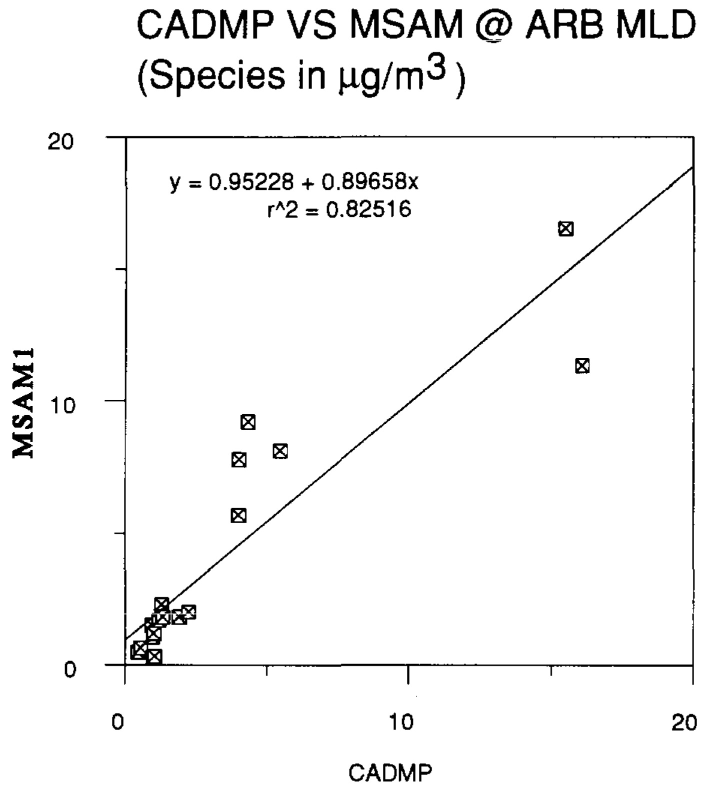

Figure 12. Comparison of MSAM and CADMP sampler for mass, sulfate, total and particulate nitrate, ammonium, ammonia, sulfur dioxide, nitric dioxide (µg/m^3)

3.1.2 Evaluation of Tests

The results produced by intercomparison of samplers were very informative about the first design of the MSAM sampler. As indicated from the figures above, the MSAM sampler performed well in reproduction of data as well as correlating well with the CADMP sampler in quantifying most of the acidic deposition species. Figure 13 shows the comparison of the MSAM and CADMP samplers for all the species except HNO_3, Particulate Nitrate, NH_3 and mass. Phase I testing also showed several problems especially in the comparison of HNO_3, particulate nitrate, NH_3 and mass. With the modifications to the MSAM sampler completed, MSAM samplers have great potential. The problems with solutions to be tested in Phase II are listed as follows:

1. The most significant problem encountered was an excessive pressure drop over the impregnated filter cassettes, especially the filter cassette containing the Teflon, citric acid and potassium carbonate impregnated filters. The high pressure drop caused a loss of impregnate and increased the flow by approximately 20 to 30 percent. The loss of impregnant was evidenced as glycerol residue on the cassette following the impregnated filters. The problem was resolved two ways; first by reducing the pressure drop across the filter pack by moving the citric acid

impregnated filter to the cassette containing the single Teflon, and the second by including an additional check of the filters before the filter pack leaves the laboratory. The impregnated will not only be checked for flow rate but for pressured drop. If the impregnated filter has higher than normal pressure drop and a lower than normal flow rate, the filter will be replaced and checked again.

2. Mass concentration differed greatly between the MSAM and CADMP sampler. Since the most of the Teflon filters that collect the mass precede the impregnated filters the volumes were not calculated correctly. This was corrected by implementing the solution used for the impregnated filters.

3. Although the denuder was calculated to be very efficient and the oxidized aluminum surface should collect the nitric acid vapor efficiently (John *et al.*, 1988), the denuder appears to have allowed penetration of the nitric acid vapor. This problem can be solved by coating the denuder. Additional tests on oxidized aluminum denuders can be conducted at a later date.

4. Although the test for total nitrate from the MSAM agreed with the CADMP (MSAM/CADMP=0.91-0.96), the ARB recommended from experience that the Nylasorb filter be preceded with a Teflon filter to prevent clogging of the total nitrate channel. To facilitate this recommendation, a Teflon pre filter was added in front of the Nylasorb filter. To calculate the total nitrate and sulfate, ion chromatography will be performed on both the Teflon and Nylasorb filters. The nitrate from both filters will be added together to get a total nitrate number. The same will be done to produce total sulfate numbers.

5. Although ammonium can be analyzed from the total nitrate Nylasorb filter, as per the DRI Laboratory, it is easier and more accurate to analyze ammonium from a Teflon or quartz prefilter due to the buffer solution required to extract the Nylasorb filter for nitrates. This can be solved by analyzing the Teflon prefilter from the total nitrate channel for ammonium. The Teflon prefilter will also be analyzed for nitrates and sulfates for the calculation of total nitrates and sulfates.

With the above noted modifications to the MSAM sampler Phase II of the testing protocol proceeded. In July 1992, the MSAM was field deployed at a CADMP intensive study at Barton Flats in the San Bernardino National Forest.

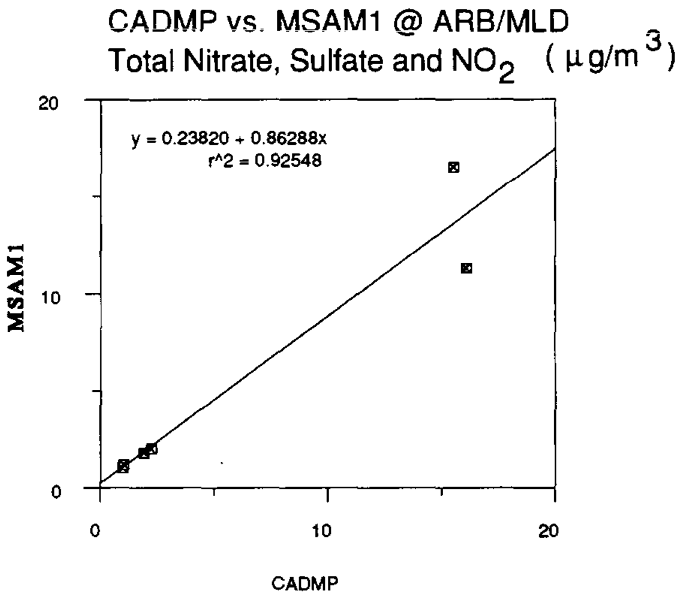

Figure 13. CADMP versus MSAM1 at Air Resources Board Monitoring and Laboratory Division for species total nitrate, sulfate and NO_2.

See Appendix A for complete data set.

3.2 Comparisons at Barton Flats, CA

During the period from August 5, 1992 to November 6, 1992, the Modular System for Acid deposition Monitoring (MSAM) sampler continued with Phase II testing. Phase II testing sampled with a co-located CADMP sampler at Barton Flats. This served two purposes. The first determined if the modifications to the MSAM sampler corrected the problems encountered in the test at ARB/MLD. Table 5 contains the filters and analysis used in Phase II of the MSAM sampler tests. The configuration of the MSAM sampler can be found in Figure 14. The modifications to the MSAM sampler included the movement of the citric acid filter from the afterfilter cassette to the cassette containing the Teflon filter for mass, laser and elemental analysis. A second modification placed a Teflon filter in front of the total nitrate Nylasorb filter. Teflon - Nylasorb filter cassette follows the same setup as the CADMP sampler. The last modification involved the coating of the denuder with sodium carbonate. This coating would increase the efficiency of the denuder to adsorb the nitric acid. The second purpose was to work out the logistics of sample handling between the laboratory and the field.

Table 5. Filters and Analysis Used for MSAM Sampler (Phase II)

CHANNEL	AIR FLOW RATE	MEASUREMENT
IMPACTOR-SO_2	10.0 lpm	Stage B: $PM_{2.5-0.3}$, Elemental Analysis (Na-Pb) Stage C: $PM_{0.3-0.068}$, Elemental Analysis(Na-Pb) Afterfilter: $PM_{\leq 0.068}$, Elemental Analysis(Na-Pb) K_2CO_3 impregnated filter: Ion Chromatography (SO_2)
TEFLON-CITRIC ACID	5.0 lpm	Teflon filter: $PM_{2.5}$ Mass, Elemental Analysis (Na-Pb) Citric acid impregnated filter: Automated Colorimetry (NH_3)
TEFLON-TEA	2.5 lpm	Teflon filter: $PM_{2.5}$ Mass, Elemental analysis (Na-Pb) TEA Impregnated filter: Automated Colorimetry (NO_2)
TOTAL NITRATE - BACKUP FILTER	2.5	Teflon filter: Ion Chromatography (NO_3^-,NH_4^+, $SO_4^=$) Nylasorb filters: Ion Chromatography (NO_3^-, $SO_4^=$)
PARTICULATE NITRATE	2.7	Nylasorb filter: Ion Chromatography (Particulate NO_3^-, $SO_4^=$)

During the test period, the MSAM sampler collected 14 day averaged samples and the CADMP sampler collect was one day in six. During the day the CADMP sampler was operating, the sampler collected for two periods, 6 AM - 6 PM and 6 PM - 6 AM. This represented a problem with direct comparisons between the MSAM and CADMP sampler. Since the CADMP sampler only collects aerosols two or three days out of the fourteen days the MSAM collects for, this represents only a 14 to 21 percent overlap of sample collection. Since only two or three days are averaged for the 14 day average for the CADMP sampler, the comparison should be used only as a rough estimate. On November 6, 1992, field tests at the Barton Flats CADMP concluded with four two-week periods of air monitoring. These tests were evaluated and the following results were collected. This section covers all results from these tests and provides an evaluation and conclusions of the MSAM sampler at the end of Phase II.

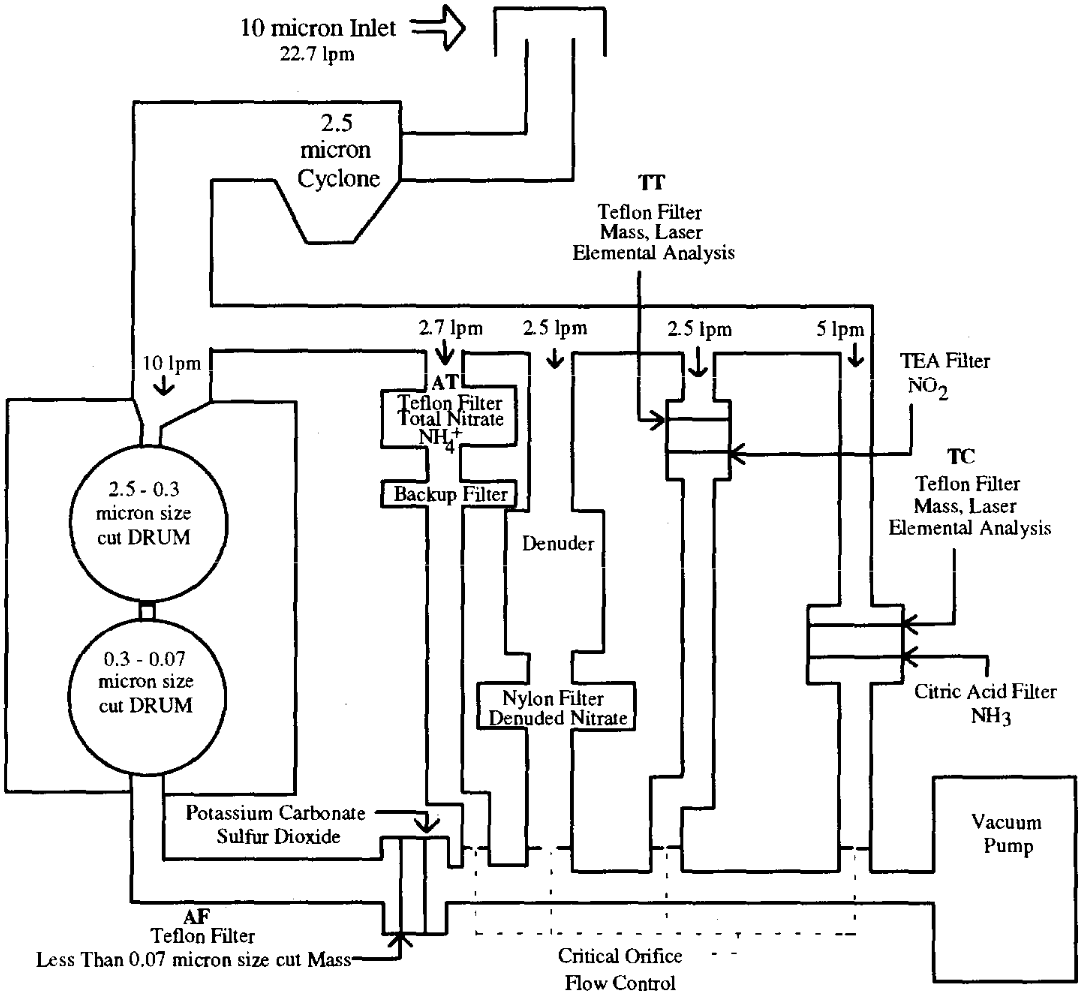

Figure 14. Schematic of MSAM sampler during Phase II trials

3.2.1 Summary of Data

Figure 15 and Table 6 shows the improvement of the MSAM sampler in Phase II. Figure 15 shows the correlation between the species in which there were problems from Phase I. The Figure 15 shows a general agreement between the MSAM and CADMP samplers. In Table 6 the ratios of the species are shown for both Phase I and II. Although not all the modifications to the MSAM sampler were successful, Table 6 shows an improvement from Phase I to Phase II. Figure 15 also shows an improvement by plotting the correlation between the MSAM and CADMP samplers, for the same species found in Table 6.

Table 6. MSAM filters for NH_4^+, Particulate NO_3^-, NH_3 and mass.

SPECIES	Trial 1 DATE	MSAM1:CADMP	Trial 2 DATE	MSAM1:CADMP
NH_4^+				
	8-14 April	0.909	4-16 Aug.	0.857
	15-21 April	0.956	28 Aug.-3 Oct.	0.971
	22-29 April		9 Oct.-21 Oct.	0.775
PARTICULATE NO_3^-				
	8-14 April	1.433	4-16 Aug.	1.411
	15-21 April	1.646	28 Aug.-3 Oct.	0.929
	22-29 April		9 Oct.-21 Oct.	1.208
NH_3				
	8-14 April	0.314	4-16 Aug.	0.890
	15-21 April	0.305	28 Aug.-3 Oct.	0.935
	22-29 April		9 Oct.-21 Oct.	0.926
MASS				
	8-14 April	2.122	4-16 Aug.	0.828
	15-21 April	1.485	28 Aug.-3 Oct.	1.326
	22-29 April		9 Oct.-21 Oct.	1.032

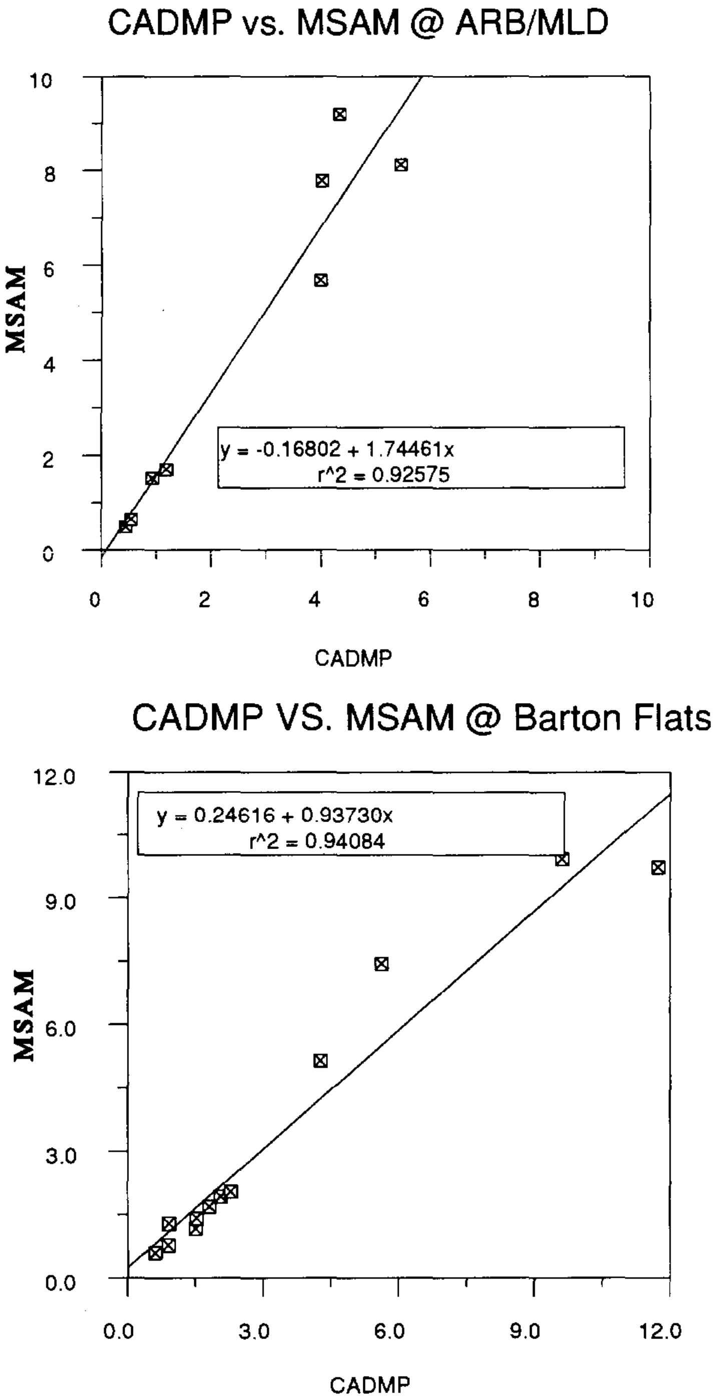

Figure 15. Improvement for MSAM species: mass, particulate nitrate, ammonium and ammonia. ($\mu g/m^3$).

Figure 16 shows the four channels of the MSAM used for collecting mass concentration. Channels TC (Teflon filter in front of the Citric Acid Filter), TT (Teflon filter in front of the TEA filter) and AT (Teflon filter in front of the Nitrate filter) collect $PM_{2.5}$ at 2.5, 5.0 and 2.5 liters per minute, respectively. Channel AF is the Teflon filter following the two stage impactors. This Teflon filter collects particulate matter less than .07 microns. In Figure 16, channels TT, TC and AT are essentially equivalent (less than 5 percent variation, using ANOVA test). In Figure 17, the mass measured by the CADMP and MSAM samplers are compared. The chart shows the first three periods of the MSAM agreeing with the CADMP mass concentration averages. During the fourth period, the sampler suffered from a leak in the system, as reported by the field operator. The amounts reported by the MSAM sampler are considerably lower in the fourth period than the CADMP sample. These data indicate that the modifications done on the sampler corrected the mass differences between MSAM and CADMP encountered in Phase I of this project.

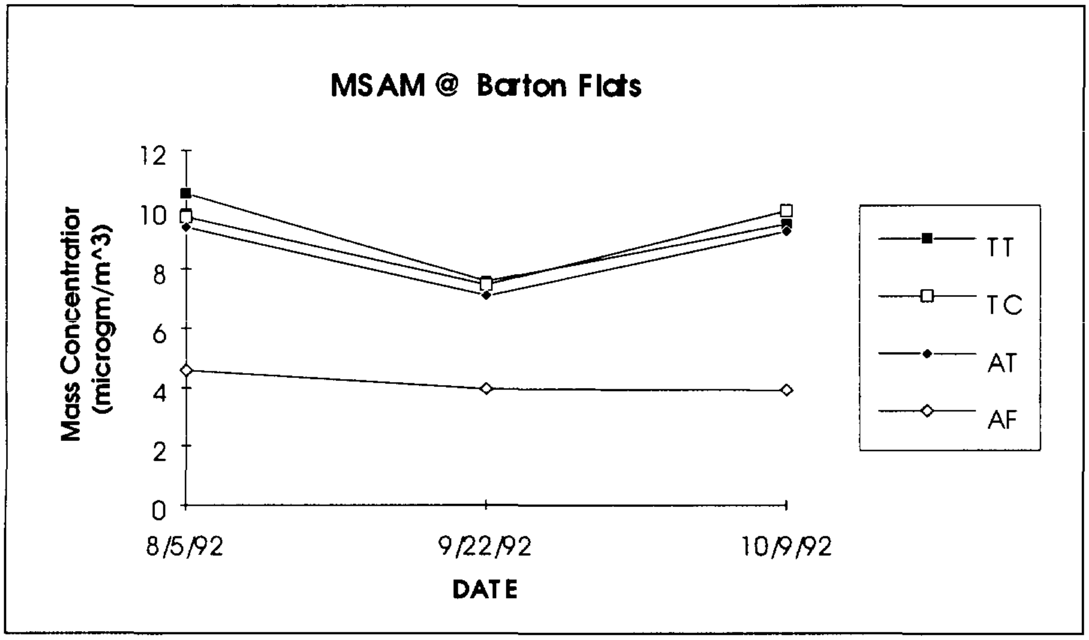

Figure 16. Linear plot of mass concentration of $PM_{2.5}$ from the MSAM sampler located at Barton Flats.

The ion chromatography and automated colorimetry data provided by DRI showed some improved results due to the modifications completed on the MSAM sampler. In Figures 18 and 19, correlation plots show the result of using a different substrate (Teflon) for the analysis of ammonium. Although the collection of NH_4^+ appears to lower than the CADMP sampler (slope = 0.644), as shown in Figure 18, this could be attributed to the CADMP's selective sample period of one day six and not a true 14 day average. In the case of NH_3, the species showed a marked improvement from Phase I to Phase II (CADMP/MSAM ≈ 0.33 for Phase I and = 0.84 for Phase II). Both the NH_3 and NH_4^+ ions have greater agreement than in Phase I trials (r^2 = 0.9999 in Figure 18 and r^2 =

0.9836 in Figure 19). As with the mass concentrations, the ions for the CADMP's one day in six samples were also averaged to represent an MSAM 14 day average. In Table 26 of Appendix B, similar results were found in the case of SO_2. In the cases of NH_3 and SO_2, quality assurance of the impregnated filters helped in producing better results in Phase II than in Phase I as shown in Table 6.

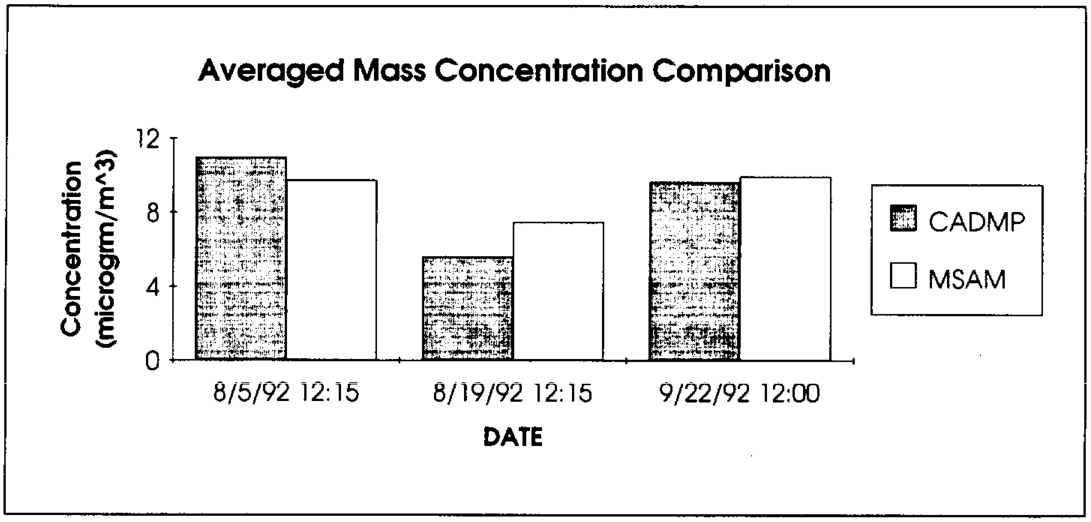

Figure 17. Bar Chart of MSAM versus CADMP mass concentration. The MSAM samples are a 14 day average of mass concentration and the CADMP sample represents an arithmetic average of 1 day in 6 samples falling in between the MSAM sample period.

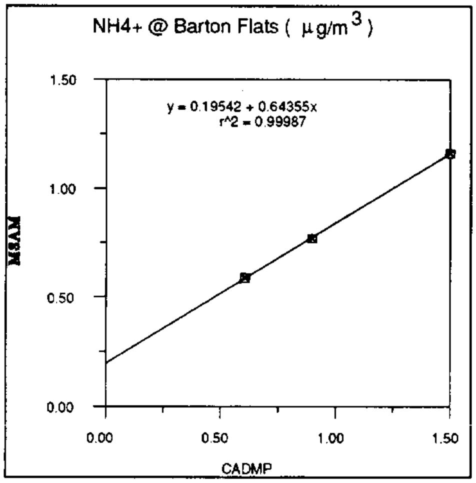

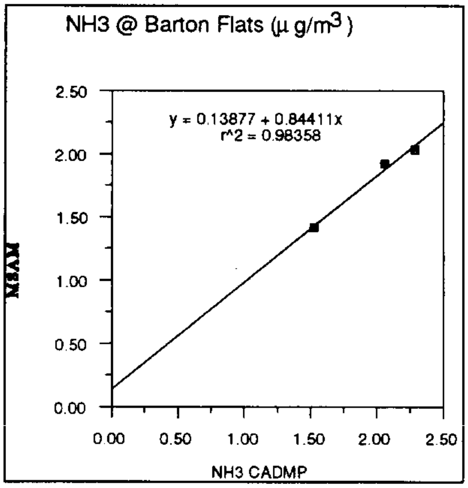

Figure 18 (left). Comparison of CADMP and MSAM NH_4^+ ions.
Figure 19 (right). Comparison of CADMP and MSAM NH_3 ions.

With respect to the collection of nitrate and sulfate, the MSAM sampler had mixed results. A concern of the MSAM sampler was the ability to quantify the amount of nitric acid from the aerosol. During Phase I, the MSAM failed to show that the denuder was operating properly. Before Phase II testing, two major modifications were done. The first modification resulted in the coating of the denuder with sodium carbonate. The sodium carbonate would enhance the nitric acid scrubbing efficiency as opposed to aluminum alone. The second modification created a Teflon-Nylasorb combination filter pack. The ARB had recommended, from experience, that the Teflon-Nylasorb combination would reduce the possibility of filter clogging as opposed to single a Nylasorb filter. As a result, the total nitrate would be calculated from the addition of the Teflon filter plus the Nylasorb filter.

During the period the MSAM sampler collected, the amount of nitric acid, according to the CADMP sampler, was low. In Figure 20, the low amount of nitric acid is represented by the near 1:1 correlation between the total and particulate nitrates reported by the CADMP sampler. Table 27 of Appendix B displays the amount of nitric acid by subtracting the denuded nitrate from the total nitrate of the CADMP sampler. As the table points out, during most of the period of the value for nitric acid was low.

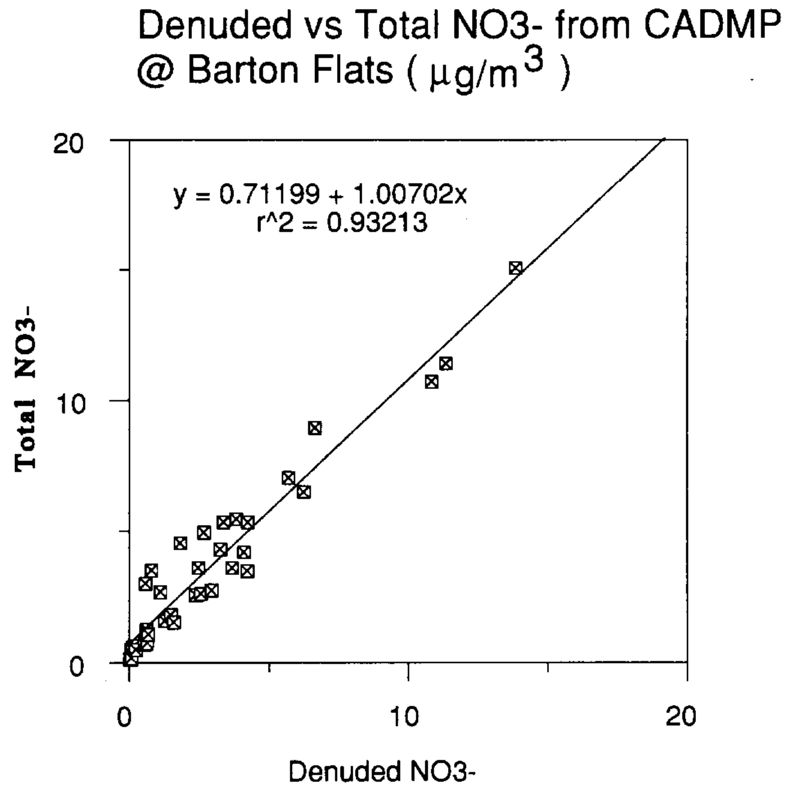

Figure 20. Correlation between Denuded NO_3^- and Total NO_3^- from the CADMP sampler at Barton Flats.

Because of the low amount of nitric acid during the sampler period at Barton Flats, the MSAM denuder's capabilities were not tested to its fullest. But as Figure 21 shows, the CADMP and MSAM ratios differ by about 20 percent (slope = 1.21). Again the difference between the MSAM and CADMP measurements were attributed to the different sampling schedules. In Figure 22, the comparison of CADMP and MSAM total nitrates is presented. As the figure shows, the MSAM reports far less total nitrates than the CADMP sampler. This difference could be attributed to the new filter configuration for collecting the total nitrate. The single Nylasorb filter was replaced with a Teflon-Nylasorb filter combination to reduce the chances of filter clogging. The filters were placed in a double cassette. It was later determined that because of the filter cassette's construction, the nitric acid that passed through the Teflon filter could have been absorbed by the plastic support grid and the plastic filter cassette walls before reaching the Nylasorb filter. This would reduce the amount of nitric acid collected by the Nylasorb filter.

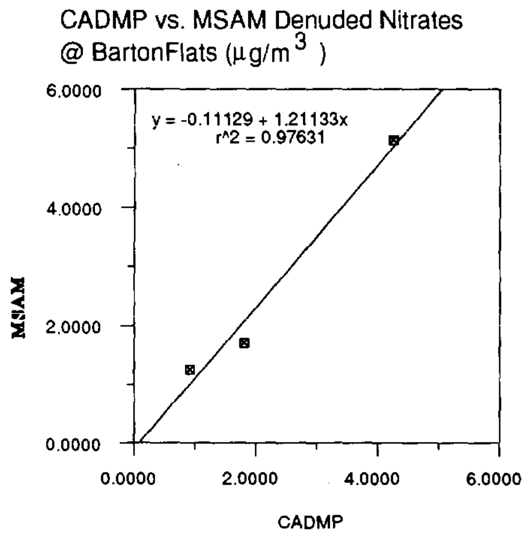

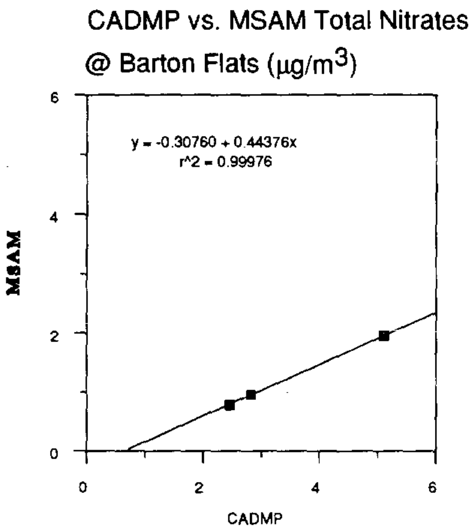

Figure 21 (left). CADMP denuded nitrate versus MSAM denuded nitrate at Barton Flats. The agreement is fairly good (within 20 percent) considering the CADMP schedule of one day in six versus the MSAM schedule of a true 14 day average.

Figure 22 (right). Correlation plot of MSAM denuded nitrates and CADMP total nitrates. The plots are show the MSAM's Teflon filter volatilization of nitrates due to length of time before analysis.

To check that the total and particulate nitrate filters were collecting the same amount of material, the sulfate from both channels were compared. In Figure 23, the sulfate from the total nitrate channel is regressed against the particulate nitrate channel. As Figure 23 shows, the sulfates from both channels agree (slope =1.05, and r^2=.9934). The results of this test shows that are no systematic problems with the sampler (i.e. the MSAM contained no leaks, or flow rate problems).

Since the sulfates from both channel agree, flow rate is not the problem. The problem appears to related to the collection of nitrates onto the Teflon. From experience, a large percentage (about 50 percent) of nitrates is driven of the Teflon filter while sampling. In Table 7, the Teflon shows very little nitrate capture compared to the Nylasorb filter. Although the Nylasorb filters will collect the remaining nitrate particles and gases, the remaining nitrate on the Teflon is very volatile. Because the MSAM Teflon filters were not analyzed for at least eight weeks, this gave the nitrate particles time to volatilize off of the Teflon filter.

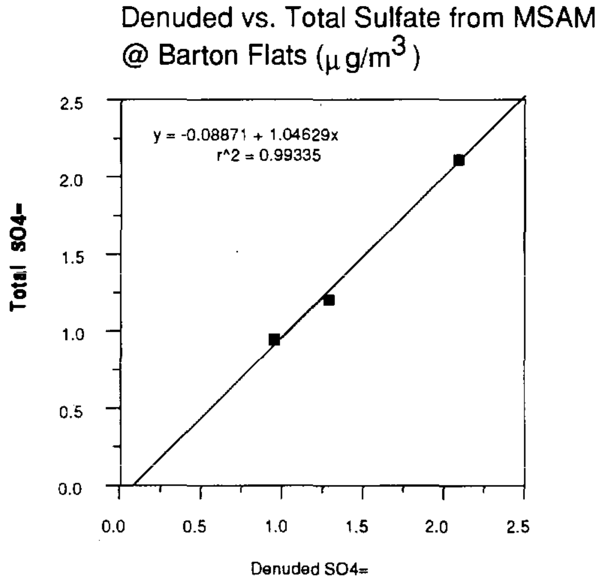

Figure 23. Correlation between Denuded $SO_4^=$ versus Total $SO_4^=$ from the MSAM sampler at Barton Flats. This shows that were no systematic problems with the MSAM total and particulate nitrate channels.

Table 7. Comparison of nitrate off the Teflon and Nylasorb from the total nitrate and particulate nitrate channel.

DATE	Total Nitrate off Teflon	Total Nitrate off Nylasorb	Total Nitrate Teflon + Nylasorb	Particulate Nitrate
Aug. 5	0.060378±0.010681	0.7111±0.0182	0.7715±0.0211	1.285751±0.041042
Sept.22	0.241477±0.025498	0.7119±0.0182	0.9534±0.0314	1.680699±0.040716
Oct. 9	0.064341±0.014156	1.8921±0.0580	1.9565±0.0597	2.501732±0.116211
Oct. 23	0.699383±0.060828	0.7236±0.0185	1.4230±0.0636	3.688564±0.042343

Another part of the tests completed at the Barton Flats site was the evaluation of the impactor channels. B channel of the two stage impactor collects particles between 2.5 μm and 0.3 μm. C channel collects particles between 0.3 μm and 0.07 μm. The After-filter follows the two stage impactor to collect ultrafine particles. Figure 24 represents the size distribution of fine sulfur particles during the field test at Barton Flats. These particles are important in visibility where B channel particles scatter light more efficiently than the C channel particles. In Figure 24, the ultrafine $PM_{\geq 0.07}$ is calculated from the 14 day average Teflon filter. It has been determined in past experiments, such the Winter Haze Intensive Tracer Experiment (WHITEX) and Southern California Air Quality Intercomparison of Carbon Species Methods, that the ultrafine ($PM_{\leq 0.07}$) particles closely correlate with particles in the C channel of the two stage impactor. The ultrafine sulfur concentrations were derived from the C channel ratio. Although the particles from the C channel and the After-filter do not follow a true one to one correspondence, the data gives a rough estimate on the percentage of ultrafine particles. These data can be converted to an equivalent sulfate number to compare with the sulfate numbers given by the CADMP sampler. In Figure 25, the MSAM sulfate values are plotted alongside the CADMP sulfate values. The plot shows, except for the period between 10/15/1992 and 10/21/92, that the data is generally in good agreement.

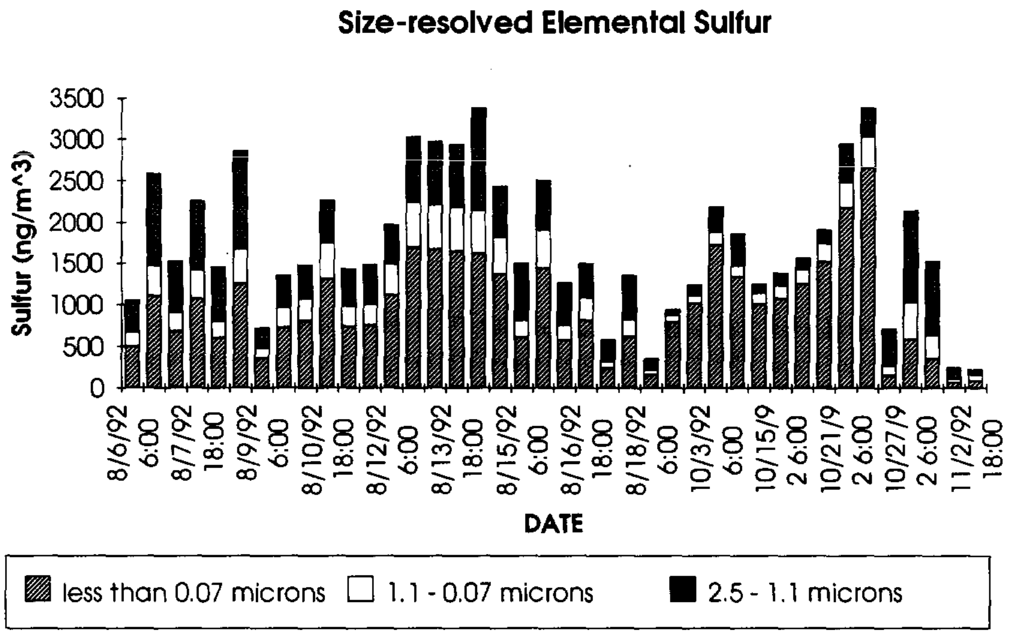

Figure 24. Elemental size-resolved sulfur by PIXE analysis from the two stage impactor at Barton Flats.

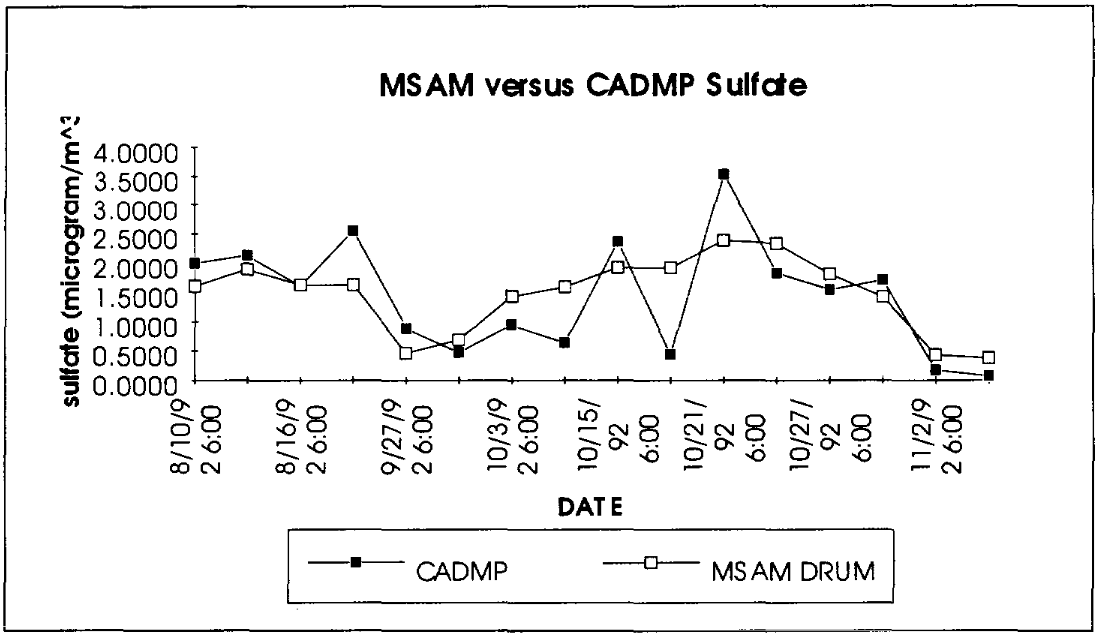

Figure 25. Time plot of MSAM and CADMP sulfate at Barton Flats, California.

3.2.2 Evaluation of Tests

The completion of Phase II testing produced very encouraging results. Most of the problems that occurred in Phase I testing were rectified with the modifications done on the MSAM sampler. Phase II also provided the first attempts at developing operating procedures for use of the MSAM in the field. These protocols were based upon the highly successful IMPROVE system. In Phase II, the MSAM sampler produced 3 valid samples out of 4. The fourth sample was invalid due to a faulty vacuum fitting which has since been corrected. As for the problems encountered in Phase I, the following solutions and data analysis of the solutions are as follows:

1. In Phase I, the most significant problem was due to heavily impregnated filters. This caused a high pressure drop and a significant loss of impregnate. The procedure for the quality assurance of the impregnated filters was changed before the start of Phase II. The old procedure just checked the flow rate across the filter. The new procedure includes the measurement of the pressure drop across the filter at the laboratory, prior to shipment of the filter pack. If the pressure drop is more than 7 inches of mercury, the filter is replaced with a new one and rechecked for pressure drop. The data from Phase II shows an improvement with species collected by impregnated filter, such as ammonia and sulfur dioxide.

2. The mass concentration differed in the Phase I tests between the MSAM and CADMP sampler was related to the filter impregnant problem. Since the filters measured for mass precede the impregnated filters, the flow rate also affected the

mass concentration calculations. The mass concentration was solved with the same solution as the impregnated filters. The mass concentration comparisons from Phase II showed the improvements Additional tests were also completed at UC Davis (see section 4.3).

3. In Phase I tests, the denuder appeared to have allowed some penetration of the nitric acid vapor. After coating the denuder with sodium carbonate, the sampler was sent to Barton Flats. During the Phase II tests, the amount of nitric acid detected by the CADMP sampler was very low.

4. Analysis of ammonium was done through automated colorimetry from a Teflon filter. The Teflon was chosen over the Nylasorb filter. In accordance with DRI Laboratory's past experience, the analysis of NH_4^+ off Teflon was easier and more accurate than a Nylasorb due to the buffer solution required to extract the Nylasorb filter for nitrates. As evidenced in Figure 19, this modification reported the MSAM's value NH_4^+ within acceptable limits (within 20 percent).

5. One problem did arise from Phase II tests of the MSAM sampler. In an effort to reduce the chances of clogging in the total nitrate channel, a Teflon filter was added in front of the Nylasorb filter. The total nitrate was extracted from both the Teflon filter and with the Nylasorb back-up filter. Unfortunately, the filters were placed incorrectly (not in accordance with ARB's instructions). The filters were to be placed one on top of each other separated by a Teflon support grid. The instructions were misinterpreted, and the filters were loaded into a plastic double cassette, separating the filter by 2 to 3 centimeters. This probably allowed the nitrates, which volatilized off the Teflon filter, to be lost to the plastic support grid and cassette walls. Also due to delays beyond the control of UCD, the filters were not analyzed until two months after sampling. This allowed more of the nitrate to volatilize off the Teflon filter. UCD recommends that the Teflon filter should be removed leaving only the Nylasorb filter to collect the total particulate nitrates, thereby removing the effect of nitric acid and nitrate absorption by the plastic support grid and cassette walls.

At the end of Phase II, it was decided to continue with testing at UC Davis. The test would provide further investigation of the mass concentration problems from Phase I and check the new impregnated filter protocols. The testing would include co-location of the IMPROVE particulate sampler for standard purposes.

See Appendix B for complete Phase II data set.

3.3 Comparisons at the University of California, Davis

During the month of December 1992, a series of side by side measurements with the well-tested IMPROVE particulate sampler was conducted. The IMPROVE sampler was designed and built by the University of California, Davis to collect $PM_{2.5}$ using the same cyclone incorporated by the MSAM sampler. These samplers are used by the National Park Service as a part of their visibility monitoring program. These tests were specifically aimed to determine if the MSAM sampler had resolved the mass differences found in Phase I testing. Although Phase II showed an improvement in mass concentrations further tests were completed to confirm Phase II's results. It also gave UCD a chance to compare the data between the MSAM and IMPROVE samplers. Table 8 contains the filters and analysis used in the final version of the MSAM sampler. The sampler's final configuration is found in Figure 26's schematic.

Table 8. Filters and Analysis Used for MSAM Sampler in final UC Davis tests.

CHANNEL	AIR FLOW RATE	MEASUREMENT
IMPACTOR-SO_2	10.0 lpm	Stage B: $PM_{2.5\text{-}0.3}$, Elemental Analysis (Na-Pb) Stage C: $PM_{0.3\text{-}0.068}$, Elemental Analysis (Na-Pb) Afterfilter: $PM_{\leq 0.068}$, Elemental Analysis (Na-Pb) K_2CO_3 impregnated filter: Ion Chromatography (SO_2)
TEFLON-CITRIC ACID	5.0 lpm	Teflon filter: $PM_{2.5}$ Mass, Laser, Elemental Analysis (H, Na-Pb) Citric acid impregnated filter: Automated Colorimetry (NH_3)
TEFLON-TEA	2.5 lpm	Teflon filter: Ion Chromatography (NH_4^+) TEA Impregnated filter: Automated Colorimetry (NO_2)
TOTAL NITRATE	2.5	Nylasorb filters: Ion Chromatography (Total NO_3^-, $SO_4^=$)
PARTICULATE NITRATE	2.7	Nylasorb filter: Ion Chromatography (Particulate NO_3^-, $SO_4^=$)

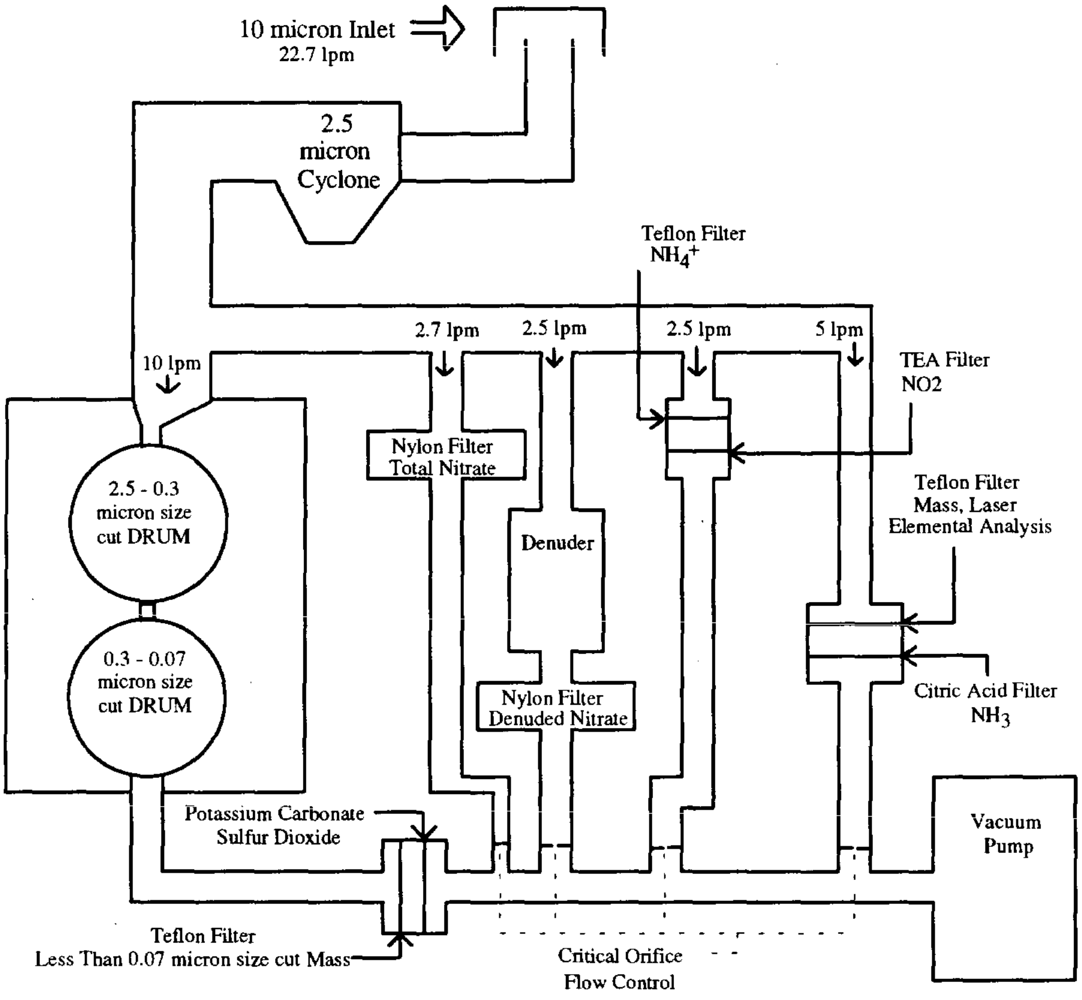

Figure 26. Schematic of final version of the MSAM sampler.

3.3.1 Summary of Data

The results of the comparison are shown in Figures 27 and 28. Figure 27 plots the two $PM_{2.5}$ filters from the MSAM (TC and TT) sampler versus the IMPROVE sampler (A1). Three IMPROVE samplers and on MSAM sampler were setup at the field study site located on the campus of UCD. Daily 24-hour samples were taken over a two week period. Every period, except one, shows good agreement. The sample taken December 22, 1992, has a mass problem that occurred due to pump malfunction in the IMPROVE sampler. Figure 28 shows the correlation between the MSAM and IMPROVE $PM_{2.5}$ mass concentration without the sample taken December 22, 1992. From these results, it was determined that the mass problem has been corrected.

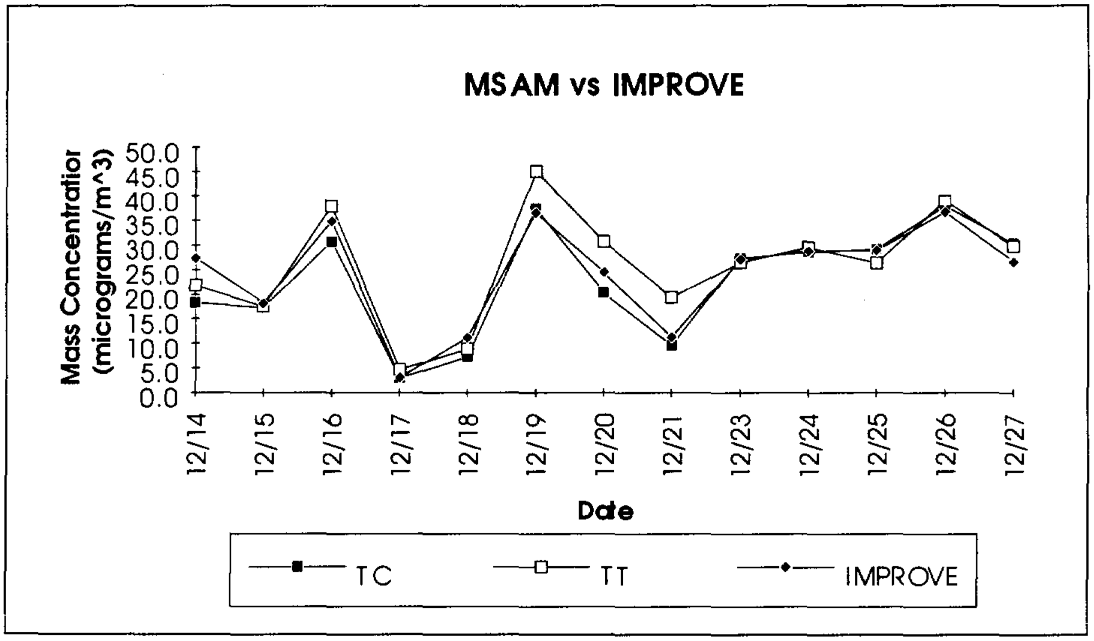

Figure 27. Time plot of mass concentrations (μg/m3) of the IMPROVE sampler and the MSAM sampler. TC and TT refer to mass taken from two of the MSAM Teflon filters.

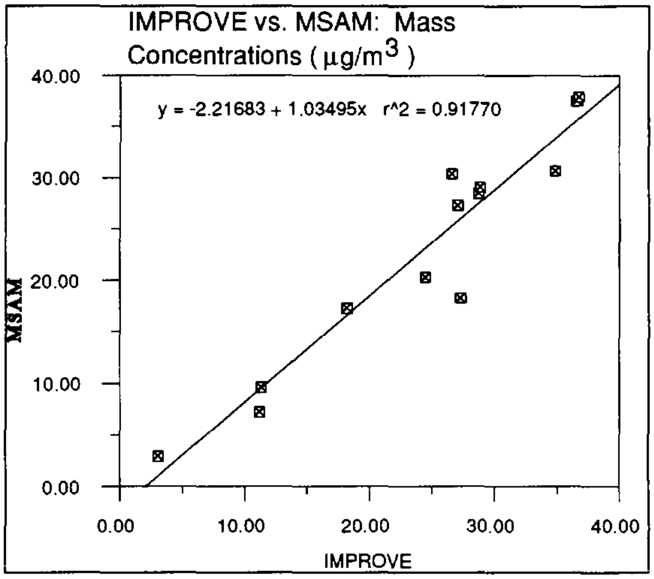

Figure 28. Correlation plot of IMPROVE vs. MSAM mass concentrations in μg/m^3.

3.3.2 Evaluation of Tests

The tests completed at the University of California, Davis produced additional data to support the modifications done on the MSAM sampler during Phase II to measure mass concentrations. The modifications included additional quality assurance of impregnated filters and the arrangement of filter cassette packs.

3.4 Final Evaluation

Following Phase I, there were many problems to overcome. Because of UCD's experience with the aerosol samplers, most of the problems were identified and modifications completed before Phase II. Although Phase II clearly shows an improvement in the sampler, additional problems occurred. After Phases I and II, an agreement can be shown with most of the species except for total nitrate and nitric acid. Since nitric acid is dependent upon total nitrate measurements, accurate total nitrate measurement is essential for the success of the MSAM sampler. But with the successes in the measurement of mass concentration, sulfates, ammonia, ammonium, NO_2, SO_2, size-time resolved particles and elemental analysis, UCD believes with a few more modifications and tests the MSAM sampler has great potential.

3.5 Cost Considerations

One of the main objectives was keeping the cost for running the MSAM sampler low. Costs were kept low because the number of samples needed to be analyzed, as compared the CADMP, are substantially lower and the design of the sampler simplified.

The cost for construction of a MSAM site is approximately $11,000.00. The costs will vary based upon the amount ordered. The cost includes the fabrication of the on site stand and module along with two filter packs. The site would then be setup by UCD or ARB personnel. Once the site is set up the majority of the cost will be filter analyses. The filters available for analysis and their cost per two weeks is shown in Table 9. As Table 9 shows to analyze all the filters from one site per year would cost less than $7,000.

Table 9. Cost of Filter Analysis

CHANNEL	MEASUREMENT	Total Cost/2 week
IMPACTOR-SO_2	1. Afterfilter: $PM_{\leq 0.068}$, Elemental Analysis (Na-Pb) 2. K_2CO_3 impregnated filter: Ion Chromatography (SO_2)	1. $53.00 1. $28.47
TEFLON-CITRIC ACID	1. Teflon filter: $PM_{2.5}$ Mass, Laser, Elemental Analysis (H, Na-Pb) 2. Citric acid impregnated filter: Automated Colorimetry (NH_3)	1. $53.00 2. $25.72
TEFLON-TEA	1. Teflon filter: Ion Chromatography (NH_4^+) 2. TEA Impregnated filter: Automated Colorimetry (NO_2)	1. $25.72 2. $25.72
TOTAL NITRATE	1. Nylasorb filters: Ion Chromatography (Total NO_3^-, $SO_4^=$)	1. $28.47
PARTICULATE NITRATE	1. Nylasorb filter: Ion Chromatography (Particulate NO_3^-, $SO_4^=$)	1. $28.47
	Total / two weeks	**$268.57**
	Total / year	**$6,982.82**

All of the filters would be analyzed once a minimal amount of filters are collected to reduce cost of data processing. Once the filters are analyzed, the impactor's strips would subsequently analyzed. To keep analysis costs down, only time periods of interest would be analyzed. The time periods would be picked based upon the available meteorological and filter analysis. Once the desired impactor strips are chosen, UCD would analyze the samples. The cost for analysis per 4-hour period is $13. If a full strip were to be analyzed (eighty-four 4-hour time periods), the cost would total $1,092. For two full strips the total cost would be $2,184. The maximum cost for a MSAM two week sample would be $2,470.75.

4.0 Project Summary

4.1 Major Findings

Following Phase I and Phase II testing, the MSAM sampler has met most of the goals set out in the proposal to the California Air Resources Board. Once the question of the lack of total nitrate is resolved, UCD believes that the MSAM sampler will developed into a low maintenance, highly resolved aerosol monitor for use in the forests of California and elsewhere that the California Air Resource Board sees fit.

4.2 Phase I

Phase I offered the first field test of the MSAM sampler. The MSAM sampler ran opposite a California Air Resources' acid deposition sampler (CADMP) at the downtown Sacramento CADMP site. In the initial test, the results were quite positive. They included agreements in sulfates, sulfur dioxide, total nitrates, ammonia and nitric oxide. Other positive results include the excellent agreement with the two side by side MSAM samplers. They not only agreed with the species extracted from the filters but also with the elements taken from the impactor substrates.

The Phase I tests did include some minor discrepancies between the MSAM and the CADMP samplers. They included mass concentrations, denuded nitrates and ammonium. After a review of the design of the MSAM sampler, the problems were identified and modifications were done. After the modifications to the samplers were completed the MSAM was prepared for Phase II trials.

4.3 Phase II

Phase II provided the first true field tests. The MSAM sampler was set up at the CADMP test site located at Barton Flats, near the San Bernardino Mountains. Not only did Phase II set the stage for tests of the modifications completed on the MSAM sampler but the logistics of maintaining a site through the mail. With the lessons learned in Phase I, the modified sampler resolved most of the problems encountered in the tests conducted at the Sacramento CADMP site. Since the collocated CADMP sampler ran on a one day in six schedule versus the MSAM full 14 day average, the data provided by the CADMP was used as a guide rather than a direct comparison. With the comparison of the data you would expect a 10 percent to 30 percent differences between the means (general observation) of the CADMP and MSAM sampler, due to the differing operating schedules. Also in remote areas, a 30 percent to 50 percent accuracy is very good since the ambient levels are generally low (probably close to a few micrograms per cubic meter. After examining the data from the Phase II trials, the MSAM sampler performed well except for the collection of total nitrate. The problem stems from the use of the Teflon filter to capture and retain nitrate particles. From UCD's experience, it is very difficult to collect and analyze nitrate from Teflon. Although this can be done, special precautions must be followed. The Teflon filter should be kept cold and analyzed as soon as possible to assure that the nitrates on the filter are not lost to volatilization. Because of the long time delay between sampling and analysis, this could not be assured during Phase II testing.

4.4 Phase III

The results from Phase I showed a less than satisfactory agreement between the MSAM and CADMP for mass concentration. Because of the small number of samples collected in Phase II, it was decided to continue the mass concentration tests at UCD. The tests were conducted using the MSAM sampler and collocating it with the IMPROVE particulate sampler. Since collection of mass will show that the sampler's flow system is operating to specifications, Phase III testing was developed. As the tests show, the modifications done between Phase I and II showed that the mass concentration agreement between each of the filters in the MSAM sampler and IMPROVE particulate sampler were within a 5 percent agreement.

5.0 CONCLUSIONS

The objective of the MSAM project was to develop and demonstrate a monitoring system that can be economically deployed throughout the state and provide data comparable to that of the standard CADMP sampler. The design of the MSAM sampler consisted of old technologies merged in new ways. Sample collection was based upon techniques developed and used by various laboratories including University of California at Davis' Air Quality Group. These included cyclone, denuder, filter substrate and flow rate control devices. The addition of an impactor will also enhance the MSAM samplers capabilities. The impactor will provide information not only on particle size distribution modes but on particle growth. Along with sample collection techniques, sample analysis uses some of the same procedures concurrently used in the CADMP sampler, and some of the same protocols used in the IMPROVE visibility program for the National Parks, mainly elemental analysis of $PM_{2.5}$ aerosols.

After Phase I and II trials, the University of California at Davis has provided a sampler that has achieved most of the objectives of the proposals. With the results of Phase I and II testing and UCD's experience with aerosol sampling, UCD believes that it can overcome the problems occurring with total nitrate collection. UCD recommends that with further modifications and testing, in a short period of time, the MSAM can provide the ARB with a sampler that could only enhance the California Acid Deposition Program.

6.0 REFERENCES

Bowers, Kenneth J., Paul Wakabayashi, Thomas A. Cahill, Robert A. Eldred, Robert Matsumura, and Steve Teague. Particulate matter by size and composition at remote USFS sites. Report to The United States Forest Service, U.S. Department of Agriculture (1990).

Cahill, Thomas A. Air quality in the Lake Tahoe basin. *Proceedings of the Lake Tahoe Research Seminar*, II. South Lake Tahoe, CA, Sep. 27. Pp. 63-68 (1974).

Cahill, Thomas A. Ion-excited x-ray analysis of environmental samples. Chapter 1 of New uses for ion accelerators. James Ziegler, Editor. Plenum Press Pp. 1-72 (1975).

Cahill, Thomas A. Comments on surface coatings for Lundgren-type impactors. *Aerosol Measurement*. Dale A. Lundgren, Editor. University Presses of Florida. Pp. 131-134 (1979).

Cahill, T.A., J. Barone, R.A. Eldred, R.G. Flocchini, D.J. Shadoan, and T.M. Dietz. Influence of sulfur size distribution on optical extinction. *Environmental and Climatic Impact of Coal Utilization*. J.J. Singh and A. Deepak, Editors. Academic Press. Pp. 213-244 (1980).

Cahill, T.A. Proton microprobes and particle-induced x-ray analytical systems. *Annual Reviews Nuclear and Particle Science* 30:211-252 (1980).

Cahill, T.A., C. Goodart, J.W. Nelson, R.A. Eldred, J.S. Nasstrom, and P.J. Feeney. Design and evaluation of the drum impactor. *Proceedings of International Symposium on Particulate and Multi-phase Processes*. Hemisphere Publishing Corporation, Washington, D.C. Teoman Ariman and T. Nejat Veziroglu, Editors. 2:319-325. (1985).

Cahill, T.A., R.A. Eldred, P.J. Feeney, R.G. Flocchini, M. Pitchford, and W. Malm. Ultra-fine sulfur-containing aerosols in the West. *Proceedings of Symposium on Heterogenenis Processes in Source-Dominated Atmospheres*. New York, NY, Oct. 8-11. R. Leifer, Editor (1985).

Cahill, Thomas A., Patrick J. Feeney, and Robert A. Eldred. Use of size selective sampling to aid in source apportionment in remote areas. *Proceedings of Fifth Symposium on Environmental Analytical Chemistry*. Provo, UT, June 18. Pp. 1-21 (1986).

Cahill, Thomas A., Robert A. Eldred, Don Wallace, and Bruce H. Kusko. The hydrogen-sulfur correlation, by PIXE plus PESA, and aerosol source identification. 4th Int. PIXE Conf. Published in *Nucl. Instr. & Methods in Phys. Res.* Tallahassee, FL, June 9-13 (1986). B22:296-300 (1987).

Cahill, Thomas A., Patrick J. Feeney, and Robert A. Eldred. Size-time composition profile of aerosols using the drum sampler. 4th Int. PIXE Conf. Published in *Nucl. Instr. & Methods in Phys. Res.* Tallahassee, FL, June 9-13 (1986). B22:344-348 (1987).

Cahill, Thomas A., Patrick J. Feeney, Robert A. Eldred, and William C. Malm. Size/time/composition data at Grand Canyon National Park and the role of ultrafine sulfur particles. In *Transactions TR-10; Visibility Protection: Research and Policy Aspects.* P. Bhardwaja, Editor. Pp. 657-667 Pittsburgh, PA: APCA (1987).

Cahill, Thomas A., Marcelle Surovik, Robert A. Eldred, Patrick J. Feeney, and Nehzat Motallebi. Visibility and particulate size at the 1986 "Carbon Shoot-out" and 1987 "WHITEX" programs. *Proceedings of the APCA 81st Annual Meeting,* Dallas, TX, June 19-24. Paper No. 88-54.2:1-20 (1988).

Cahill, Thomas, Robert Matsumura, Paul Wakabayashi, and Marcelle Surovik. Size-resolved aerosols and visibility during the Southern California air quality study. *Proceedings of the Air and Waste Mgt. Assoc. 82nd Ann. Mtg. and Exhib.* Anaheim, CA, June 25-30. Paper No. 89-154.3:1-19 (1989).

Cahill, Thomas A., Marcelle Surovik, and Ian Wittmeyer. Visibility and aerosols during the 1986 carbonaceous species methods comparison study. *Aerosol Science and Technology* 12:149-160 (1990).

Cahill, Thomas A. Particle-induced x-ray emission. *Metals Handbook Ninth Edition,* American Society for Metals. Kathleen Mills, Editor. Vol. 10, Pp. 102-108 (1990).

Cahill, Thomas A. Design constraints on aerosol samplers used in visibility studies in the southwest. In *Visibility and Fine Particles*, C.V. Mathai, Editor, Pittsburgh, PA, pp. 97-108 (1990).

Cahill, Thomas A., Robert A. Eldred, Patrick J. Feeney, Peter J. Beveridge, and L. Kent Wilkinson. The stacked filter unit revisited. In *Visibility and Fine Particles*, C.V. Mathai, Editor, pp. 213-222 (1990).

Cahill, Thomas A. and Paul Wakabayashi. Compositional analysis of size-segregated aerosol samples. Chapter in the ACS book *Measurement Challenges in Atmospheric Chemistry.* Leonard Newman, Editor. Chapter 7, Pp. 211-228 (1993).

Cahill, Thomas A., Robert T. Matsumura, and Paul Wakabayashi. Size-resolved aerosols and visibility in the south coast air basin. SCAQS Data Analysis Conference. University of California, Los Angeles, CA. July 22-23, 1992. Presented at the A&WMA Conference (1992).

Cahill, Thomas A., Paul Wakabayashi, and Terry James. Size segregated aerosols of the Kuwaiti oil fires. Presented at the Conference on Visibility and Fine Particles. Vienna, September 15-18, 1992. (1992).

Cahill, Thomas A., Paul Wakabayashi, and Terry James. Integrated studies of urban and remote aerosols for analysis of visibility reduction. Presented at the 6th International Conference on PIXE and its Analytical Applications. Tokyo, Japan (1992).

Cahill, Thomas A., Paul Wakabayashi, Kenneth Bowers, Robert A. Eldred, Otto Raabe, Steve Teague, and Mark Van de Water. Two new rotating-DRUM impactors for visibility studies: SMART and the IMPROVEd DRUM. Presented at the Conference on Visibility and Fine Particles. September 15-18, 1992. Vienna, Austria (1992).

Cahill, Thomas A., Paul Wakabayashi, Otto Raabe, and Steve Teague. A new inertial impactor for visibility-reducing aerosols. Presented at the *A&WMA* 85th Annual Meeting and Exhibition. Kansas City, June 21-26 (1992).

Eldred, Robert A., Bruce H. Kusko, and Thomas A. Cahill. The external PIXE milliprobe at Davis: Laser alignment, PIXE calibration, and quality assurance. *Nuclear Instruments and Methods* B3:579-583 (1984).

Eldred, Robert A., Thomas A. Cahill, Marc Pitchford, and William C. Malm. IMPROVE--a new remote area particulate monitoring system for visibility studies. *Proceedings of the APCA 81st Annual Meeting,* Dallas, TX, June 19-24. Paper No. 88-54.3:1-16 (1988).

Eldred, R.A., T.A. Cahill, L.K. Wilkinson, P.J. Feeney, and William C. Malm. Particulate characterization at remote sites across the U.S.: First year results of the NPS/IMPROVE Network. *Proceedings of the Air and Waste Mgt. Assoc. 82nd Ann. Mtg. and Exhib.* Anaheim, CA, June 25-30. Paper No. 89-151.3:1-16 (1989).

Eldred, Robert A., Thomas A. Cahill, L. Kent Wilkinson, Patrick J. Feeney, Judith C. Chow, and William C. Malm. Measurement of fine particles and their chemical components in the IMPROVE/NPS networks. In *Visibility and Fine Particles*, C.V. Mathai, Editor, Pittsburgh, PA, pp. 187-196 (1990).

Ewell, D.M., R.G. Flocchini, L.O. Myrup, and T.A. Cahill. Aerosol transport in the Southern Sierra Nevada. *Journal of Applied Meteorology.* Vol. 28, No. 2, Pp. 112-125, Feb. (1989).

Hering, Susanne V., Bruce R. Appel, W. Cheng, F. Salaymeh, Steven H. Cadle, Patricia A. Mulawa, Thomas A. Cahill, Robert A. Eldred, Marcelle Surovik, Dennis Fitz, James E. Howes, Kenneth T. Knapp, Leonard Stockburger, Barbara J. Turpin, James J. Huntzicker, Xin-Qui Zhang, and Peter H. McMurry. Comparison of sampling methods for carbonaceous aerosols in ambient air. *Aerosol Science and Technology* 12:200-213 (1990).

John, Walter, S.M. Wall and J.L. Ondo. Anew method nitric acid and nitrate aerosol measurement using the dichotomous sampler. *Atmospheric Enviroment.* 22:1627-1635 (1988)

Mathai, C. V., John G. Watson, Jr., C. Fred Rogers, Judith C. Chow, Ivar Tombach, Judith O. Zwicker, Thomas Cahill, Patrick Feeney, Robert Eldred, Marc Pitchford, and Peter K. Mueller. Intercomparison of ambient aerosol samplers used in western visibility and air quality studies. *Environmental Science & Technology.* Vol. 24, No. 7, Pp. 1090-1099 (1990).

Matsuda, Yatsuka and Thomas A. Cahill. Optical analysis of carbon soot in the atmosphere of the Sacramento Valley. *Atm. Env.* (1985).

Motallebi, Nehzat, Thomas A. Cahill, and Robert G. Flocchini. Influence of particulate size on statistical studies of visibility at California regions. *Atmosfera* Pp. 111-126 (1990).

Motallebi, Nehzat, Robert G. Flocchini, Leonard O. Myrup, and Thomas A. Cahill. A principal component analysis of visibility and air pollution in six California cities. *Atmosfera* Pp. 127-141 (1990).

Ouimette, J.R., S.K. Friedlander, and T.A. Cahill. A Technique for determining the contributions of aerosol chemical species to the extinction coefficient. Abstract for American Chemical Society Meetings. San Francisco, CA (1980).

Pedersen, Brian S. and Thomas A. Cahill. Ozone at a remote, high-altitude site in Sequoia National Park, California. *Transactions of Effects of Air Pollution on Western Forests, Air & Waste Management Association.* Richard K. Olson and Allen S. Lefohn, Editors. Anaheim, CA. Vol. 16, Pp. 207-220. June (1989).

Raabe, O.G., D.A. Braaten, R.L. Axelbaum, and S.V. Teague. Calibration and validation of the drum sampler. Abstract for AAAR 4th annual meeting. (Poster Session). Albuquerque, NM, Nov. 18-22 (1985).

Raabe, Otto G., David A. Braaten, Richard L. Axelbaum, Stephen V. Teague, and Thomas A. Cahill. Calibration Studies of the DRUM Impactor. *Journal of Aerosol Science* 19.2:183-195 (1988).

Roberson, John A. And Clayton T. Crowe. *Engineerin Fluid Mechanics* Houghton Milflin Co. Boston (1975).

Teague, S.V., O.G. Raabe, and R.A. Eldred. Small cyclone collection efficiency calibration for IMPROVE samplers. *Eighth Annual AAAR Meeting, 1989.* October 9-13, 1989, Reno, Nevada (1989).

Unger, Charles D. Analysis of a summertime acid rain event in the Sierra Nevada. *Transactions of Effects of Air Pollution on Western Forests, Air & Waste Management Association.* Richard K. Olson and Allen S. Lefohn, Editors. Anaheim, CA. Vol. 16, Pp. 137-146. June (1989).

Wakabayashi, Paul, Thomas A. Cahill, and Teresa James. Size and time resolved aerosols from the Kuwait fires, June-July 1991. Presented at the 6th International Conference on PIXE and its Analytical Applications. Tokyo, Japan (1992).

Wakabayashi, Paul, Thomas A. Cahill, and Teresa James. Size segregated aerosols of the Kuwaiti oil fires. Presented at the Conference on Visibility and Fine Particles. September 15-18, 1992. Vienna, Austria (1992).

Wesolowski, J.J., W. John, W. Devor, T.A. Cahill, P.J. Feeney, G. Wolfe, and R. Flocchini. Collection surfaces of cascade impactors. In *X-ray fluorescence analysis of environmental samples.* Thomas G. Dzubay, Editor. Ann Arbor Science. Pp. 121-130 (1978).

APPENDIX A

Data Set for Testing of
(Modular Sampler for Acid-Deposition Monitoring) MSAM
at the ARB/MLD Site in Sacramento

April 08-29, 1992

Table 10: $SO_4^=$ measured by CADMP (extracted and analyzed by IC by DRI), SFU (3 times PIXE sulfur), and MSAM (3 times PIXE sulfur). (in µg/m^3).

	CADMP	SFU	MSAM1	MSAM2
April 8	0.940 ± 0.065	1.185 ± 0.068		
April 9	0.905 ± 0.062	1.035 ± 0.058		
April 10	0.866 ± 0.058	0.950 ± 0.051		
April 11	1.129 ± 0.078	1.263 ± 0.067		
April 12	1.068 ± 0.073	1.141 ± 0.061		
April 13	1.473 ± 0.098	1.128 ± 0.060		
April 14	0.661 ± 0.045	0.715 ± 0.040		
April 8-14 Average SO^-_4	1.006 ± 0.070	1.060 ± 0.059	1.195 ± 0.061	1.218 ± 0.062
April 15	0.740 ± 0.050	0.783 ± 0.045		
April 16	1.981 ± 0.137	1.952 ± 0.101		
April 17	0.734 ± 0.050	0.817 ± 0.044		
April 18	0.410 ± 0.027	0.425 ± 0.024		
April 19	0.826 ± 0.056	0.904 ± 0.048		
April 20	1.281 ± 0.084	1.118 ± 0.060		
April 21	0.808 ± 0.054	0.844 ± 0.045		
April 15-21 Average SO^-_4	0.969 ± 0.073	0.977 ± 0.057	1.052 ± 0.054	1.087 ± 0.056
April 22-29 Average SO^-_4		1.012 ± 0.056	1.178 ± 0.061	1.222 ± 0.063

Table 11: NH_4^+ measured by CADMP and MSAM (extracted and analyzed by calorimetry by DRI). (in µg/m^3).

	CADMP	MSAM1	MSAM2
April 8	0.559 ± 0.037		
April 9	0.470 ± 0.031		
April 10	0.378 ± 0.024		
April 11	0.715 ± 0.047		
April 12	0.811 ± 0.055		
April 13	0.567 ± 0.038		
April 14	0.312 ± 0.021		
April 8-14 Average NH^+_4	0.545 ± 0.038	0.647 ± 0.046	0.368 ± 0.023
April 15	0.594 ± 0.041		
April 16	0.838 ± 0.058		
April 17	0.270 ± 0.017		
April 18	0.173 ± 0.010		
April 19	0.434 ± 0.028		
April 20	0.460 ± 0.031		
April 21	0.325 ± 0.020		
Apirl 15-21 Average NH^+_4	0.442 ± 0.033	0.490 ± 0.032	0.391 ± 0.027
April 22-29 Average NH^+_4		0.641 ± 0.045	0.307 ± 0.018

Table 12: NO_3^- measured by CADMP and MSAM (extracted and analyzed by IC by DRI). TN=Total Nitrate Channel, DN=Denuded Nitrate Channel. (in μg/m^3).

	CADMP		MSAM	
	TN	DN	TN	DN
April 8	1.597 ± 0.079	1.278 ± 0.079		
April 9	1.396 ± 0.071	0.716 ± 0.050		
April 10	2.601 ± 0.161	0.971 ± 0.066		
April 11	1.587 ± 0.079	1.182 ± 0.080		
April 12	1.449 ± 0.082	1.531 ± 0.106		
April 13	4.374 ± 0.266	1.335 ± 0.092		
April 14	2.585 ± 0.153	1.279 ± 0.087		
April 8-14 Average NO_3^-	2.227 ± 0.144	1.185 ± 0.082	(MSAM1) 2.025 ± 0.142	1.698 ± 0.118
			(MSAM2) 1.946 ± 0.133	1.794 ± 0.124
April 15	1.672 ± 0.084	1.290 ± 0.089		
April 16	1.584 ± 0.083	0.974 ± 0.067		
April 17	1.335 ± 0.081	0.282 ± 0.017		
April 18	0.880 ± 0.051	0.247 ± 0.017		
April 19	1.999 ± 0.103	0.872 ± 0.060		
April 20	3.819 ± 0.204	1.532 ± 0.103		
April 21	2.012 ± 0.104	1.259 ± 0.085		
April 15-21 Average NO_3^-	1.900 ± 0.111	0.922 ± 0.070	(MSAM1) 1.816 ± 0.104	1.518 ± 0.103
			(MSAM2) 1.530 ± 0.104	1.466 ± 0.101
April 22-29 Average NO_3^-			(MSAM1) 2.022 ± 0.140	1.452 ± 0.099
			(MSAM2) 1.486 ± 0.104	1.467 ± 0.101

Table 13: Nitric acid vapor measured by difference denuder techniques by CADMP and MSAM samplers (see table 4 for total and particulate nitrate values). (in μg/m^3).

	CADMP	MSAM1	MSAM2
April 8	0.319 ± 0.112		
April 9	0.680 ± 0.087		
April 10	1.630 ± 0.174		
April 11	0.405 ± 0.112		
April 12	-0.082 ± 0.134		
April 13	3.039 ± 0.231		
April 14	1.306 ± 0.176		
April 8-14 Average HNO_3	1.042 ± 0.165	0.327 ± 0.185	0.152 ± 0.182
April 15	0.382 ± 0.122		
April 16	0.610 ± 0.107		
April 17	1.053 ± 0.083		
April 18	0.633 ± 0.054		
April 19	1.127 ± 0.119		
April 20	2.287 ± 0.229		
April 21	0.753 ± 0.134		
Apirl 15-21 Average HNO_3	0.978 ± 0.131	0.298 ± 0.146	0.064 ± 0.145
April 22-29 Average HNO_3		0.570 ± 0.171	0.019 ± 0.145

Table 14: SO_2 measured by CADMP and MSAM by K_2CO_3 impregnated filter (extrated and analyzed by IC by DRI). (in $\mu g/m^3$).

	CADMP	MSAM1	MSAM2
April 8	2.003 ± 0.140		
April 9	1.288 ± 0.090		
April 10	1.203 ± 0.084		
April 11	1.248 ± 0.086		
April 12	0.552 ± 0.036		
April 13	1.725 ± 0.115		
April 14	1.210 ± 0.083		
April 8-14 Average SO_2	1.318 ± 0.095	1.818 ± 0.127	1.752 ± 0.122
April 15	0.623 ± 0.042		
April 16	1.219 ± 0.084		
April 17	0.656 ± 0.045		
April 18	0.464 ± 0.031		
April 19	1.184 ± 0.080		
April 20	3.721 ± 0.259		
April 21	1.104 ± 0.075		
April 15-21 Average SO_2	1.282 ± 0.114	2.300 ± 0.153	2.173 ± 0.151
April 22-29 Average SO_2		3.216 ± 0.224	3.268 ± 0.228

Table 15: NH_3 measured by CADMP and MSAM by citric acid impregnated filter (extrated and analyzed by colorimetry by DRI). (in µg/m^3).

	CADMP	MSAM1	MSAM2
April 8	5.993 ± 0.419		
April 9	7.091 ± 0.493		
April 10	4.093 ± 0.284		
April 11	1.856 ± 0.129		
April 12	1.409 ± 0.099		
April 13	2.907 ± 0.197		
April 14	4.607 ± 0.320		
April 8-14 Average NH_3	3.994 ± 0.309	5.676 ± 0.396	5.570 ± 0.390
April 15	2.146 ± 0.149		
April 16	6.992 ± 0.487		
April 17	3.006 ± 0.208		
April 18	1.887 ± 0.234		
April 19	3.342 ± 0.233		
April 20	7.383 ± 0.511		
April 21	3.336 ± 0.231		
April 15-21 Average NH_3	4.013 ± 0.322	7.774 ± 0.543	7.264 ± 0.507
April 22-29 Average NH_3		9.270 ± 0.648	9.497 ± 0.664

Table 16: NO_2 measured by CADMP and MSAM by TEA impregnated filter (extrated and analyzed by colorimetry by DRI). (in μg/m^3).

	CADMP	MSAM1	MSAM2
April 8	22.697 ± 1.298		
April 9	17.980 ± 1.245		
April 10	0.220 ± 0.037		
April 11	15.572 ± 1.058		
April 12	16.847 ± 1.166		
April 13	13.957 ± 0.936		
April 14	21.177 ± 1.466		
April 8-14 Average NO_2	15.493 ± 1.117	16.528 ± 1.156	16.228 ± 1.135
April 15	16.920 ± 1.152		
April 16	15.484 ± 1.084		
April 17	10.533 ± 0.734		
April 18	7.065 ± 0.486		
April 19	27.114 ± 1.896		
April 20	19.629 ± 1.309		
April 21	15.887 ± 1.088		
April 15-21 Average NO_2	16.090 ± 1.181	11.331 ± 0.791	11.332 ± 0.792
April 22-29 Average NO_2		10.745 ± 0.748	10.866 ± 0.759

Table 17: Particulate Mass measured by CADMP, MSAM, and SFU (Filter pre and post weights by UCD). (in $\mu g/m^3$).

	CADMP	SFU	MSAM1	MSAM2
April 8	4.238 ± 0.233	29.652 ± 0.452		
April 9	3.144 ± 0.173	24.525 ± 0.353		
April 10	2.830 ± 0.170	16.353 ± 0.344		
April 11	5.356 ± 0.170	6.336 ± 0.341		
April 12	7.073 ± 0.173	12.589 ± 0.348		
April 13	4.533 ± 0.378	7.420 ± 0.344		
April 14	3.184 ± 0.171	6.702 ± 0.342		
April 8-14 Average Mass	4.337 ± 0.222	14.797 ± 0.363	9.203 ± 0.102	8.252 ± 0.104
April 15	4.661 ± 0.228	6.208 ± 0.443		
April 16	4.517 ± 0.171	6.612 ± 0.367		
April 17	4.072 ± 0.169	7.536 ± 0.331		
April 18	4.537 ± 0.169	5.366 ± 0.344		
April 19	8.329 ± 0.174	9.106 ± 0.350		
April 20	7.286 ± 0.383	9.234 ± 0.345		
April 21	4.836 ± 0.169	7.318 ± 0.342		
April 15-21 Average Mass	5.463 ± 0.222	7.340 ± 0.362	8.114 ± 0.100	10.043 ± 0.102
April 22		7.153 ± 0.208		
April 23		13.973 ± 0.342		
April 24		10.416 ± 0.343		
April 25		7.014 ± 0.344		
April 26		8.703 ± 0.348		
April 27		9.006 ± 0.346		
April 28		4.902 ± 0.340		
April 22-28 Average Mass		8.738 ± 0.328	10.841 ± 0.101	9.973 ± 0.102

Table 18: Elemental Analysis of MSAM and SFU Filters by PIXE in ng/m^3

MSAM PROJECT FILTERS PIXE ANALYSIS

Filter	**Date**	**H**	**Na**	**Mg**	**Al**	**Si**	**P**	**S**	**Cl**
PERIOD 1									
SFU 01	8 Apr	318.1	99.3	0	0	219.9	0	394.9	0
SFU 02	9 Apr	221.5	163.9	0	34.9	86.3	0	345.1	0
SFU 03	10 Apr	226.2	71.5	37.1	34.9	117.1	0	316.5	0
SFU 04	11 Apr	260.4	97.4	0	0	147.7	0	421.1	0
SFU 05	12 Apr	408.9	0	0	16.4	41.0	0	380.3	0
SFU 06	13 Apr	225.9	281.4	0	13.8	61.0	0	376.0	0
SFU 07	14 Apr	233.0	195.9	26.1	0	105.1	0	238.3	0
AVERAGE	**8-14 Apr**	**270.5714**	**129.9143**	**9.028571**	**14.28571**	**111.1571**	**0**	**353.1714**	**0**
MSAM1T1	**8-14 Apr**	**254.8**	**98.6**	**0**	**0**	**127.4**	**0**	**398.4**	**0**
MSAM2T1	**8-14 Apr**	**250.3**	**110.1**	**8.4**	**36.3**	**140.4**	**0**	**406.0**	**27.1**
PERIOD 2									
SFU 08	15 Apr	196.9	0	0	24.9	67.5	0	261.1	0
SFU 09	16 Apr	235.8	85.7	0	24.9	83.3	0	650.5	0
SFU 10	17 Apr	169.1	126.1	0	0	337.3	0	272.4	373.0
SFU 11	18 Apr	206.1	0	0	0	310.3	0	141.8	0
SFU 12	19 Apr	381.5	136.0	0	0	165.6	0	301.3	0
SFU 13	20 Apr	236.9	386.4	0	0	97.5	0	372.5	396.2
SFU 14	21 Apr	225.0	266.6	0	0	107.0	0	281.2	230.4
AVERAGE	**15-21 Apr**	**235.9**	**142.9714**	**0**	**7.114286**	**166.9286**	**0**	**325.8286**	**142.8**
MSAM1T2	**15-21 Apr**	**235.3**	**149.2**	**0**	**63.7**	**251.6**	**0**	**350.8**	**181.4**
MSAM2T2	**15-21 Apr**	**242.6**	**146.5**	**0**	**65.5**	**240.3**	**0**	**362.2**	**168.4**
PERIOD 3									
SFU 15	22 Apr	283.9	253.8	0	36.7	143.7	0	243.4	79.2
SFU 16	23 Apr	523.9	69.3	24.6	129.5	389.6	0	396.7	0
SFU 17	24 Apr	503.1	0	0	116.1	295.6	0	456.6	0
SFU 18	25 Apr	325.8	0	0	100.4	225.0	0	329.3	0
SFU 19	26 Apr	202.9	195.0	0	0	128.9	0	359.3	95.4
SFU 20	27 Apr	338.9	121.6	0	0	199.9	0	379.0	0
SFU 21	28 Apr	230.6	58.7	0	73.9	212.2	0	195.9	0
AVERAGE	**22-28 Apr**	**344.1571**	**99.77143**	**3.514286**	**65.22857**	**227.8429**	**0**	**337.1714**	**24.94286**
MSAM1T3	**22-28 Apr**	**340.4**	**59.9**	**0**	**121.4**	**350.7**	**0**	**392.8**	**0**
MSAM2T3	**22-28 Apr**	**317.3**	**68.1**	**0**	**154.7**	**334.3**	**0**	**407.2**	**0**

MSAM

Filter	**K**	**Ca**	**Ti**	**V**	**Cr**	**Mn**	**Fe**	**Ni**	**Cu**
PERIOD 1									
SFU 01	57.0	61.9	0	0	0	0	83.3	0	3.1
SFU 02	48.6	28.8	3.5	0	0	0	43.3	0	2.6
SFU 03	35.5	31.4	0	0	0	0	52.1	0	2.1
SFU 04	39.6	37.6	5.1	0	0	1.3	49.0	0	2.2
SFU 05	38.8	26.0	3.8	2.6	2.3	0	40.0	0	2.9
SFU 06	31.3	30.9	1.8	3.2	0	1.2	44.4	0	1.8
SFU 07	28.2	53.5	0	2.0	1.4	0	44.6	0	2.5
AVERAGE	**39.85714**	**38.58571**	**2.028571**	**1.114286**	**0.528571**	**0.357143**	**50.95714**	**0**	**2.457143**
MSAM1T1	**47.4**	**45.9**	**2.9**	**0**	**0**	**1.0**	**61.2**	**0**	**1.4**
MSAM2T1	**46.7**	**49.3**	**3.9**	**0**	**0**	**0**	**66.9**	**0**	**2.1**
PERIOD 2									
SFU 08	28.6	32.1	0	4.3	1.8	3.5	33.5	0	2.3
SFU 09	27.4	32.1	1.3	2.7	0	0	31.3	0	3.0
SFU 10	61.1	118.4	5.0	0	0	2.0	81.3	0	4.1
SFU 11	57.0	76.4	3.5	0	0.5	2.7	72.9	0	6.7
SFU 12	111.9	69.9	4.7	2.2	0	0	62.0	0	2.8
SFU 13	61.3	57.5	2.2	3.1	0	1.1	49.5	0	2.6
SFU 14	41.0	45.3	2.8	0	1.5	0	50.4	0	1.9
AVERAGE	**55.47143**	**61.67143**	**2.785714**	**1.757143**	**0.542857**	**1.328571**	**54.41429**	**0**	**3.342857**
MSAM1T2	**71.3**	**90.4**	**4.7**	**0**	**0**	**2.0**	**82.4**	**0**	**2.8**
MSAM2T2	**71.0**	**89.4**	**4.0**	**0.9**	**0**	**2.0**	**80.6**	**0**	**2.9**
PERIOD 3									
SFU 15	62.1	45.6	4.6	0	1.1	2.3	67.7	0	1.6
SFU 16	118.0	74.5	12.7	0	1.8	0	155.4	0	3.3
SFU 17	135.0	58.0	8.7	2.2	0	3.0	122.4	0	10.5
SFU 18	55.3	56.0	6.1	2.4	0	1.0	93.0	0	2.9
SFU 19	43.9	46.2	4.2	0	0.8	0	51.4	0	2.4
SFU 20	51.9	54.0	6.5	1.8	0	0	82.2	0	2.1
SFU 21	59.8	42.3	10.3	0	0	1.4	77.8	0.5	1.8
AVERAGE	**75.14286**	**53.8**	**7.585714**	**0.914286**	**0.528571**	**1.1**	**92.84286**	**0.071429**	**3.514286**
MSAM1T3	**97.0**	**87.7**	**9.1**	**0.8**	**0**	**2.0**	**159.1**	**0**	**2.3**
MSAM2T3	**99.2**	**94.1**	**9.3**	**0.9**	**0**	**2.3**	**141.6**	**0**	**2.4**

MSAM

Filter	**Zn**	**Ga**	**Au**	**Hg**	**As**	**Pb**	**Se**	**Br**	**Rb**
PERIOD 1									
SFU 01	5.0	0	0	0	0	0	0	1.5	0
SFU 02	3.3	0	0	0	0	4.8	1.8	0	0
SFU 03	4.2	0	0	0	0	4.3	0	2.8	0
SFU 04	3.6	0.6	0	0	0	3.2	0	1.7	0.9
SFU 05	3.9	0	0	0	0	4.7	1.3	2.3	0
SFU 06	3.4	0	0	0	0	4.9	0.8	0	0
SFU 07	3.3	0	0	0	0	4.2	1.0	1.9	0
AVERAGE	**3.814286**	**0.085714**	**0**	**0**	**0**	**3.728571**	**0.7**	**1.457143**	**0.128571**
MSAM1T1	**4.6**	**0**	**0**	**0**	**0**	**3.4**	**0.6**	**1.5**	**0**
MSAM2T1	**5.2**	**0**	**0**	**0**	**0**	**3.2**	**0.5**	**1.6**	**0.5**
PERIOD 2									
SFU 08	2.4	0	3.0	0	0	4.5	2.3	0	0
SFU 09	2.9	0	0	0	0	0	1.2	1.3	0
SFU 10	2.6	0	0	0	0	5.1	0	1.4	0
SFU 11	2.2	0	0	0	0	2.6	1.2	1.7	0
SFU 12	3.9	0	0	0	0	5.3	1.0	4.0	0
SFU 13	2.8	0	0	0	0	4.1	2.4	2.5	1.3
SFU 14	3.1	0	0	0	0.8	3.7	0	1.5	2.4
AVERAGE	**2.842857**	**0**	**0.428571**	**0**	**0.114286**	**3.614286**	**1.157143**	**1.771429**	**0.528571**
MSAM1T2	**3.4**	**0**	**0**	**0**	**0**	**3.2**	**0.6**	**2.1**	**0.6**
MSAM2T2	**3.7**	**0**	**0**	**0**	**0**	**3.0**	**0.6**	**1.8**	**0**
PERIOD 3									
SFU 15	4.0	0	0	0	0	4.7	0	2.7	1.4
SFU 16	5.9	0	0	0	0	3.9	0	3.2	0
SFU 17	22.6	0	0	0	0	8.0	0	2.4	0
SFU 18	3.7	0	0	0	0	3.7	0	2.5	0
SFU 19	2.7	0	0	0	0	4.3	0	2.4	0
SFU 20	5.2	0	0	0	1.0	4.3	1.1	2.2	0
SFU 21	2.7	0	0	0	0	3.0	0.5	1.6	0
AVERAGE	**6.685714**	**0**	**0**	**0**	**0.142857**	**4.557143**	**0.228571**	**2.428571**	**0.2**
MSAM1T3	**8.8**	**0**	**0**	**0**	**0**	**4.6**	**0**	**2.0**	**0**
MSAM2T3	**7.7**	**0**	**0**	**0**	**0**	**5.1**	**0**	**2.2**	**0.5**

MSAM

Filter	**Sr**	**Y**	**Zr**	**Mo**	**Ru**	**Pd**	**Ag**	**Cd**
PERIOD 1								
SFU 01	0	0	0	0	0	0	0	0
SFU 02	6.4	0	0	0	0	0	0	0
SFU 03	1.7	0	0	0	0	0	0	0
SFU 04	2.0	0	0	0	0	0	0	0
SFU 05	0	1.1	0	0	0	0	0	0
SFU 06	0	0	0	0	0	0	8.3	0
SFU 07	0	0	0	0	0	0	0	8.0
AVERAGE	**1.442857**	**0.157143**	**0**	**0**	**0**	**0**	**1.185714**	**1.142857**
MSAM1T1	**0.9**	**0**	**0**	**0**	**0**	**0**	**0**	**0**
MSAM2T1	**0.9**	**0**	**0**	**0**	**0**	**0**	**0**	**0**
PERIOD 2								
SFU 08	0	0	0	0	0	0	0	0
SFU 09	0	0	0	0	0	0	0	0
SFU 10	2.2	0	0	0	0	0	0	0
SFU 11	0	0	3.1	0	0	0	0	0
SFU 12	4.5	2.1	0	0	0	3.6	0	0
SFU 13	0	0	2.3	0	0	0	0	5.1
SFU 14	1.6	0	0	0	0	0	0	0
AVERAGE	**1.185714**	**0.3**	**0.771429**	**0**	**0**	**0.514286**	**0**	**0.728571**
MSAM1T2	**1.0**	**0**	**0**	**0**	**0**	**0**	**0**	**2.5**
MSAM2T2	**1.4**	**0**	**0**	**0**	**0**	**0**	**0**	**0**
PERIOD 3								
SFU 15	0	0	0	0	0	0	0	0
SFU 16	0	0	0	2.6	0	0	0	0
SFU 17	7.6	0	0	0	0	0	0	0
SFU 18	1.4	0	0	0	0	0	0	0
SFU 19	1.9	0	0	0	0	0	0	0
SFU 20	1.6	0	0	0	3.7	0	0	0
SFU 21	0	0	0	0	0	5.6	0	0
AVERAGE	**1.785714**	**0**	**0**	**0.371429**	**0.528571**	**0.8**	**0**	**0**
MSAM1T3	**1.7**	**0**	**0**	**0**	**0**	**0**	**0**	**0**
MSAM2T3	**2.5**	**0**	**0**	**0**	**0**	**0**	**0**	**0**

MSAM

Filter	**BABS**	**OMH**	**KNON**	**NHSO**	**SOIL**	**RCMA**	**MASS**
PERIOD 1							
SFU 01	1.567	3016.40625	7.02	1628.9625	859.862	5763.3871	29625.0
SFU 02	1.426	1859.34375	22.62	1423.5375	481.855	4206.22555	24525.0
SFU 03	1.314	2022.28125	4.24	1305.5625	551.559	4064.15445	16353.0
SFU 04	0.975	2132.96875	10.2	1737.0375	571.815	4699.65	6336.0
SFU 05	2.087	4315.09375	14.8	1568.7375	305.442	6210.0976	12589.0
SFU 06	1.456	1813.625	4.66	1551.0	350.081	4424.8028	7420.0
SFU 07	1.379	2384.59375	1.44	982.9875	458.852	4318.2682	6702.0
AVERAGE	**1.457714**	**2506.33**	**9.282857**	**1456.832**	**511.3523**	**4812.369**	**14792.86**
MSAM1T1	**1.135**	**2134.0**	**10.68**	**1643.4**	**560.725**	**4599.634**	**9203.0**
MSAM2T1	**1.12**	**2046.0**	**6.56**	**1674.75**	**688.463**	**4693.703**	**8252.0**
PERIOD 2							
SFU 08	1.249	1809.84375	8.5	1077.0375	368.148	3266.9917	6208.0
SFU 09	1.031	1006.15625	8.62	2683.3125	404.856	4320.6943	6612.0
SFU 10	0.755	1388.75	12.32	1123.65	1256.563	4101.49875	7536.0
SFU 11	0.689	2346.4375	13.26	584.925	1098.951	4048.91195	5366.0
SFU 12	1.697	4209.90625	74.7	1242.8625	790.019	6687.4526	9106.0
SFU 13	1.321	1976.90625	31.6	1536.5625	504.798	5028.5728	9234.0
SFU 14	1.324	2127.125	10.76	1159.95	482.733	4451.4382	7318.0
AVERAGE	**1.152286**	**2123.589**	**22.82286**	**1344.043**	**700.8669**	**4557.937**	**7340.0**
MSAM1T2	**1.031**	**2029.5**	**21.86**	**1447.05**	**1153.106**	**5033.312**	**8114.0**
MSAM2T2	**0.955**	**2090.688**	**22.64**	**1494.075**	**1122.677**	**5105.433**	**10483.0**
PERIOD 3							
SFU 15	1.539	3066.9375	21.48	1004.025	715.711	5451.32245	7153.0
SFU 16	2.858	5839.96875	24.76	1636.3875	1811.809	9496.22215	13973.0
SFU 17	2.053	5348.0625	61.56	1883.475	1485.274	8803.09815	10416.0
SFU 18	1.206	3347.78125	- 0.5	1358.3625	1108.604	5814.10805	7014.0
SFU 19	0.87	1554.78125	13.06	1482.1125	547.087	4089.80825	8703.0
SFU 20	1.973	3357.0625	2.58	1563.375	800.917	6029.06515	9006.0
SFU 21	1.35	2497.34375	13.12	808.0875	986.533	4457.14975	4902.0
AVERAGE	**1.692714**	**3573.134**	**19.43714**	**1390.832**	**1065.134**	**6305.825**	**8738.143**
MSAM1T3	**1.426**	**3330.25**	**1.54**	**1620.3**	**1688.106**	**6790.633**	**10841.0**
MSAM2T3	**1.453**	**2963.125**	**14.24**	**1679.7**	**1706.78**	**6539.864**	**9973.0**

APPENDIX B

Data Set for Testing of (Modular Sampler for Acid-Deposition Monitoring) MSAM at Barton Flats, California

August 05 - November 06, 1992

Table 19: Elemental analysis by PIXE (in $\mu g/m^3$). Sample is all aerosols ≤ 2.5µm in diameter.

SAMDAT	STTIM	H	NA	MG	AL	SI	P	S	CL	ZN	GA	AU	HG	AS	PB	SE	BR	RB
Aug. 10-15	1215	189.01	0	0	28.2	85.1	0	267.2	0	2.16	0	0	0	0	1.98	0	1.81	0
Sept. 21-Oct. 3	1200	266.58	0	0	151.57	419.65	0	387.11	0	4.05	0	0	0	0	2.94	0	2.39	0.42
Oct. 9-21	1225	395.87	132.93	0	113.44	252.32	0	549.94	0	6.22	0	0	0	0.89	3.11	0	2.78	0
Oct. 27-Nov. 2	1000	137.12	0	0	24.59	57.86	0	232.32	0	2.36	0	0	0	0	1.51	0	1.22	0

Table 20: NO_3^- measured by CADMP (extracted and analyzed by IC by DRI). TN=Total Nitrate Channel,DN=Denuded Nitrate Channel. ($\mu g/m^3$)

DATE	ST. TIME	TN	DN
August 4	6:00:00 AM	1.2477±0.0424	0.6050±0.0289
August 4	6:00:00 PM	1.5326±0.0464	1.5867±0.0721
August 10	6:00:00 AM	4.5593±0.1077	1.8178±0.0809
August 10	6:00:00 PM	1.1787±0.0422	0.5941±0.0285
August 16	6:00:00 AM	2.9923±0.0769	0.5628±0.0273
August 16	6:00:00 PM	1.0782±0.0429	0.6691±0.0315
August 28	6:00:00 AM	4.3208±0.1038	3.2519±0.1437
August 28	6:00:00 PM	2.6103±0.0713	2.5693±0.1170
September 3	6:00:00 AM	7.0401±0.1710	5.6997±0.2532
September 3	6:00:00 PM	4.2061±0.1089	4.0876±0.1963
September 9	6:00:00 AM	8.9589±0.2033	6.6474±0.2927
September 9	6:00:00 PM	1.5935±0.0515	1.2656±0.0570
September 15	6:00:00 AM	5.4764±0.1313	3.8296±0.1690
September 15	6:00:00 PM	3.6035±0.0942	3.6644±0.1618
September 21	6:00:00 AM	4.9523±0.1184	2.6669±0.1217
September 21	6:00:00 PM	3.4949±0.0889	4.2209±0.2027
September 27	6:00:00 AM	3.5124±0.0874	0.7803±0.0363
September 27	6:00:00 PM	0.6454±0.0375	0.1931±0.0175
October 3	6:00:00 AM	3.6038±0.0875	2.4501±0.1146
October 3	6:00:00 PM	0.6992±0.0387	0.5494±0.0274
October 9	6:00:00 AM	5.3579±0.1336	3.3709±0.1489
October 9	6:00:00 PM	1.8033±0.0540	1.4787±0.0662
October 15	6:00:00 AM	5.3374±0.1339	4.2281±0.2052
October 15	6:00:00 PM	0.4879±0.0376	0.2319±0.0187
October 21	6:00:00 AM	15.0817±0.3637	13.8539±0.8032
October 21	6:00:00 PM	2.5638±0.0758	2.3625±0.1056
October 27	6:00:00 AM	11.427±0.2833	11.3577±0.5107
October 27	6:00:00 PM	10.7234±0.2638	10.8351±0.4907
November 2	6:00:00 AM	2.6720±0.0771	1.1034±0.0501
November 2	6:00:00 PM	0.4762±0.0381	0.0596±0.0165
November 8	6:00:00 AM	6.5043±0.1524	6.2420±0.2761
November 8	6:00:00 PM	2.7346±0.0739	2.9474±0.1320
November 14	6:00:00 AM	0.5870±0.0388	0.0950±0.0169
November 14	6:00:00 PM	0.1759±0.0361	0.0733±0.0167
November 20	6:00:00 AM	0.7528±0.0410	0.6309±0.0303
November 20	6:00:00 PM	0.1120±0.0369	0.0527±0.0164
November 26	6:00:00 AM	0.2817±0.0356	0.0525±0.0164
November 26	6:00:00 PM	0.1101±0.0352	0.0036±0.0160

Table 21: $SO_4^=$ measured by CADMP extracted and analyzed by IC by DRI. ($\mu g/m^3$)

DATE	ST. TIME	CONC.
August 4	6:00:00 AM	2.0259±0.0905
August 4	6:00:00 PM	2.2193±0.0986
August 10	6:00:00 AM	1.9996±0.0895
August 10	6:00:00 PM	2.1259±0.0948
August 16	6:00:00 AM	1.6039±0.0728
August 16	6:00:00 PM	2.5518±0.1129
August 28	6:00:00 AM	1.1333±0.0553
August 28	6:00:00 PM	1.2739±0.0600
September 3	6:00:00 AM	1.9837±0.0889
September 3	6:00:00 PM	1.7876±0.0806
September 9	6:00:00 AM	1.8296±0.0826
September 9	6:00:00 PM	1.1623±0.0565
September 15	6:00:00 AM	1.7137±0.0779
September 15	6:00:00 PM	1.9983±0.0897
September 21	6:00:00 AM	1.5305±0.0703
September 21	6:00:00 PM	1.7159±0.0780
September 27	6:00:00 AM	0.8878±0.0479
September 27	6:00:00 PM	0.4747±0.0371
October 3	6:00:00 AM	0.9301±0.0498
October 3	6:00:00 PM	0.6327±0.0413
October 9	6:00:00 AM	1.1058±0.0553
October 9	6:00:00 PM	0.6925±0.0429
October 15	6:00:00 AM	2.3637±0.1051
October 15	6:00:00 PM	0.4456±0.0372
October 21	6:00:00 AM	3.5326±0.2724
October 21	6:00:00 PM	1.8266±0.0825
October 27	6:00:00 AM	1.5456±0.0711
October 27	6:00:00 PM	1.7100±0.0778
November 2	6:00:00 AM	0.1747±0.0343
November 2	6:00:00 PM	0.0744±0.0335
November 8	6:00:00 AM	0.5755±0.0407
November 8	6:00:00 PM	0.5513±0.0398
November 14	6:00:00 AM	0.1961±0.0338
November 14	6:00:00 PM	0.2104±0.0336
November 20	6:00:00 AM	0.3589±0.0367
November 20	6:00:00 PM	0.3296±0.0359
November 26	6:00:00 AM	0.6370±0.0408
November 26	6:00:00 PM	0.2736±0.0337

Table 22: NH_3 measured by CADMP on citric acid impregnated filter (extracted and analyzed by colorimetry by DRI). ($\mu g/m^3$)

DATE	ST. TIME	CONC.
August 4	6:00:00 AM	1.5815±0.0730
August 4	6:00:00 PM	1.0476±0.0540
August 10	6:00:00 AM	2.9752±0.1631
August 10	6:00:00 PM	1.1372±0.0570
August 16	6:00:00 AM	3.5776±0.1816
August 16	6:00:00 PM	1.4528±0.0683
August 28	6:00:00 AM	2.7938±0.1579
August 28	6:00:00 PM	1.5256±0.0709
September 3	6:00:00 AM	3.9265±0.1926
September 3	6:00:00 PM	1.4549±0.0683
September 9	6:00:00 AM	3.7863±0.1921
September 9	6:00:00 PM	1.1735±0.0595
September15	6:00:00 AM	4.1666±0.2054
September15	6:00:00 PM	1.9922±0.0895
September21	6:00:00 AM	4.3668±0.2112
September21	6:00:00 PM	3.2435±0.1757
September27	6:00:00 AM	1.7696±0.0809
September27	6:00:00 PM	0.5819±0.0426
October 3	6:00:00 AM	1.7867±0.0819
October 3	6:00:00 PM	0.5985±0.0436
October 9	6:00:00 AM	1.5201±0.0720
October 9	6:00:00 PM	0.8806±0.0508
October 15	6:00:00 AM	2.8262±0.1644
October 15	6:00:00 PM	0.2304±0.0370
October 21	6:00:00 AM	1.7101±0.0789
October 21	6:00:00 PM	0.9273±0.0517
October 27	6:00:00 AM	2.9752±0.1698
October 27	6:00:00 PM	1.1676±0.0591
November 2	6:00:00 AM	1.5004±0.0714
November 2	6:00:00 PM	0.4614±0.0426
November 8	6:00:00 AM	1.0074±0.0546
November 8	6:00:00 PM	0.4212±0.0415
November 14	6:00:00 AM	0.4970±0.0434
November 14	6:00:00 PM	0.1270±0.0366
November 20	6:00:00 AM	0.2314±0.0380
November 20	6:00:00 PM	0.0000±0.0368
November 26	6:00:00AM	0.0492±0.0359
November 26	6:00:00PM	0.0000±0.03598

Table 23: NH_4^+ measured by CADMP (extracted and analyzed by colorimetry by DRI). ($\mu g/m^3$)

DATE	ST. TIME	CONC.
August 4	6:00:00 AM	0.8140±0.0447
August 4	6:00:00 PM	1.0572±0.0544
August 10	6:00:00 AM	0.9140±0.0485
August 10	6:00:00 PM	0.9709±0.0509
August 16	6:00:00 AM	0.6957±0.0413
August 16	6:00:00 PM	1.0077±0.0523
August 28	6:00:00 AM	0.9143±0.0487
August 28	6:00:00 PM	0.9896±0.0518
September 3	6:00:00 AM	1.6025±0.0789
September 3	6:00:00 PM	1.6909±0.0828
September 9	6:00:00 AM	1.1375±0.0584
September 9	6:00:00 PM	0.7053±0.0427
September 15	6:00:00 AM	1.3080±0.0660
September 15	6:00:00 PM	1.5299±0.0759
September 21	6:00:00 AM	0.9809±0.0517
September 21	6:00:00 PM	1.2887±0.0651
September 27	6:00:00 AM	0.3490±0.0380
September 27	6:00:00 PM	0.2414±0.0334
October 3	6:00:00 AM	0.4685±0.0471
October 3	6:00:00 PM	0.3014±0.0350
October 9	6:00:00 AM	0.4864±0.0485
October 9	6:00:00 PM	0.3597±0.0390
October 15	6:00:00 AM	1.1536±0.0592
October 15	6:00:00 PM	0.2330±0.0340
October 21	6:00:00 AM	5.4194±0.3182
October 21	6:00:00 PM	1.3427±0.0674
October 27	6:00:00 AM	3.8367±0.1826
October 27	6:00:00 PM	3.5963±0.1715
November 2	6:00:00 AM	0.0956±0.0338
November 2	6:00:00 PM	0.0401±0.0334
November 8	6:00:00 AM	1.0614±0.0555
November 8	6:00:00 PM	0.7598±0.0450
November 14	6:00:00 AM	0.0860±0.0331
November 14	6:00:00 PM	0.0816±0.0327
November 20	6:00:00 AM	0.1547±0.0343
November 20	6:00:00 PM	0.0381±0.0334
November 26	6:00:00 AM	0.2110±0.0329
November 26	6:00:00 PM	0.0666±0.0319

Table 24: SO_2 measured by CADMP on K_2CO_3 impregnated filter (extrated and analyzedby IC by DRI). (µg/m^3)

DATE	ST. TIME	CONC.
August 4	6:00:00 AM	0.4770±0.0776
August 4	6:00:00 PM	0.2948±0.0760
August 10	6:00:00 AM	1.6907±0.1014
August 10	6:00:00 PM	1.4898±0.0959
August 16	6:00:00 AM	1.0643±0.0868
August 16	6:00:00 PM	1.4263±0.0949
August 28	6:00:00 AM	0.9087±0.0838
August 28	6:00:00 PM	1.1361±0.0878
September 3	6:00:00 AM	1.3542±0.0930
September 3	6:00:00 PM	0.8779±0.0829
September 9	6:00:00 AM	1.4822±0.0996
September 9	6:00:00 PM	0.5440±0.0833
September 15	6:00:00 AM	1.1020±0.0925
September 15	6:00:00 PM	0.6744±0.0857
September 21	6:00:00 AM	1.2850±0.0955
September 21	6:00:00 PM	0.9089±0.0882
September 27	6:00:00 AM	0.8744±0.0873
September 27	6:00:00 PM	0.3273±0.0810
October 3	6:00:00 AM	0.5591±0.0851
October 3	6:00:00 PM	0.3031±0.0825
October 9	6:00:00 AM	1.4683±0.1009
October 9	6:00:00 PM	0.8414±0.0887
October 15	6:00:00 AM	0.2178±0.0813
October 15	6:00:00 PM	0.2742±0.0810
October 21	6:00:00 AM	0.6151±0.0853
October 21	6:00:00 PM	0.3237±0.0818
October 27	6:00:00 AM	0.7960±0.0881
October 27	6:00:00 PM	0.2072±0.0799
November 2	6:00:00 AM	0.4991±0.0849
November 2	6:00:00 PM	0.1341±0.0823
November 8	6:00:00 AM	0.9193±0.0904
November 8	6:00:00 PM	0.3188±0.0831
November 14	6:00:00 AM	0.2512±0.0823
November 14	6:00:00 PM	0.2291±0.0817
November 20	6:00:00 AM	0.3520±0.0837
November 20	6:00:00 PM	0.2786±0.0833
November 26	6:00:00 AM	0.5101±0.0830
November 26	6:00:00 PM	0.2129±0.0807

Table 25: $PM_{2.5}$ measured by CADMP (µg/m^3)

DATE	ST. TIME	CONC.
August 4	6:00:00 AM	7.3384±1.1705
August 4	6:00:00 PM	11.4723±1.2213
August 10	6:00:00 AM	7.8846±1.1811
August 10	6:00:00 PM	11.4723±1.2213
August 16	6:00:00 AM	8.0909±1.1853
August 16	6:00:00 PM	19.4893±1.3829
August 28	6:00:00 AM	6.7949±1.1703
August 28	6:00:00 PM	9.6877±1.1963
September 3	6:00:00 AM	12.1154±1.2371
September 3	6:00:00 PM	10.4525±1.2066
September 9	6:00:00 AM	12.292±1.3023
September 9	6:00:00 PM	5.1838±1.2288
September 15	6:00:00 AM	8.6915±1.2733
September 15	6:00:00 PM	11.3832±1.3070
September 21	6:00:00 AM	6.2799±1.2378
September 21	6:00:00 PM	13.1642±1.3205
September 27	6:00:00 AM	4.8217±1.2212
September 27	6:00:00 PM	2.3740±1.2082
October 3	6:00:00 AM	4.4590±1.2499
October 3	6:00:00 PM	2.5634±1.2345
October 9	6:00:00 AM	9.0573±1.2891
October 9	6:00:00 PM	4.5293±1.2505
October 15	6:00:00 AM	8.6426±1.2661
October 15	6:00:00 PM	0.7494±1.2101
October 21	6:00:00 AM	27.514±1.6508
October 21	6:00:00 PM	7.1933±1.2501
October 27	6:00:00 AM	19.7171±1.4671
October 27	6:00:00 PM	19.6118±1.4313
November 2	6:00:00 AM	2.1013±1.2466
November 2	6:00:00 PM	0.9059±1.2379
November 8	6:00:00 AM	11.1368±1.3211
November 8	6:00:00 PM	4.7383±1.2518
November 14	6:00:00 AM	2.3564±1.2342
November 14	6:00:00 PM	0.9645±1.2239
November 20	6:00:00 AM	1.8912±1.2460
November 20	6:00:00 PM	0.4205±1.2446
November 26	6:00:00 AM	2.7296±1.2166
November 26	6:00:00 PM	0.4088±1.2099

Table 26: Comparison of one day in six averaged over 14 days for the CADMP and true 14 day average for the MSAM (μg/m^3)

SPECIES	DATES	CADMP	MSAM
$SO_4^=$	Aug.10-16	2.0882±0.0539	2.1130±0.6803
	Sept. 21-Oct. 3	1.2909±0.0407	1.2048±0.0439
	October 9-21	2.3119±0.0594	1.4183±0.0565
NH_4^+	Aug.10-16	0.8971±0.0483	0.7690±0.0132
	Sept. 21-Oct. 3	0.6050±0.0451	0.5873±0.0102
	October 9-21	1.4991±0.0944	1.1614±0.0142
NH_3	Aug.10-16	2.2857±0.1175	2.0347±0.2172
	Sept. 21-Oct. 3	2.0578±0.1060	1.9236±0.2054
	October 9-21	1.3491±0.0758	1.4127±0.1515
NO_3^-(TN)	Aug.10-16	2.4521±0.0674	0.8003±0.0211
	Sept. 21-Oct. 3	2.8180±0.0764	0.9416±0.0314
	October 9-21	5.1053±0.1331	2.0116±0.0597
NO_3^-(DN)	Aug.10-16	0.9110±0.0421	1.2858±0.0410
	Sept. 21-Oct. 3	1.8101±0.0867	1.6807±0.0407
	October 9-21	4.2543±0.2246	5.1400±0.1162
HNO_3	Aug.10-16	1.5412±0.0801	-0.4855±0.0462
	Sept. 21-Oct. 3	0.9728±0.1431	-0.7391±0.0514
	October 9-21	0.8058±0.1226	-3.1285±0.1307
SO_2	Aug.10-16	1.4178±0.0948	1.4996±0.0417
	Sept. 21-Oct. 3	0.7096±0.0866	0.5535±0.0459
	October 9-21	0.6234±0.0865	0.7246±0.0594
MASS	Aug.10-16	11.7343±1.2427	9.7200±0.0752
	Sept. 21-Oct. 3	5.6104±1.2454	7.4400±0.0757
	October 9-21	9.6143±1.3195	9.9200±0.0895

Table 27: HNO_3 measured by CADMP by denuder difference technique. ($\mu g/m^3$)

DATE	ST. TIME	CONC.
August 4	6:00:00 AM	0.6530±0.0679
August 4	6:00:00 PM	-0.0550±0.0990
August 10	6:00:00 AM	2.7854±0.1981
August 10	6:00:00 PM	0.5940±0.0677
August 16	6:00:00 AM	2.4684±0.1257
August 16	6:00:00 PM	0.4156±0.0715
August 28	6:00:00 AM	1.0860±0.2089
August 28	6:00:00 PM	0.0417±0.1610
September 3	6:00:00 AM	1.3618±0.3585
September 3	6:00:00 PM	0.1204±0.2698
September 9	6:00:00 AM	2.3485±0.4417
September 9	6:00:00 PM	0.3331±0.0950
September 15	6:00:00 AM	1.6731±0.2551
September 15	6:00:00 PM	-0.0619±0.2227
September 21	6:00:00 AM	2.3220±0.2109
September 21	6:00:00 PM	-0.7376±0.2456
September 27	6:00:00 AM	2.7758±0.1470
September 27	6:00:00 PM	0.4595±0.0570
October 3	6:00:00 AM	1.1722±0.1809
October 3	6:00:00 PM	0.1522±0.0624
October 9	6:00:00 AM	2.0188±0.2777
October 9	6:00:00 PM	0.3298±0.1053
October 15	6:00:00 AM	1.1270±0.3012
October 15	6:00:00 PM	0.2601±0.0573
October 21	6:00:00 AM	1.2474±1.0641
October 21	6:00:00 PM	0.2045±0.1611
October 27	6:00:00 AM	0.0704±0.7441
October 27	6:00:00 PM	-0.1135±0.6995
November 2	6:00:00 AM	1.5937±0.1356
November 2	6:00:00 PM	0.4233±0.0574
November 8	6:00:00 AM	0.2665±0.3558
November 8	6:00:00 PM	-0.2162±0.1743
November 14	6:00:00 AM	0.4999±0.0588
November 14	6:00:00 PM	0.1042±0.0547
November 20	6:00:00 AM	0.1239±0.0672
November 20	6:00:00 PM	0.0602±0.0557
November 26	6:00:00 AM	0.2329±0.0541

Appendix C

Analysis of Nitrate Results from the Barton Flats test of MSAM

Introduction

The improvements made in the MSAM sampler prior to the Barton Flats tests resulted in improved performance in almost every category of sampling except the nitrates. This was unexpected and very disturbing, since MSAM (and IMPROVE, using identical protocols) had performed very well in this measurements from even the very first tests. This "Appendix C" is designed to examine in some depth the problems of the Barton Flats nitrate measurements, to see if it is a problem inherent to the MSAM protocols or merely a blunder or fluke that can be avoided in the future.

Analysis

MSAM uses the "Denuder Difference Method" to measure nitrates. The method relies on capture of nitrate on two parallel filters, each Nylasorb, one accepting the aerosols and gasses directly, the other accepting only aerosols since it is placed behind a denuder designed to collect acidic vapors and gases. The two filters are analyzed by ion chromatography for ions such as nitrates, sulfates, and chlorides. The subtraction of the "total nitrate" channel from the "denuded nitrate" channel gives the value for acidic gasses and vapors in general, and nitric acid in particular. This method had the best performance of any in the 1985 nitrate intercomparison ("The Nitrogen Species Methods Comparison", Lawson, 1988), and was the basis for the SCAQS and CADMP measurements and the IMPROVE nitrate Channel B, now used all over the US.

After the experience of clogging on the nylon filters used in some SCAQS samples, it was recommended that a Teflon pre-filter be added to the MSAM "total nitrate" just prior to the Barton Flats tests. In retrospect, it was a mistake to add an unproven protocol to this test at the last moment, but the opportunity to run side by side with the CADMP sampler was essential to analysis of the performance of MSAM. Unfortunately, a series of errors was made that ruined the nitrate results:

Error #1. The Teflon pre-filter was placed in a separate cassette well in front of the Nylasorb filter, not directly in the same cassette with the Nylasorb filter.

This error was understandable since this is the standard way we handle filter pairs that use mass/elemental/optical analysis. Placing two filters in contact ruins such measurements in many cases. But in this case, it was wrong. The Teflon filter will collect a significant fraction of the particulate nitrates that is present in the atmosphere, never less than 30 percent, often approaching 100 percent. This is shown in the results of tests recently concluded in Davis in summer, 1991, in situations of high heat and low humidity that maximize evolution of particulate nitrates into gaseous nitrates, and subsequent loss from a Teflon filter.

Figures C-1 and C-2 show the results of these tests. From a detailed analysis of these results, we have extracted loss rates of nitrate versus filter loading, mass, etc. But the main point is that nitrates are lost from Teflon in these conditions. It is also important to recognize that about 30 percent of the nitrate was retained, even in such extreme conditions.

These tests gave almost the precise experience of the WRAQS tests (as presented by Dr. Warren White, ACS Meeting, Denver, 1987) that showed up to 66 percent loss of nitrates in summer but almost total collection in winter from Teflon filters at sites throughout the arid west.

In the MSAM test, the Teflon filter was in a standard plastic holder, which placed the filter directly on plastic support structures, grids, etc., and well upstream of the Nylasorb filter. Thus, any particulate nitrate that evolves into nitric acid during sampling must passes directly over and through plastic grids, support matrices, and surfaces before it reaches the Nylasorb filter. Clearly, knowing the affinity of nitric acid for reducing surfaces, much of the evolved nitric acid would never reach the Nylasorb filter. Since we cannot measure nitrates off such surfaces, this fraction was lost to MSAM, reducing the "total nitrate" result.

Error #2 The Teflon filter was not analyzed for about 8 weeks, sitting in a petri dish in the field and, later, in the laboratory under ambient conditions.

Again, this is understandable considering the standard Air Quality Group (AQG), UCD protocols. We often use guard filter to protect gaseous-collecting filter packs, and then never analyze the filters. This was the assumption of our laboratory personnel in this case, an error in training and protocols but again caused in part by the last minute changes in the Barton Flat test procedures.

We know from the tests above that at least 30 percent of the nitrate collected in the worst conditions stays on a Teflon filter. But the conditions in the Barton Flats tests were not nearly as severe as the Davis tests, since temperatures were much lower (actually chilly at night) and humidities were higher. Thus we expect that a large fraction of all particulate nitrate would be collected on the Teflon filter and stay on the Teflon filter.

But upon analysis, after the 8 week delay, almost no nitrates were found on the Teflon filter. The assumption is almost inescapable that the nitrates slowly evolved off the filter in this period and collected on the walls of the petri dishes used to store the samples. Recall that, unlike our normal protocols, the Teflon filters were handled as non-analyzable "guard filter" and stored at room temperature, not under refrigeration as is our normal protocol.

The results of these two errors was to reduce the "total nitrate" results by losing material to the Teflon filter support structures during sampling, and the petri dish during extended storage. There is no way to recover these data.

The conclusion is inescapable that the results of the "total nitrate" channel of MSAM in the Barton Flats tests are biased low, which was what was observed in the results.

We further conclude, on the basis of the earlier tests, that the MSAM is capable of properly collecting materials when the filter media are correctly configured and sample handling protocols are followed.

Conclusion

The nitrate results from the MSAM tests at Barton Flats are incorrect due to problems in sampling and problems in analysis that guarantee loss of a major fraction of nitrate captured on the Teflon pre-filter. This filter was added at the last moment to handle a potential problem with clogging as seen in SCAQS. It was not present in the earlier (and successful) MSAM tests of nitrates. It has nothing to do with the MSAM design and/or the MSAM analytical protocols. Thus, based upon all the evidence, MSAM is capable of excellent measurements of all forms of nitrate.

REPORT DOCUMENTATION PAGE

1. AGENCY USE ONLY *(Leave Blank)*

PB94189222

2. REPORT DATE

July 1993

3. REPORT TYPE AND DATES COVERED

Final Report

4. TITLE AND SUBTITLE

Development of a Modular System for Acidic Deposition Monitoring

5. FUNDING NUMBERS

A132-102

6. AUTHOR(S)

Thomas A. Cahill, Kenneth Dowers, Teresa A. Jones, and
Paul H. Wakabayashi

7. PERFORMING ORGANIZATION NAME(S) AND ADDRESS(ES)

University of California, Davis
Department of Crocker Nuclear Laboratory
Davis, CA 95616-8569

8. PERFORMING ORGANIZATION REPORT NUMBER

9. SPONSORING/MONITORING AGENCY NAME(S) AND ADDRESS(ES)

California Air Resources Board
Research Division
2020 L Street
Sacramento, CA 95814

10. SPONSORING/MONITORING AGENCY REPORT NUMBER

ARB/R-94/525

11. SUPPLEMENTARY NOTES

12a. DISTRIBUTION/AVAILABILITY STATEMENT

Release Unlimited. Available from National Technical Information Service
5285 Port Royal Road
Springfield, VA 22161

12b. DISTRIBUTION CODE

13. ABSTRACT *(Maximum 200 Words)*

The objective of this project was to develop and demonstrate a monitoring system that can be economically deployed throughout the State and provide data comparable to that of the standard CADMP sampler. The study had two phases. In Phase I, the MSAM was tested in Sacramento for three one-week periods. The data analyses showed good agreement between collocated MSAM units and fair agreement between the MSAM and CADMP samplers. During the period from August 5, 1992, to November 6, 1992, the MSAM was deployed at a CADMP intensive study site at Barton Flats in the San Bernardino National Forest. Phase II compared the MSAM and CADMP samplers under field conditions. During phase II, the MSAM collected two-week sample averages, while the CADMP continued to collect on its normal one-day-in-six protocol. The results showed a general agreement between the MSAM and CADMP samplers except for the collection of total nitrate.

14. SUBJECT TERMS

Nylasorh filters, Correlation Coefficient Colorimetry, Denuder Tubes

15. NUMBER OF PAGES

16. PRICE CODE

17. SECURITY CLASSIFICATION OF REPORT

Unclassified

18. SECURITY CLASSIFICATION OF THIS PAGE

Unclassified

19. SECURITY CLASSIFICATION OF ABSTRACT

Unclassified

20. LIMITATION OF ABSTRACT

Unlimited

CARB-RD Version (Org. 5-93) of Federal Standard Form 298 (Rev. 2-89)